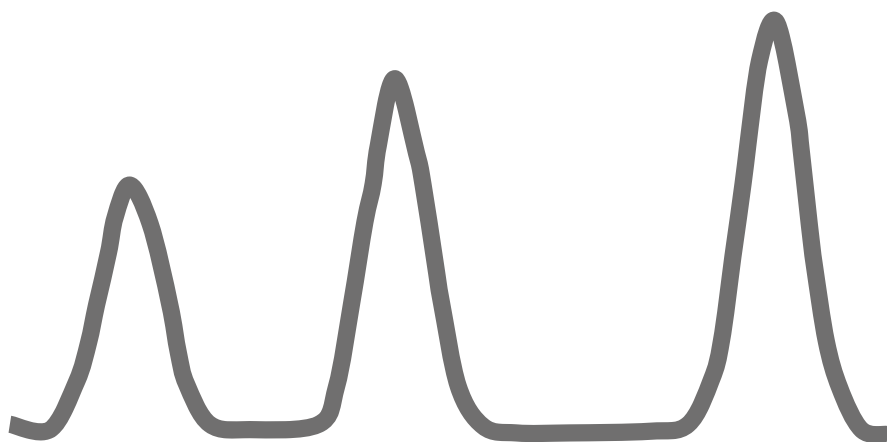


AMPERE NMR SCHOOL

BOOK OF ABSTRACTS

18th – 24th June 2023
ZAKOPANE, POLAND



AMPERE NMR SCHOOL

BOOK OF ABSTRACTS

ZAKOPANE

18th – 24th June 2023

AMPERE NMR SCHOOL 2023

18th – 24th June 2023

organized by
The NanoBioMedical Centre
Adam Mickiewicz University in Poznań, Poland



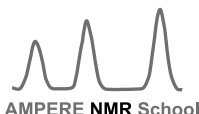
Organizing Committee

Danuta Kruk
Roksana Markiewicz
Nataliya Babayevska
Jacek Jenczyk
Alicja Joras
Grzegorz Nowaczyk
Tomasz Zalewski

Scientific Committee

Danuta Kruk (Olsztyn, Poznań) Poland
Bernhard Blümich (Aachen), Germany
Anja Böckmann (Lyon), France
Janez Dolinšek (Ljubljana), Slovenia
Matthias Ernst (Zürich), Switzerland
Wiktor Koźmiński (Warsaw), Poland
David Lurie (Aberdeen), Scotland, UK
Alexander MacKay (Vancouver), Canada
Beat Meier (Zürich), Switzerland
Daniel Topgaard (Lund), Sweden

The School is supported by the Groupement AMPERE and Softcomp
with the financial sponsorship by JEOL Ltd and Stelar.



AMPERE NMR School

The School is held under the Honorary Patronage
of the Rector of Adam Mickiewicz University, Poznań, Poland



Honorary Patronage
RECTOR OF ADAM MICKIEWICZ
UNIVERSITY
POZNAŃ

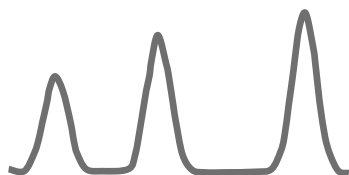
SPEAKERS	9
SOLID-STATE NMR OF THE MULTIDRUG ABC TRANSPORTER BMRA Denis Lacabanne, Thomas Wiegand, Cédric Orelle, Jean-Michel Jault, Beat H. Meier and Anja Böckmann	11
BICOMPONENT FLUIDS IN POROUS MEDIA: WHAT NMR CAN DO FOR YOU Siegfried Stapf, Niklas Siebert, Timo Spalek, Vincent Hartmann, Bulat Gizatullin, Carlos Mattea	12
PROTEIN FAST MAS NMR AT HIGH FIELD Beat H. Meier, Morgane Callon, Dominique Luder, Alexander A. Malär, Thomas Wiegand, Vaclav Rimal, Lauriane Lecoq, Ago Samoson and Anja Böckmann	13
THE MAGICAL WORLD OF PURE SHIFT NMR Adolfo Botana, Peter Kiraly and Paul Bowyer	14
HIGH DIMENSIONALITY AND HIGH RESOLUTION NMR EXPERIMENTS FOR BIOMOLECULES Wiktor Kozmiński	15
PRACTICAL ASPECTS OF ¹³C QNMR Adolfo Botana	16
USE OF A BENCHTOP MAGNETIC RESONANCE IMAGING SYSTEM FOR FOOD APPLICATIONS Mecit Halil Oztop, Esmanur Ilhan and Erdem Mercan	17
BASICS OF MRI & FIELD-CYCLING IMAGING David J. Lurie	18
EFFECT OF SURFACTANT AGGREGATION ON CLOUD FORMATION Anne Selent, Pär Håkansson, Sampo Vepsäläinen, Ilari Ainasoja, Sanna Komulainen, Pau Mayorga Delgado, Otto Mankinen, Jiří Mareš, Ritu Ghanghas, Silvia Calderón, Vladimir V. Zhivonitko, Jack J. Lin, Jussi Malila, Ville-Veikko Telkki and Nønne L. Prisle	19
OBSERVING SHORT-RANGE ORIENTATIONAL ORDER: FROM LIQUID CRYSTALS TO SMALL-MOLECULE LIQUIDS Anton Gradišek, Tomaž Apih, Maria J. Beira, Carlos Cruz, Susete N. Fernandes, M. Helena Godinho and Pedro J. Sebastião	20
LOW FIELD MRI SOLUTIONS: FIXED FIELD, PRE-POLARIZED OR FIELD-CYCLED? Esteban Anoardo	21
ASYMMETRY IN THREE-SITE RELAXATION-EXCHANGE NMR Bernhard Blümich, Matthew Partiale and Matthew Augustine	22
TRANSLATIONAL MOTION AND MAGNETIC FIELD GRADIENTS Daniel Topgaard	23
EXPLORING NMR LABORATORY OPERATIONS IN MEDICINAL CHEMISTRY: INSIGHTS FROM EVERYDAY CHALLENGES AT CELON PHARMA SA Arkadiusz Leniak	24
NMR OF QUADRUPOLEAR NUCLEI IN SOLIDS AT ULTRA-HIGH MAGNETIC FIELDS Olivier Lafon	25
⁶⁹GA AND ⁷¹GA AS PROBES OF LOCAL SYMMETRY IN DIAMAGNETIC COMPLEX METALLIC PHASES Magdalena Wencka	26
LOOKING INTO POROUS MATERIALS WITH SOLID STATE NMR AND RELAXOMETRY Lucia Calucci, Silvia Borsacchi, Elisa Della Latta, Marco Geppi, Francesca Martini and Francesca Nardelli	27
FIELD-CYCLING NMR RELAXOMETRY OF PARAMAGNETIC-LABELED PROTEINS Giacomo Parigi	28
NMR RELAXATION PROCESSES IN SOLUTIONS OF SUPERPARAMAGNETIC NANOPARTICLES Danuta Kruk	29

ANALYSIS OF STRONGLY DIPOLAR COUPLED SOLIDS BY TIME-DOMAIN NMR	
<u>Leonid Grunin, Maria Ivanova</u>	30
CHEMICAL EXCHANGE RATE STUDIED BY NMR CPMG METHOD	
<u>Janez Stepišnik and Aleš Mohorič</u>	31
ASSESSING THE MOLECULAR DYNAMICS IN PARAMAGNETIC LIQUID SYSTEMS	
<u>Maria J. Beira and Pedro J. Sebastião</u>	32
IONIC-LIQUID BASED HYBRID GEL POLYMER ELECTROLYTES AS SEEN BY NMR	
<u>Claudia Schmidt</u>	33
CHALLENGES OF NON-EXPONENTIAL NMR RELAXATION PROCESS	
<u>Adriane Consuelo Leal Auccaise, Elzbieta Masiewicz and Danuta Kruk</u>	34
ON-LINE LABORATORY TRAININGS	35
JASON WORKSHOP: PRACTICAL ASPECTS	
<u>Adolfo Botana and Peter Kiraly</u>	37
MAGIC ANGLE	
<u>Jacek Jencyk</u>	38
FFC-NMR TUTORIAL	
<u>Elzbieta Masiewicz</u>	39
MRI: BASIC PRINCIPLES AND APPLICATION	
<u>Tomasz Zalewski and Marek Kempka</u>	40
NMR DIFFUSION	
<u>Michał Bielejewski</u>	41
PARTICIPANTS POSTERS	43
P1. INSIGHTS INTO GELATION MECHANISMS AND GEL PROPERTIES OF LMWG/PC: A COMPARATIVE STUDY USING DSC/TGA, NMR, AND CONFOCAL FLUORESCENCE MICROSCOPY	
<u>Farooq Ahmad, Natalia Bielejewska, Michał Bielejewski</u>	45
P2. MAGNETIC RESONANCE IMAGING OF HYDROCARBON GAS AT VARIOUS PRESSURES	
<u>M. Anikeeva, A. N. Pravdivtsev, E. Peschke and J-B. Hövener</u>	46
P3. SYNTHESIS OF NOVEL TRACERS FOR DEUTERIUM MAGNETIC RESONANCE IMAGING	
<u>Fatima Anum, Arne Brahms, Philip Saul, Maria Anikeeva, Rainer Herges, Jan-Bernd Hövener, Andrey N. Pravdivtsev</u>	47
P4. INSIGHTS TO NMR RELAXATION AND SUSCEPTIBILITY REPRESENTATION	
<u>Ruben Auccaise, Adriane Consuelo Leal Auccaise and Danuta Kruk</u>	48
P5. SYNTHESIS AND CHARACTERIZATION OF GD-BASED DENDRITIC POLYMERS AS A POTENTIAL CONTRAST AGENT	
<u>Nataliya Babayevska, Katarzyna Fiedorowicz, Jacek Jencyk</u>	49
P6. FAST PKA DETERMINATION FOR LEAD OPTIMISATION APPLICATION OF CHEMICAL SHIFT IMAGING AND CHEMICAL GRADIENTS INTO ANALYSIS OF APIS	
<u>K. Baj, A. Hindle, S.H. Marsden, J. Brammer, S. Demanze, M. Wallace, J.A. Iggo</u>	50
P7. UNDERSTANDING WATER AND OIL HOLDING PROPERTIES OF COCOA FIBER-GUM MIXTURES WITH NMR RELAXOMETRY	
<u>Murad Bal, Mecit H. Oztop</u>	51

P8. THREE MUSKETEERS OF MRI CONTRASTING: INFLUENCE OF METAL ADDITION ON PHOTOTHERMAL AND RELAXIVITY PROPERTIES OF POROUS POLYDOPAMINE NANOPARTICLES	
<u>Magdalena J. Bigaj-Józefowska, Emerson L. Coy, Karol Załęski, Radosław Mrówczyński, Bartosz F. Grześkowiak</u>	52
P9. SPEEDING UP RESTRICTED DIFFUSION NMR MEASUREMENTS FOR POROUS STRUCTURE DETERMINATION OF BIOCOMPATIBLE GELS	
<u>Marek Czarnota, Sylwester Domański and Mateusz Urbańczyk</u>	53
P10. GMO@DTPA-BSA-GD NANOPARTICLES AS NOVEL POTENTIAL MRI CONTRAST AGENTS	
<u>K. Gębicka, D. Flak, T. Zalewski, M. Kempka, G. Nowaczyk, M. Banaszak</u>	54
P11. CHARACTERIZATION OF POLYMER-CERAMIC COMPOSITE ELECTROLYTES USING MULTIDIMENSIONAL SOLID-STATE NMR	
<u>Pedram Ghorbanzade and Juan Miguel López del Amo</u>	55
P12. INVESTIGATING SYNERGISTIC EFFECTS BETWEEN CELLULOSE AND LIGNIN FOR ADVANCED FOREST CARBON FIBERS: MASS TRANSPORT CHARACTERIZATION WITH MAGNETIC RESONANCE METHODS	
<u>F. Guerroudj, J. Bengtsson, K. Jedvert and D. Bernin</u>	56
P13. 1D 1H NMR SPECTRA OF NOVEL GLYCERYL MONOOLEATE / GLYCERYL MONOLAURATE LIPID LIQUID CRYSTALLINE NANOPARTICLES	
<u>Jakub Jagielski, Łukasz Popenda, Karolina Gębicka, Grzegorz Nowaczyk</u>	57
P14. 1H-NMR LOW TEMPERATURE SPECTROSCOPY AND RELAXOMETRY STUDIES OF HYDRATION FROM GASEOUS PHASE OF FOLIOSE LICHENIZED FUNGI: PSOROMA HYPNORUM FROM ANTARCTICA	
<u>D. Jakubiec, K. Kubat, M. A. Olech, A. Casanova-Katny, K. Strzałka and H. Harańczyk</u>	58
P15. INSIGHTS INTO STRUCTURE AND DYNAMICS OF MINIMAL HDV LIKE RIBOZYME DRZ-MTGN-1	
<u>Soumyadip Jana, Silke Johannsen, Roland K.O. Sigel</u>	59
P16. MECHANISMS OF MOLECULAR MOTION BY MEANS OF NMR RELAXOMETRY	
<u>Adam Kasparek, Maciej Osuch, Danuta Kruk</u>	60
P17. A TD-NMR INVESTIGATION FOR THE FOOD-GRADE PICKERING EMULSIONS	
<u>Esratur Kaya, Esmanur İlhan and Mecit Halil Öztop</u>	61
P18. METHODS OF FUNCTIONALIZATION OF SMART HYDROGEL SURFACES BASED ON HYALURONIC ACID	
<u>Marietta Koźlarek, Roksana Markiewicz and Grzegorz Nowaczyk</u>	62
P19. EVALUATION OF MIXING EFFICIENCY IN BUBBLE REACTORS FOR CARBON DIOXIDE CAPTURE USING MRI	
<u>Feryal Guerroudj, Emmanouela Leventaki, Saeed Khoshhal Salestan, Francisco M. Baena-Moreno, Diana Bernin</u>	63
P20. IN-HOUSE FABRICATION OF MICROWAVE WAVEGUIDES AND RESONATORS FOR EFFICIENT DYNAMIC NUCLEAR POLARIZATION	
<u>Jake Lumsden, Zhenfeng Pang, Utsab Banerjee, Kong Ooi Tan</u>	64
P21. NOVEL 1D ZNO NANOMATERIALS WITH PROMISING PHOTOELECTROCHEMICAL PROPERTIES FOR BIOSENSING AND WATER SPLITTING APPLICATIONS	
<u>Andrii Lys, Irfan Hanif and Igor Iatsunskyi</u>	65
P22. STRUCTURE AND MOLECULAR INTERACTIONS IN AMMONIUM IONIC LIQUIDS	
<u>Roksana Markiewicz, Adam Klimaszyk, Marcin Jarek, Michał Taube</u>	66
P23. WATER DYNAMICS IN ARTIFICIAL TISSUES BY MEANS OF NMR RELAXOMETRY	
<u>Elzbieta Masiewicz, Farman Ullah, Adrianna Mieloch and Danuta Kruk</u>	67

P24. ANALYSIS MOLECULAR DYNAMIC PROCESSES IN THE COMPLEX OF HUMAN S100B PROTEIN WITH Aβ PEPTIDE ON BASE ^{15}N RELAXATION DATA	
<u>Thomas Okoth, Wojciech Kwiatek, Maciej Kozak and Igor Zhukov</u>	68
P25. FREQUENCY OPTIMIZATION IN MULTIDIMENSIONAL DIFFUSION-RELAXATION CORRELATION MRI ON A FIXED MOUSE BRAIN	
<u>Pak Shing Kenneth Or, Maxime Yon, Omar Narvaez, Alejandra Sierra Lopez, Dan Benjamini and Daniel Topgaard</u>	69
P26. LUNG CANCER RADIOMICS INVESTIGATION: CT-MRI FEATURES COMPARISON AND SOFTWARE CONSISTENCY	
<u>Agnese Robustelli-Test, Alessandra Pinto, Chandra Bortolotto, Raffaella Cabini, Francesca Brero, Manuel Mariani, Ian Postuma, Lorenzo Preda, Alessandro Lascialfari</u>	70
P27. INSIGHT INTO MASS TRANSFER WITHIN A SUPERABSORBENT POLYMER USING MRI	
<u>Saeed Khoshhal Salestan, Emmanouela Leventaki, Feryal Guerroudj, Diana Bernin</u>	71
P28. INVESTIGATION OF THE INTERACTION OF SODIUM IONS WITH ZIF-8 IN SODIUM-ION BATTERY ELECTROLYTES USING ^{23}Na AND ^1H NMR	
<u>Dominika Tubacka, Kosma Szutkowski, Patryk Florczak</u>	72
P29. ^{13}C SOLID-STATE NMR PROVIDING CRUCIAL INSIGHTS INTO PULPING OF NON-WOODEN CELLULOSE RESOURCES	
<u>Joanna Wojtasz-Mucha, Diana Bernin</u>	73
P30. THE POSITIVE INTERPLAY BETWEEN IMAGING AND THERAPEUTIC AGENTS ENCAPSULATED IN THERANOSTIC LIPOSOMES TARGETING ORAL CANCER	
<u>Tomasz Zalewski, Grzegorz Nowaczyk and Paulina Skupin-Mrugalska</u>	74
P31. NMR DEPTH PROFILING OF PAINTED WALLS: OSTIA ANTICA	
<u>Matea Urbanek, Jan Bader, Daniel Krüger, A. Yong, Jürgen Frick, Jens Anders, E. Del Federico, P. Tomassini, Bernhard Blümich</u>	75
P32. CONTRAST ENHANCEMENT IN MRI USING COMBINED DOUBLE ACTION CONTRASTAGENTS AND IMAGE POST-PROCESSING IN THE BREAST CANCER MODEL	
<u>D. MacDonald, A. Dash, F.C.J.M. van Veggel, B. Tomanek, and B. Błasiak</u>	76
P33. EXPLORING TEMPERATURE RELATED PROTON DYNAMICS INHYDRATED STARCH BY TIME DOMAIN NMR	
<u>Jana van Rooyen, Leonid Grunin, Mecit Oztop and Marena Manley</u>	77
LIST OF SCHOOL SPEAKERS	78
LIST OF TRAINERS	79
LIST OF PARTICIPANTS	80
NOTES	81

SPEAKERS



AMPERE NMR School

Solid-state NMR of the Multidrug ABC Transporter BmrA

Denis Lacabanne^{a,b}, Thomas Wiegand^{a,c,d}, Cédric Orelle^e, Jean-Michel Jault^e,
Beat H. Meier^a and Anja Böckmann^e

^a *Physical Chemistry, ETH Zurich, 8093 Zurich, Switzerland*

^b *current address: Medical Research Council Mitochondrial Biology Unit, University of
Cambridge, Cambridge, United Kingdom*

^c *current address: Max-Planck-Institute for Chemical Energy Conversion, Stiftstr. 34-36,
45470 Mülheim an der Ruhr, Germany*

^d *current address: Institute of Technical and Macromolecular Chemistry, RWTH Aachen
University, Worringerweg 2, 52074 Aachen, Germany*

^e *Molecular Microbiology and Structural Biochemistry, UMR5086 CNRS/University of Lyon*

Membrane proteins presented an interesting target for solid-state NMR studies, since they could be studied in a lipid environment. Also, NMR can reveal chemical properties of the protein, by chemical-shift perturbations caused by binding events. Molecular motors are interesting in this context, since they use ATP as a fuel to power molecular machines. ABC transporters are such machines, since they act as pumps to import and export molecules from cells. This is for instance important in antibiotic resistance, where these large proteins remove the antibiotics from bacterial cells. The pumping mechanisms proceeds as a function of ATP hydrolysis.

The detailed mechanism of ATP hydrolysis in ATPbinding cassette (ABC) transporters is still not fully understood. We here present results from solid-state NMR which we used to probe the conformational changes and dynamics during the catalytic cycle by locking the multidrug ABC transporter BmrA in prehydrolytic, transition, and posthydrolytic states, using a combination of mutants and ATP analogues. The NMR spectra reveal that ATP binds strongly in the prehydrolytic state to both ATP-binding sites, but that in the transition state of wild-type BmrA, the symmetry of the dimer is broken and only a single site is tightly bound to ADP:Mg²⁺:vanadate. In the posthydrolytic state, weak binding is observed for both sites. Our results show that after ATP binding, the symmetry of the ATP-binding sites of BmrA is lost in the ATP-hydrolysis step, but is then recovered in the posthydrolytic ADP-bound state.

FIGURE 1. This is Style for Figure Captions. All text should be 10 pt. The text “FIGURE 1” which labels the caption should be bold and capital. Center this text under the figure. If figures have more than one part should be labels (a), (b), etc.

Acknowledgements

We thank the French ANR and ANRS for support.

BICOMPONENT FLUIDS IN POROUS MEDIA: WHAT NMR CAN DO FOR YOU

Siegfried Stapf, Niklas Siebert, Timo Spalek, Vincent Hartmann,
Bulat Gizatullin, Carlos Mattea

Dept. of Technical Physics II, TU Ilmenau, PO Box 100 565, 98684 Ilmenau, Germany

The theoretical description of the T_1 dispersion of liquids in metal-free porous systems has been established decades ago, distinguishing between the limiting cases of strong and weak adsorption of the molecules on the native glass surface [1]. The model predicts vanishing T_1 dispersion in the weak adsorption case, and strongly pronounced dispersion for those molecules that encounter preferential orientation on the surface, experiencing the surface curvature via anomalous diffusion. Therefore, this process is intramolecular by nature and is expected to lead to identical dispersions for protons and deuterons [2].

In very small pores, such as in the 4 nm pores of Vycor or on the surface of silica particles of similar size, T_1 dispersion is present for all liquids, indicating non-negligible surface interaction. We have carried out ^2H relaxation dispersion measurements of perdeuterated liquids and ^1H and ^2H studies of binary systems of two fluids in Vycor that are either miscible or immiscible in the bulk, e.g. protic (water, ethanol) and aprotic liquids (acetone, THF, cyclohexane, n-alkanes) [3,4]. Combining NMRD relaxation between 0.2 mT and 1 T with relaxation and diffusion experiments at 7 T, a particularly strong ^2H relaxation dispersion was observed that is at variance with either of the established relaxation models. Moreover, we found a strong tendency of preferential surface adsorption of the non-polar liquid, but also an apparent phase separation between bulk miscible liquids such as acetone and cyclohexane, suggesting that the latter is entirely removed from the silica surface.

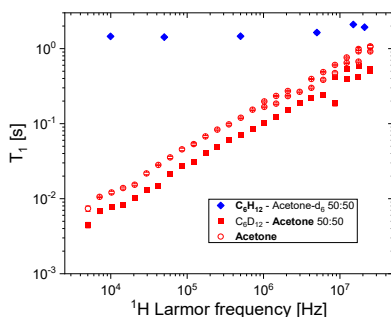


FIGURE 1. Relaxation dispersion $T_1(\nu)$ of the ^1H nuclei of liquids in Vycor porous glass for partially deuterated mixtures of acetone and cyclohexane at 50%:50% volume fraction compared with pure acetone in Vycor.

References

- [1] T. Zavada, R. Kimmich, J. Chem. Phys. **109**, 6929-6939 (1998)
- [2] S. Stapf, R. Kimmich, R.-O. Seitter, Phys. Rev. Lett. **75**, 2855-2858 (1995)
- [3] C. Mattea, R. Kimmich, I. Ardelean et al., J. Chem. Phys. **121**, 10648 (2004)
- [4] J. Ward-Williams, L.F. Gladden, Magn. Reson. Imaging **56**, 57-62 (2019)
- [5] S. Stapf, N. Siebert, T. Spalek, V. Hartmann, B. Gizatullin, C. Mattea, Magn. Reson. Lett., *in press*

Protein fast MAS NMR at high field

Beat H. Meier^{1*}, Morgane Callon^{1*}, Dominique Luder¹, Alexander A. Malär¹, Thomas Wiegand¹, Vaclav Rimal¹, Lauriane Lecoq², Ago Samoson³ and , Anja Böckmann²

¹ Physical Chemistry, ETH Zürich, 8093 Zürich, Switzerland^{SEP}

² Molecular Microbiology and Structural Biochemistry (MMSB) UMR 5086

CNRS/Université de Lyon, Labex Ecofect, 7 passage du Vercors, 69367 Lyon, France

³ Institute of Health technologies, Tallin University of Technology Akadeemia tee 15a, 12618 Tallinn, Estonia

The NMR resonances of protein side chain protons provide important information not only about protein structure and dynamics, but also about the mechanisms that regulate interactions between macromolecules. However, these resonances are particularly difficult to resolve spectrally, even in relatively small proteins. The recent development of MAS frequencies up to 160 kHz has been shown to significantly improve resolution. Indeed, NMR spectroscopy, the only technique capable of accessing interactions and dynamic processes in a sample under physiological conditions, has so far been limited when applied to large protein assemblies. We characterise the gain in resolution by increasing the MAS frequency from 110 to 160 kHz MAS frequencies and find a drastic improvement in the spectral resolution of this crowded region in the ¹H-¹³C dimensions, allowing the identification of these essential proton resonances in fully protonated samples. These improvements allowed us to assign 60% of the aliphatic protons of the core protein (Cp), which is organised in a large 120-dimer assembly to form the hepatitis B virus capsid. This opens up new possibilities for further characterisation of protein-protein or protein-nucleic acid interactions.

The magical world of pure shift NMR

Adolfo Botana^a, Peter Kiraly^b and Paul Bowyer^a

^aJEOL UK Ltd, Silver Court, Watchmead, Welwyn Garden City AL7 1LT

^bJEOL UK Ltd, 4 Bankside, Long Hanborough, Witney OX29 8LJ

NMR is an enormously powerful analytical technique, yielding unrivalled insights into the chemical structure and dynamics of organic molecules. Unfortunately, the information that can be readily extracted from the NMR spectrum is sometimes limited by overlap between neighboring peaks, a problem which is often exacerbated by the presence of broad peak “multiplets” due to J-splittings. This is particularly a problem in proton spectra, where the narrow chemical shift range and manifold J-couplings between protons can lead to severe peak overlap. In recent years, much work has been done to develop NMR methods that yield spectra where the peak multiplet structure is completely suppressed; these so-called “pure shift” spectra show much higher resolution than conventional spectra [1]. We introduce the basic principles of pure shift NMR and describe some of the most important pure shift methods that have been developed to date.

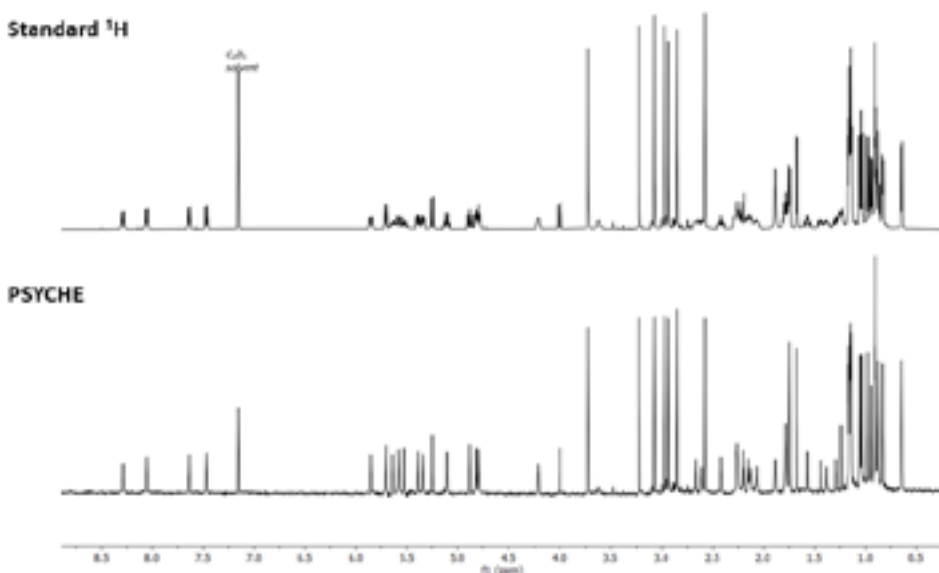


FIGURE 1. Standard single proton pulse acquisition and a pure shift spectrum of cyclosporine.

References

[1] Bowyer, Paul “An Introduction to Pure Shift NMR” <https://attendee.gotowebinar.com/register/7480233097627308048>. Accessed 8 Dec. 2022.

High dimensionality and high resolution NMR experiments for biomolecules

Wiktor Koźmiński

Faculty of Chemistry, Biological and Chemical Research Centre, University of Warsaw, Warsaw, Żwirki i Wigury 101, 02-089 Warsaw, Poland

Studies of biomolecular structure and dynamics by NMR spectroscopy at atomic resolution require acquisition of multidimensional spectra. However, the recording time of sufficiently resolved multidimensional spectra is often very long due to the sampling limitations. A variety of different methods, mostly based on non-uniform sampling, were proposed to overcome this limitation in multidimensional NMR spectroscopy. They could be utilized in two different ways, either to shorten the experiment duration without loss of resolution, or to perform experiments that are not obtainable conventionally, i.e. with significantly improved resolution and/or of high dimensionality. Most often first of these two, so called “Fast NMR” approach, is shown as the example of the utility of these methods, as it saves expensive spectrometer time. However, in many cases spectra which are not possible to record conventionally, featuring extraordinary resolution and high number of dimensions may be more interesting from scientific point of view as they reveal effects that are hidden, when spectral lines are broad, or enable resolving spectral ambiguities when peaks are overlapped. This second approach we refer to as “Accurate NMR”. Its full potential is manifested when the overall experiment time is less important than a new information available from spectra of high dimensionality (4-6D) or of high resolution approaching natural line-width. The new methods were applied for NMR studies of intrinsically disordered proteins, where the structural disorder in combination with highly repetitive amino-acid sequences causes severe peak overlap in the spectra. Several novel 4-7D pulse sequences are proposed. The new experiments employ non-uniform sampling that enables achieving high resolution in indirectly detected dimensions.

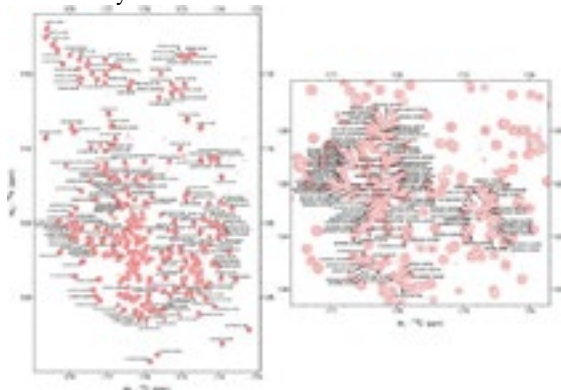


Figure 1 Resonance assignment of Tau3x (354 aa) shown on CON projection from 3D HNCO [1]

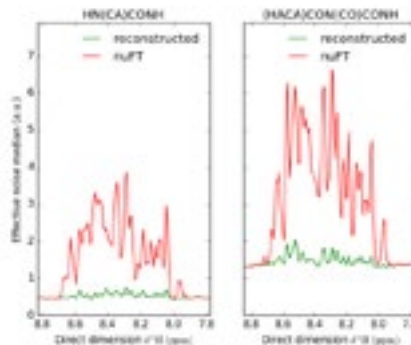


Figure 2 Noise median for 5D HN(CA)CONH (left) and 5D (HACA)CON(CO)CONH (right) SSA-reconstructed and ruFT spectra with respect to direct dimension ^1H chemical shift [2]

Acknowledgements

Polish National Science Centre MAESTRO grant 2015/18/A/ST4/00270 is gratefully acknowledged.

References

1. S. Żerko, P. Byrski, P. Włodarczyk-Pruszyński, M. Górka, K. Ledolter, E. Masliah, R. Konrat, W. Koźmiński, J. Biomol. NMR. 65 (2016).
2. K. Kosiński, J. Stanek, M.J. Górka, S. Żerko, W. Koźmiński, J. Biomol. NMR. 68 (2017) 129–138.
3. K. Kazimierczuk, J. Stanek, A. Zawadzka-Kazimierczuk, W. Koźmiński, ChemPhysChem. 14 (2013) 3015–3025
4. M. Nowakowski, S. Saxena, J. Stanek, S. Żerko, W. Koźmiński, Prog. Nucl. Magn. Reson. Spectrosc. 90–91 (2015) 49–73.

Practical aspects of ^{13}C qNMR

Adolfo Botana

JEOL UK Ltd, Silver Court, Watchmead, Welwyn Garden City AL7 1LT

Quantitative NMR is one of the most important tools for the quantification of chemical species in samples. It is most commonly run through the measurement of ^1H detected single pulse experiments[1], but severe spectral overlap makes the quantification of analytes a challenging task. ^{13}C detected NMR alleviates the spectral overlap problem, and with modern instruments achieving higher sensitivity, ^{13}C qNMR becomes a suitable alternative to ^1H qNMR. For example, the resolution achieved in ^{13}C data enables the determination of long-chain branching in polymers[2].

Several aspects such as the acquisition of data with low signal-to-noise ratio and the larger bandwidth required to excite the ^{13}C spectrum lead to a number of considerations that must be taken into account when acquiring ^{13}C qNMR. Here we describe some of the practical aspects and consideration to take into account to acquire accurate ^{13}C qNMR data[3].

References

- [1] Pauli, Guido F., et al. "Quantitative ^1H NMR. Development and Potential of an Analytical Method: An Update." *Journal of Natural Products*, vol. 75, no. 4, 6 Apr. 2012, pp. 834–851, DOI: 10.1021/np200993k.
- [2] Ishii, Yuya, et al. "Determination of Low Degrees of Long-Chain Branching in Polybutadiene by Double-Bond Hydrogenation Followed by ^{13}C NMR and DEPT Spectroscopies." *Polymer*, vol. 185, Dec. 2019, p. 121965, DOI: 10.1016/j.polymer.2019.121965.
- [3] Botana, Adolfo "Quantitative ^{13}C NMR" <https://attendee.gotowebinar.com/register/2577550346473705743> . Accessed 8 Dec. 2022.

USE OF A BENCHTOP MAGNETIC RESONANCE IMAGING SYSTEM FOR FOOD APPLICATIONS

Mecit Halil Oztop^a, Esmanur Ilhan^a and Erdem Mercan^a.

^aDepartment of Food Engineering, Middle East Technical University, Ankara, Turkey

Magnetic Resonance Imaging enables us to visualize the interior tissues of food samples and thus it becomes possible to observe the infected tissues in fresh produce, oil/water distribution in high-fat foods, moisture uptake during storage, and many other processes relevant to food science and processing.

In addition, it can be used to conduct flow imaging, and an MRI system can be transferred to an online viscometer. In this study, steps on how to conduct an image will be explained using a benchtop MR imaging system. T_1 , T_2 measurements, Spin Echo Imaging, T_2 mapping, and T_1 mapping will be discussed with examples. In addition, a flow MR imaging experiment will be performed to calculate the rheological properties of some food samples.

Acknowledgements

This study has received funding from the European Union's Horizon 2020 Research and Innovation Programme under grant agreement 101008228.

BASICS OF MRI & FIELD-CYCLING IMAGING

David J. Lurie

*School of Medicine, Medical Sciences & Nutrition, University of Aberdeen,
Foresterhill, Aberdeen AB25 2ZD, Scotland, UK*

MRI uses magnetic field gradients to encode spatial information into NMR signals. In frequency-encoding, the NMR signal is recorded while a field gradient is applied. Since the magnetic field varies with position along the gradient direction (e.g. X), Larmor frequency is a function of position, so the detected signal contains a range of frequencies; analysing the frequency content generates a one-dimensional projection of the water-distribution within the patient. Phase-encoding is employed in the second in-plane dimension (e.g. Y); here, the gradient is pulsed on and off prior to measurement of the signal, altering the phase of the NMR signal as a function of position. The image slice is defined using selective-excitation, in which the excitation 90° radiofrequency pulse is shaped (typically a sinc function) and is applied in the presence of a field gradient perpendicular to the slice plane (e.g. along Z for a transaxial X-Y slice). An excellent primer textbook on MRI has been published by McRobbie *et al.* [1].

During the last decade, the laboratory in Aberdeen has focused on the development of Field-Cycling Imaging (FCI), based on combining MRI with Fast Field-Cycling (FFC) magnetic resonance. By switching field strength during an experiment, this technique exploits the variation of T_1 with magnetic field (T_1 -dispersion), with the aim of increasing the diagnostic potential of MRI [2,3]. FCI aims to obtain spatially-resolved T_1 -dispersion data, by collecting images at a wide range of evolution field strengths. A range of FCI equipment has been built, including two whole-body human sized scanners, operating at detection fields of 0.06 T [4] and 0.2 T [5]. The 0.2 T system uses a single resistive magnet, composed of three coaxial coils.

Results have shown that FFC methods can detect changes in human cartilage induced by osteoarthritis [6]. Experiments on resected tissues from breast cancer patients have demonstrated significant differences in the dispersion curves between normal and diseased tissues [7]. Studies on patients with acute ischaemic stroke have been performed; FCI images exhibited increased intensity in stroke-affected regions, with maximum contrast typically at the lowest field used (0.2 mT) [8]. Studies on patients with brain cancer and patients with breast cancer are underway. All human studies were conducted following approval of the relevant Research Ethics Committees and with informed consent. Work to improve the hardware and software is ongoing, including the implementation of improved RF coils [9].

References

- [1] McRobbie D.W., *et al.*, “MRI from Picture to Proton”, 3rd Edition, Cambridge University Press (2017).
- [2] Lurie D.J., Aime S., *et al.*, *Comptes Rendus Physique* **11**, 136-148 (2010).
- [3] Lurie D.J., Ross P.J. and Broche L.M., “Techniques and Applications of Field-cycling Magnetic Resonance in Medicine”, in: “Field-cycling NMR Relaxometry: Instrumentation, Model Theories and Applications”; New Developments in NMR No. 18, Kimmich R., ed., Royal Society of Chemistry, UK, pp 358-384 (2018).
- [4] Lurie D.J., Foster M.A., *et al.*, *Phys.Med.Biol.* **43**, 1877-1886 (1998).
- [5] Broche L.M., *et al.*, *Scientific Reports* **9**:10402 (2019).
- [6] Broche L.M., Ashcroft G.P and Lurie D.J., *Magn.Reson.Med.* **68**, 358-362 (2012).
- [7] Masiewicz E., *et al.*, *Scientific Reports* **10**:14207 (2020).
- [8] Broche L.M., *et al.*, 11th Conference on FFC NMR Relaxometry, Pisa, Italy, p6 (2019).
- [9] Stormont R.S., *et al.*, *Phys.Med.Biol.* **68**, 055016 (2023).

EFFECT OF SURFACTANT AGGREGATION ON CLOUD FORMATION

Anne Selent,^a Pär Håkansson,^a Sampo Vepsäläinen,^b Ilari Ainasoja,^a Sanna Komulainen,^a Pau Mayorga Delgado,^a Otto Mankinen,^a Jiří Mareš,^a Ritu Ghanghas,^a Silvia Calderón,^{b,c} Vladimir V. Zhivonitko,^a Jack J. Lin,^{b,d} Jussi Malila,^b Ville-Veikko Telkki^a and Nønne L. Prisle^{b,d}.

^a*NMR Research Unit, University of Oulu, P.O. Box 3000, FI-90014, Finland*

^b*NANOMO Research Unit, University of Oulu, P.O. Box 3000, FI-90014, Finland*

^c*Finnish Meteorological Institute, P.O. Box 1627, FI-70211, Kuopio, Finland*

^d*Center for Atmospheric Research, University of Oulu, P.O. Box 4500, FI-90014, Finland*

Organic surfactants, which are common constituents of atmospheric aerosols, change both surface tension and water activity of cloud droplets. The aggregation of surfactants significantly affect the cloud droplet growth, inducing yet not well-known potential effects on global climate.

This work aims at improved understanding of aggregation phenomena of surfactants in aqueous solutions as well as the effect of aggregation on cloud droplet growth. We combine advanced relaxation and diffusion NMR techniques with state-of-the-art relaxation modelling, in which dynamic and structural parameters are extracted from MD simulations, to elucidate the aggregation of surfactants. Aqueous sodium decanoate was used as a representative model system. Furthermore, we use thermodynamic models and Köhler theory to estimate the effect of aggregation on growth of cloud droplets.

Contrary to the common understanding, our NMR analysis implies that surfactants form small clusters below the critical micelle concentration (CMC). Furthermore, it shows that the micelle size above the CMC is significantly smaller than the value provided by a conventional empirical model. Water diffusion experiments revealed water-encapsulating aggregates at higher concentrations and exchange rates between the encapsulated and free water pools were determined by ultrafast diffusion exchange spectroscopy. Thermodynamic modelling of aerosol hygroscopic growth and cloud droplet formation showed that the aggregation phenomena may significantly affect the hygroscopic growth factors at lower humidity conditions, leading to misrepresenting the aerosol cooling potential. [1,2]

References

- [1] O. Mankinen et al. Ultrafast diffusion exchange NMR. *Nat. Commun.* 11, 3251 (2020).
- [2] A. Selent et al. Surfactant aggregation may bias aerosol cooling potential. To be submitted.

OBSERVING SHORT-RANGE ORIENTATIONAL ORDER: FROM LIQUID CRYSTALS TO SMALL-MOLECULE LIQUIDS

Anton Gradišek^a, Tomaž Apih^a, Maria J. Beira^{b,c}, Carlos Cruz^{b,c}, Susete N. Fernandes^d, M. Helena Godinho^d, and Pedro J. Sebastião^{b,c}.

^a*Jožef Stefan Institute, Jamova Cesta 39, 1000 Ljubljana, Slovenia.*

^b*Center of Physics and Engineering of Advanced Materials, Instituto Superior Técnico, Universidade de Lisboa, Av. Rovisco Pais, 1049-001 Lisboa, Portugal.*

^c*Department of Physics, Instituto Superior Técnico, Universidade de Lisboa, Av. Rovisco Pais, 1049-001 Lisboa, Portugal.*

^d*CENIMAT/I3N, Departamento de Ciência Dos Materiais, Faculdade de Ciências E Tecnologia, UNL, 2829-516 Caparica, Portugal.*

We used NMR relaxometry to demonstrate the existence of dynamic clusters with short-range orientational order in nominally isotropic liquids consisting of elongated molecules. In those clusters the local ordering is driven by polar, steric, and hydrogen-bond interactions between the molecules. In the case of liquid crystals [1-3], measuring the local orientational order fluctuations allowed us to observe the size of these clusters diverging when approaching the phase transition from the isotropic to the nematic phase. These fluctuations are described in terms of rotational elasticity as a consequence of the correlated reorientations of the neighbouring molecules. Our quantitative observations of the dynamic clusters in liquids, numbering about ten or fewer molecules, indicate that this is a general phenomenon in various types of liquids [4].

Acknowledgements

AG and TA acknowledge the funding from Slovenian Research Agency, Basic core funding grant P1-0125. PJS, MB, and CC acknowledge FCT—Portuguese Foundation for Science and Technology projects UID/CTM/04540/2013 (CeFEMA), UID/CTM/04540/2019 (CeFEMA), MB was funded through FCT fellowships PD/BD/142858/2018 and COVID/BD/152743/2022). SNF, MGH acknowledge the FCT—Portuguese Foundation for Science and Technology projects PIDDAC (POCI-01-0145-FEDER-007688, Reference UIDB/50025/2020- 2023), PTDC/CTM-REF/30529/2017 (NanoCell2SEC).

References

- [1] P.J. Sebastião, et al., "Fast Field-Cycling NMR Relaxometry Study of Chiral and Nonchiral Nematic Liquid Crystals", *J. Phys. Chem. B* **115**, 14348-14358 (2011)
- [3] Alina Aluculesei, et al., "1H NMR study of molecular order and dynamics in CBC9CB Liquid Crystal", *Phys. Chem. Chem. Phys.* **21**, 4523-4537 (2019)
- [2] Magdalena Knapkiewicz, et al., "NMR studies of molecular ordering and molecular dynamics in a chiral liquid crystal with the SmC α^* phase", *Phys. Rev. E* **101**, 052708 (2020)
- [4] Anton Gradišek et al., "Observing short-range orientational order in small-molecule liquids", *Sci. Reports* **12**, 22500 (2022)

LOW FIELD MRI SOLUTIONS: FIXED FIELD, PRE-POLARIZED OR FIELD-CYCLED?

Esteban Anoardo^a

^a*Laboratorio de Relaxometría y Técnicas Especiales (Larte), FaMAF - Universidad Nacional de Córdoba and IFEG-CONICET. Córdoba, Argentina.*

The development of low-cost & low-field MRI solutions is a hot topic worldwide by these days. A main reason stimulating this increased activity in the field relies in the possibility to popularize the access of MRI for human diagnosis. However, there is also an in-progress impact in education with possibilities for training in engineering, radiology and biomedical sciences, basic & applied research and industrial applications [1]. We will analyze general technical issues of fixed-field instruments operating at low-field. Then we will discuss pros and cons of the pre-polarized approach, from both physical and technical perspectives. Permanent magnet and electromagnet technology will be confronted. Finally, magnetic field-cycling is introduced as an alternative technique, where field-dependent relaxation and MRI experiments are useful for the development of new contrast mechanisms [2,3]. As field-cycled machines usually deal with switched currents in electromagnets, magnetic field instability and inhomogeneity are the main limiting factors affecting image quality [4,5].

Acknowledgements

To the colleagues, collaborators, disciples and students behind our work in this field, specially: Gonzalo G. Rodriguez (now at Max Planck Institute, Göttingen), Agustín J. Romero (now at R+D Centre of New Technologies, University of Warsaw), Eustaquio M. Erro, Eduardo J. Farrher, Sofia G. Cinquegrani, Guillermo O. Forte, Alexis Berté, Leandro J. Gerbino, German D. Farrher, S. Kruber and Juan J. Ortiz. Financial support from FONCYT, CONICET and Secyt-UNC (Argentina) are kindly acknowledged.

References

- [1] E. Anoardo and G. G. Rodriguez, *New challenges and opportunities for low-field MRI*, J. Magn. Reson. Open 14-15, 100086 (2023).
- [2] G. G. Rodriguez, E. M. Erro and E. Anoardo, *Fast iron oxide-induced low-field magnetic resonance imaging*, J. Phys. D: Appl. Phys. 54, 025003 (2021).
- [3] G. G. Rodriguez and E. Anoardo, *Proton double irradiation field-cycling nuclear magnetic resonance imaging: testing new concepts and calibration methods*, IEEE Trans. Instrum. Meas. 70, 4501608 (2021).
- [4] J. A. Romero, G. G. Rodriguez and E. Anoardo, *A fast field-cycling MRI relaxometer for physical contrast design and pre-clinical studies in small animals*, J. Magn. Reson. 311, 106682 (2020).
- [5] G. G. Rodriguez, A. Salvatori and E. Anoardo, *Dual k-space and image-space post-processing for field-cycling MRI under low magnetic field stability and homogeneity conditions*, Magn. Reson. Imag. 87, 157 (2022).

Asymmetry in Three-Site Relaxation-Exchange NMR

Bernhard Blümich¹, Matthew Partiale², and Matthew Augustine²

¹ *Institut für Technische und Makromolekulare Chemie, RWTH Aachen University, Germany*

² *Department of Chemistry, UC Davis, USA*

Asymmetry of peak integrals in 2D relaxation maps of exchange between three sites reports circular flow between the relaxation sites. This disagrees with detailed balance according to which the exchange between any pair of sites must be balanced in thermodynamic equilibrium. Confined diffusion of particles jumping randomly under thermodynamic constraints on a 2D checkerboard grid to any of their eight neighbor positions and confined gas diffusion were modelled to explore the impact of topological constraints on diffusion. Both models produce density variations across the pore. The checkerboard simulations reveal that up to 1% of the molecules may move in circular paths near the walls. This motion is argued to result from stochastic pore resonance corresponding to diffusion eigenmodes. If confirmed by experiment, it can be concluded with certainty that T_2 - T_2 exchange maps can be asymmetric, and that detailed balance of multi-site exchange is strictly valid only in the absence of topological constraints. The lecture will discuss the significance of detailed balance in textbook physics, how it can be probed in relaxation exchange NMR experiments, and the Monte Carlo simulations executed to test the validity of the principle.

Reference

B. Blümich, M. Parziale, M. Augustine, Monte-Carlo Analysis of Asymmetry in Three-Site Relaxation Exchange: Probing Detailed Balance, Magnetic Resonance, Preprint under review, 22 May 2023, <https://mr.copernicus.org/preprints/mr-2023-8/>

TRANSLATIONAL MOTION AND MAGNETIC FIELD GRADIENTS

Daniel Topgaard^a

^aDepartment of Chemistry, Lund University, Lund, Sweden

Micrometer-scale structures in porous media are imprinted on the time/frequency-dependent (“restricted”) and anisotropic self-diffusion of the pore liquids, which may be investigated with magnetic resonance methods employing magnetic field gradients to encode the signal with information about translational motion. The simplest and most commonly used methods rely on a pair of gradient pulses to study displacements in the direction of the gradient [1]. These methods are sensitive to a wide range of fundamentally different aspects of motion, including bulk diffusivity, restriction, anisotropy, flow, and exchange. While it may be convenient to have a single method to study multiple phenomena, the lack of specificity prevents unambiguous microstructural interpretation of the data [2]. More detailed information can be obtained by capitalizing on the formal analogies between investigating translational motion with magnetic field gradients and measuring rotational correlation functions and interaction tensor anisotropies in solid-state NMR spectroscopy [3]. This lecture includes the basic relations between structure and translational motion in porous media, the physical principles of using pulsed and modulated gradients to separate and correlate specific aspects of translational motion, and examples of applications to liquid crystals, yeast cells, and brains as illustrated in Figure 1.

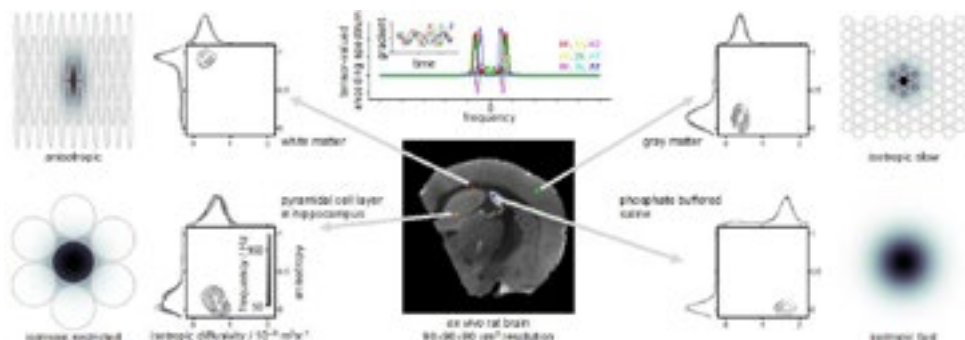


FIGURE 1. Diffusion encoding by double-rotation gradient waveform [4] (top center) and frequency-dependent diffusion tensor distributions for selected voxels of an *ex vivo* rat brain. The multidimensional distributions are visualized as projections onto the 2D plane of isotropic diffusivity and normalized anisotropy for a series of frequencies (gray scale of contour lines), where restriction results in a shift of the distribution with frequency (bottom left). For each voxel, the underlying tissue structure is shown schematically with gray lines representing partially permeable cell membranes and “ink stains” illustrating water diffusion during the 10 ms timescale of diffusion encoding.

References

- [1] Stejskal, *J. Chem. Phys.* **42**, 288 (1965). doi: 10.1063/1.1695690
- [2] Topgaard, *J. Magn. Reson.* **306**, 150 (2019). doi: 10.1016/j.jmr.2019.07.024
- [3] Narvaez, *arXiv:2111.07827* (2021). doi: 10.48550/arXiv.2111.07827
- [4] Jiang, *Magn. Reson.* **4**, 73 (2023). doi: 10.5194/mr-4-73-2023

Exploring NMR Laboratory Operations in Medicinal Chemistry: Insights from Everyday Challenges at Celon Pharma SA

Arkadiusz Leniak

Celon Pharma SA. , Ogrodowa 2A, 05-092 Kielpin

Working in a pharmaceutical company's NMR lab combines the need for fast data analysis and accurate results, particularly in the medicinal chemistry department. The intricacies of this work differ from those found in academic settings, and the solutions employed are uniquely tailored to the fast-paced world of drug discovery.

In this presentation, I will provide an insider's perspective on our NMR laboratory at Celon Pharma SA. From compound characterization to reaction monitoring, NMR spectrometers are crucial tools that enable us to analyze and validate our synthesized molecules. My talk will focus on presenting practical aspects such as quantitative analysis and stoichiometry control. Furthermore, I will delve into a few interesting examples of structural analysis problems. I will also demonstrate how to effectively use titration methods and variable temperature measurements to obtain desired results and plan experiments. Additionally, I will briefly discuss how NMR can be used to screen libraries of small-molecule compounds and how to work without the use of deuterated solvents for rapid analyses of reaction mixtures straight from the reaction flask. Moreover, I will present the spectrometers we work with and the software that facilitates our daily tasks. I will also discuss our future plans, including further laboratory equipment, potential techniques, and analytical methods.

Furthermore, this short presentation goes beyond basic measurements and delves into more interesting cases encountered in our NMR laboratory. I will present a few real-life case studies and examples that highlight the intricacies of working with challenging samples and problems.

NMR OF QUADRUPOLEAR NUCLEI IN SOLIDS AT ULTRA-HIGH MAGNETIC FIELDS

Olivier Lafon^a

^aUniv. Lille, CNRS, UCCS, Lille, France.

Quadrupolar nuclei with spin $I \geq 1$, such as ^{11}B , ^{14}N , ^{17}O , ^{33}S , ^{35}Cl , $^{63,65}\text{Cu}$, ^{67}Zn and ^{71}Ga , represent over 74% of stable NMR-active nuclei and are present in a broad range of solids. Nevertheless, the solid-state NMR of these nuclei remains often challenging because of their large the density matrix and the large anisotropic quadrupolar interaction, which broadens the NMR spectra and complicates the spin dynamics. As a result, NMR spectra of quadrupolar nuclei often lack resolution and many techniques developed for spin-1/2 isotopes are not suitable for quadrupolar nuclei.

This lecture will present a brief overview of the main techniques used to improve the resolution and the sensitivity of NMR spectra of quadrupolar nuclei. In particular, multiple-quantum magic-angle spinning (MQMAS) experiments can be employed to remove the broadening of the signals by quadrupolar interaction. The sensitivity for the detection of quadrupolar nuclei can be improved by the acquisition of a train of echoes using Carr-Purcell Meiboom-Gill (CPMG) sequence as well as population transfers between the different energy levels of the quadrupolar nucleus.

More recently the sensitivity and the resolution of NMR spectra of these quadrupolar nuclei has been greatly improved using ultra-high field magnetic fields produced either by persistent hybrid superconducting magnets built from high- and low-temperature superconductors (LTS) with a static magnetic field (B_0) of 28.2 T, *i.e.*, ^1H Larmor frequency ($\nu_0(^1\text{H})$) of 1.2 GHz, and DC powered hybrid magnets combining LTS and resistive wires with $B_0 = 35.2$ T and $\nu_0(^1\text{H}) = 1.5$ GHz. The sensitivity for the detection of quadrupolar nuclei has also been improved using indirect detection via protons [1,2] and dynamic nuclear polarization (DNP) [3]. These innovative approaches open new avenues for the detection of quadrupolar nuclei with low gyromagnetic ratio, low natural abundance or large quadrupolar coupling, such as ^{33}S , $^{63,65}\text{Cu}$ and ^{67}Zn , in a wide range of solids.

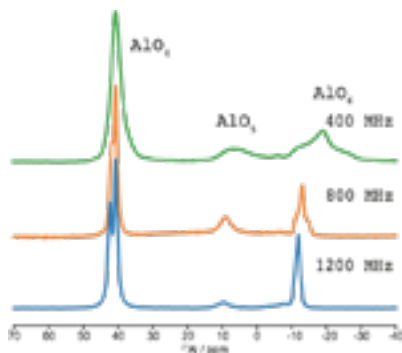


FIGURE 1. 1D ^{27}Al NMR spectra of a sample of the crystalline microporous aluminophosphate VPI-5 recorded on 400, 800 and 1200 MHz NMR spectrometers.

References

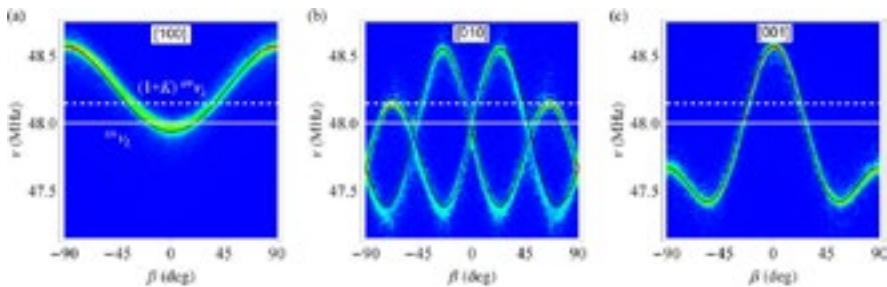
- [1] R. Bayzou *et al.*, *J. Chem. Phys.* **2022**, 156, 064202.
- [2] R. Bayzou *et al.*, *Solid State Nucl. Magn. Reson.* **2022**, 122, 101835.
- [3] E. Bellan *et al* *submitted*.

⁶⁹Ga AND ⁷¹Ga AS PROBES OF LOCAL SYMMETRY IN DIAMAGNETIC COMPLEX METALLIC PHASES

Magdalena Wencka

*Jožef Stefan Institute, Jamova 39, SI-1000, Slovenia
& Institute of Molecular Physics, Polish Academy of Sciences,
Smoluchowskiego 17, 60-179 Poznań, Poland*

The ⁶⁹Ga and ⁷¹Ga of the GaPd, GaPd₂ and Ga₃Ni₂ intermetallic catalysts NMR experiments allow to determine the electronic density of states at the Fermi level (DOS) from the Knight shift and the spin-lattice relaxation rate, which are both determined by the magnetic interaction of the nuclear spins with the spins of conduction electrons. The resolution of the Knight shift and the quadrupolar shift can be done for monocrystalline samples, by recording rotation patterns of the NMR spectra about different orthogonal crystallographic directions. Our determination of the ⁶⁹Ga and ⁷¹Ga gallium electric-field-gradient (EFG) tensor, the Knight shift and the spin-lattice relaxation rate on monocrystalline samples were performed [1, 2]. In a case of the orthorhombic GaPd₂ intermetallic compound we could determine the rotation patterns of the ⁶⁹Ga and ⁷¹Ga central lines (-1/2 ↔ +1/2 transition of a spin $I = 3/2$ spectrum) because of the large quadrupole frequency $\nu_Q = e^2qQ/(2h)$ of both isotopes (where $eq = V_{zz}$ is the largest EFG tensor eigenvalue, $Q(^{69}\text{Ga}) = 17.1 \times 10^{-30} \text{ m}^2$ and $Q(^{71}\text{Ga}) = 10.7 \times 10^{-30} \text{ m}^2$ are the nuclear electric quadrupole moments of the two isotopes and h is the Planck's constant), which made the satellite transitions unobservable. The figure below shows the rotation patterns of the ⁶⁹Ga NMR central lines at $T = 300 \text{ K}$ around the [010] – the (a) panel, [010] – (b) and [001] – (c) crystal axes. A small nonzero value of the quadrupolar asymmetry parameter $\eta = 0.034$ in the GaPd₂ and $\eta = 0.030$ in the Ga₃Ni₂ as compared to $\eta = 0$ in the cubic GaPd means that the local charge distribution around the Ga site in the GaPd₂ is close to be axially symmetric, whereas it is fully axially symmetric in the GaPd. More advanced structurally examples of ²⁷Al-based complex phases like a high-entropy alloy and a decagonal quasicrystal will be discussed during the lecture as well [3, 4, 5].



References

- [1] M. Klanjšek et al., *J. Phys. Condens. Matter* 24 (2012) 085703
- [2] M. Wencka et al., *Intermetallics* 67 (2015) 35
- [3] M. Wencka et al., *Phys. Rev. B* 105 (2022) 174208
- [4] M. Wencka et al., *Scientific Reports* 12 (2022) 2271
- [5] M. Bobnar et al., *Phys. Rev. B* 85 (2012) 024205

LOOKING INTO POROUS MATERIALS WITH SOLID STATE NMR AND RELAXOMETRY

Lucia Calucci^a, Silvia Borsacchi^a, Elisa Della Latta^b, Marco Geppi^b, Francesca Martini^b, and Francesca Nardelli^a.

^a*Istituto di Chimica dei Composti Organometallici, Consiglio Nazionale delle Ricerche, Via G. Moruzzi 1, 56124 Pisa, Italy*

^b*Dipartimento di Chimica e Chimica Industriale, Università di Pisa, via G. Moruzzi 13, 56124 Pisa, Italy.*

Solid porous materials find widespread domestic and industrial applications, including construction and building, gas separation and storage, filtration and purification, ion exchange, energy storage, and heterogeneous catalysis. This class of materials encompasses fully inorganic or organic systems and organic/inorganic hybrid systems, with both crystalline and amorphous structure. The macroscopic behaviour of porous materials is strongly related to the structural and dynamic properties of their building units at molecular level, as well as to the interactions of the porous matrix with guest molecules.

Solid-state NMR (SSNMR) spectroscopy and NMR relaxometry represent very powerful techniques for characterizing microscopic properties over wide space and time scales and drawing structure-properties relationships in porous materials. Thanks to the possibility of exploiting many different NMR-active nuclei and a variety of nuclear observables, the application of NMR methods allows molecular and supramolecular structure and motions of specific moieties of the porous materials to be investigated. In addition, information can be acquired on the dynamics of gaseous or liquid guests hosted in the porous matrix, as well as on host-guest interactions.

In this lecture, the applicability of SSNMR spectroscopy and relaxometry experiments for looking inside porous materials will be discussed presenting several examples taken from the recent research work of the Pisa SSNMR group. In particular, the lecture will focus on structural properties and hydration of innovative cements characterized by multinuclear SSNMR [1,2] and ¹H relaxometry [3,4] and on structural and dynamic properties and host-guest interactions of metal organic frameworks (MOFs) [5] and polymers of intrinsic microporosity (PIMs) for CO₂ capture investigated by multinuclear SSNMR.

Acknowledgements

PRIN MUR (DOMINO project n. 2020P9KBKZ) is acknowledged for partially financing the research.

References

- [1] M. Tonelli, F. Martini, L. Calucci, E. Fratini, M. Geppi, F. Ridi, S. Borsacchi, P. Baglioni, *Dalton Trans.*, **2016**, 45, 3294.
- [2] F. Martini, M. Tonelli, E. Fratini, M. Geppi, F. Ridi, S. Borsacchi, L. Calucci, *Cem. Concr. Res.*, **2017**, 102, 60-67.
- [3] F. Martini, S. Borsacchi, M. Geppi, M. Tonelli, F. Ridi, L. Calucci, *Micropor. Mesopor. Mater.*, **2018**, 269, 26-30.
- [4] F. Martini, S. Borsacchi, M. Geppi, C. Forte, L. Calucci, *J. Phys. Chem. C* **2017**, 121, 26851–26859.
- [5] M. Cavallo, C. Atzori, M. Signorile, F. Costantino, D. Morelli Venturi, A. Koutsianos, K.A. Lomachenko, L. Calucci, F. Martini, A. Giovanelli, M. Geppi, V. Crocellà, M. Taddei, *J. Mater. Chem. A*, **2023**, 11, 5568.

FIELD-CYCLING NMR RELAXOMETRY OF PARAMAGNETIC-LABELED PROTEINS

Giacomo Parigi

*Magnetic Resonance Center (CERM), University of Florence, and CIRMMP, via Luigi
Sacconi 6, 50019 Sesto Fiorentino, Italy*

Field-cycling relaxometry can provide the nuclear longitudinal relaxation rates as a function of the applied magnetic field over 4 orders of magnitude. These measurements permit to have a direct access to spectral density functions, so that information on molecular structure and dynamics of macromolecules in solution can be obtained. ^1H relaxometry profiles are very useful for the characterization of paramagnetic molecules, especially in the field of the development of contrast agents for MRI.

The interaction of paramagnetic complexes with macromolecules present in biological systems can cause an increase of the paramagnetic relaxivity [1,2], which in turn increases the MRI contrast. The paramagnetic relaxivity is defined as the relaxation rate enhancement due to the presence of 1 mmol/dm³ concentration of the paramagnetic species. The strategy to reduce the risks associated with the administration of MRI gadolinium(III) contrast agents can pass through the use of complexes with higher efficiency, i.e. higher relaxivity, so that the injected dose can be sizably reduced. Molecular reorientation times in the nanosecond timescale are needed to achieve the highest efficiency at the fields of MRI scanners. This can be achieved by functionalizing low molecular weight gadolinium(III) complexes to bind noncovalently to macromolecules, by confining them within nanosized matrices, like nanogels, or by exploiting nanosized gadolinium(III)-based compounds.

The relaxivity profiles of Gd-labeled large protein assemblies, as the tetrameric protein asparaginase or the protein cages AaLS-13 and OP, show a remarkably high relaxivity at MRI fields, ca. five times higher than that of clinically used contrast agents. The analysis of the relaxivity profiles can shed light on the origin of the observed relaxivity enhancement, mainly ascribed to a correlation time modulating the proton-electron dipole-dipole interaction of few nanoseconds [3,4].

Hydrogel nanoparticles composed of chitosan and hyaluronan and incorporating Gd-complexes with different hydration number were also characterized through ^1H NMR relaxometry [5]. These nanoparticles exhibit enhanced relaxivity, over six times that of the free complexes, thanks to a restricted molecular dynamics and fast exchange of the metal-bound water molecule(s). Also the ^1H relaxivity profiles of Gd-HP-DO3A in crosslinked hyaluronic acid, used for monitoring the relaxation properties of contrast agents in tissues, show a modest interaction of the Gd(III) complex with the hydrogel and a slowed mobility of the water molecules [6].

References

- [1] Parigi et al. *Prog. NMR Spectrosc.* 2021, 124–125, 85.
- [2] Li et al. *J. Am. Chem. Soc.* 2019, 141, 6224.
- [3] Licciardi et al. *Bioconj. Chem.* 2022, 33, 2411.
- [4] Kaster et al. *ACS Appl. Bio Mater.* 2023, 6, 591.
- [5] Carniato et al. *ACS Appl. Bio Mater.* 2020, 3, 9065; *Inorg. Chem.* 2022, 61, 5380.
- [6] Fragai et al. *ChemPhysChem* 2019, 20, 2204.

NMR RELAXATION PROCESSES IN SOLUTIONS OF SUPERPARAMAGNETIC NANOPARTICLES

Danuta Kruk

*Department of Physics and Biophysics, University of Warmia and Mazury in Olsztyn,
Oczapowskiego 4, 10-719 Olsztyn, Poland.*

Superparamagnetic nanoparticles are considered as a novel solution for achieving high contrast in NMR imaging (MRI). The concept lies in exploiting the high magnetic moment of superparamagnetic nanoparticles that leads to very strong dipole-dipole interactions with magnetic moments of ^1H nuclei of surrounding water (solvent) molecules.

The mechanism of ^1H (generally, spin $\frac{1}{2}$) spin-lattice relaxation in solutions of superparamagnetic nanoparticles includes numerous factors that affect the relaxation rates. As already stated, the relaxation pathway is constituted by dipole-dipole interactions between the magnetic moment of the nanoparticle and the nucleus. The interactions fluctuate in time as a result of translation diffusion of the solvent molecules. One should, however, also consider the possibility that the solvent molecules (typically water) form a layer (hydration shell) around the nanoparticle staying attached to it for a time comparable (or longer) to the rotational correlation time of the nanoparticles. In such a case there are also exchange processes between the bound and the “free” fractions of the solvent molecules. As far as the magnetic moment of the nanoparticle is concerned, it has two components: a mean (average) part which is parallel (longitudinal) to the external magnetic field and does not fluctuate in time, and a component that fluctuates around this average value. Both components depend on the applied magnetic field. The mean component increases, according to the Langevin function, from zero towards a saturation value at high fields [1,2]. As the mean component grows the fluctuating part of the longitudinal magnetic component gets lower, i.e. it reaches maximum at zero field and decreases towards zero with increasing the magnetic field. In consequence, the measured ^1H relaxation rate is a sum of two relaxation contributions. The first contribution is associated with the mean component of the magnetic moment and is referred to as Curie relaxation [3] and dominates at higher magnetic fields. The second one, associated with the fluctuating component of the nanoparticle magnetization is responsible for the low field relaxation [3,4]. The relaxation scenario will be explained and illustrated by experimental examples.

Acknowledgements

The work was supported by National Science Centre, Poland, project number: UMO-2018/31/B/ST5/03605.

References

- [1] Gillis, P ; Roch, A ; Brooks, R A (1999) J. Magn. Reson., 137 (2),: 402, 407
- [2] Muller R. N., Vander E. L., Roch A., Peters J. A., Csajbok E., Gillis P., Gossuin Y. (2005) Adv. Inorg. Chem. 57, 239
- [3] Roch A., Muller R.N., Gillis P. (1999) J. Chem. Phys. 110, 5403.
- [4] Roch A., Gillis P., Ouakssim A., Muller R.N. J. Magn.and Magn. Mat. 201, 77

ANALYSIS OF STRONGLY DIPOLAR COUPLED SOLIDS BY TIME-DOMAIN NMR

Leonid Grunin, Maria Ivanova

^aResonance Systems GmbH, 28 Seestrasse, Kirchheim unter Teck, Baden-Wuerttemberg, 73230, Germany

Transverse relaxation in rigid-state materials below glass-transition temperature happens to be exponential in very rare cases, mostly showing up complex shape that many authors try to fit within a mixture of Gaussian, Abrahamian, Pake and Lorentzian lines, though for the majority of samples even such variative models do not work perfectly.

The approach to characterize structures and dynamics of solids that involves moments of spectral lines is becoming more adequate and promising because the moments can be directly calculated using integration of FFT spectrum and not rely on ambiguous multi-component approximation of the TD-NMR Free Induction Decay (FID).

On the other hand, the huge community of scientists in applied areas where TD-NMR is considered as only one of the measuring tools are educated in the way of simple relaxation times approach and the use of second moments M_2 expressed in squared Tesla occurs far less convenient and demonstrative than the T_2 in microseconds.

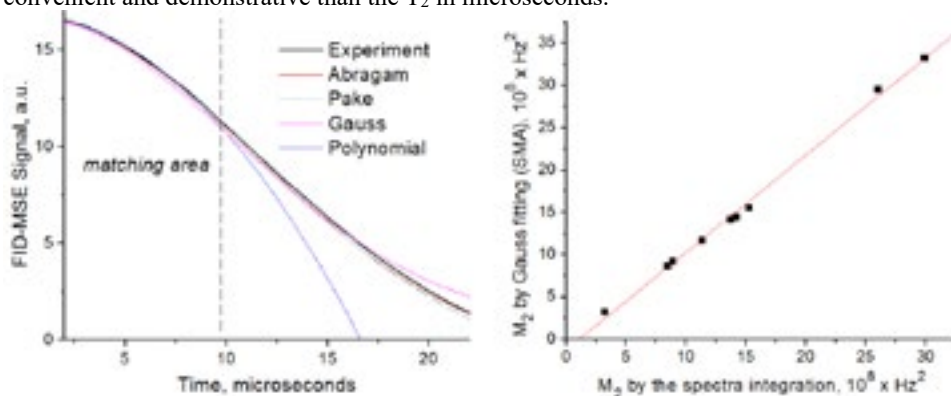


FIGURE 1. The idea of the Second Moment Approximation (SMA) applied to processing of Starch samples

The contribution pretends to bring up the way to recalculate second moments corresponding to various line shapes into timely parameter T_2^{**} with minimal distortion of information about structure of solid-state materials.

Besides the FID analysis we are discussing the use of the residual dipolar constant, acquired via Double Quantum Build-up Curve experiment for the additional insights at solids structure.

Acknowledgements

This work was partially funded from the European Union's Horizon 2020 Research and Innovation programme – MSCA-RISE under grant agreement No 101008228.

CHEMICAL EXCHANGE RATE STUDIED BY NMR CPMG METHOD

Janez Stepišnik and Aleš Mohorič

Faculty of mathematics and physics, University of Ljubljana, Slovenia

Various nuclear magnetic resonance method, which manipulate the spin dynamic of atomic nuclei in order to convey information about their environment i.e. the structure and dynamics in matter, are used in chemistry, physics, material science, biology, and medicine. Particularly useful NMR method for the study of the molecular dynamics is the Carr-Purcell-Meiboom-Gill sequence (CPMG)[1] with a train of π -radiofrequency pulses, which was originally introduced to provide reliable spin measurements relaxation, but later on it turned out that it in combination with an inhomogeneous magnetic field provides the direct insight into the spectrum of the molecular velocity auto-correlation[3,4], which is the key dynamic quantity of molecular translation motion. It is less known that by using CPMG sequences we can also obtain detailed information about the fluctuation of molecular electronic orbitals, which are the result of chemical processes such as also chemical exchange[2].

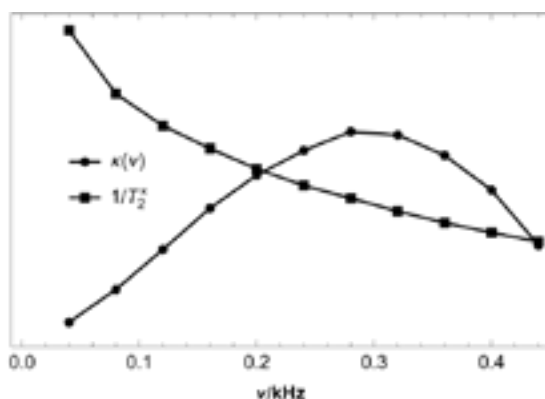


FIGURE 1. Spectrum of chemical exchange rate $\kappa(\nu)$ in aqueous sugar solutions obtained from the effective relaxation decay $1/T_2^*$ measured by the CPMG method

We will show, that with the CPMG measurements of liquids[5] in which there is a processes, such as chemical exchange, the decline of the peak of the spin echo is directly proportional to the value of the spectrum of the exchange rate at the value of the spin phase modulation frequency, which is determined by the frequency of π pulses. The method not provide just chemical exchange spectrum between only two molecular conformations, but it could result from several exchanges effecting the molecular conformation.

References

- [1] Carr, H.Y., Purcell, E.M. Phys. Rev. 94 (1954), 630–38,.
- [2] McConnell, H.M., J. Chem. Phys., 28 (1958), 430–431.
- [3] Stepišnik J., Physica 104B (1981) 350- 361.
- [4] Callaghan P.T., Stepišnik, J. Advances in Magnetic and Optical Resonance, ed. Warren S. Warren, Vol. 19, (1996), , pp. 326–89.
- [5] Stepišnik J., Mattea C., Stapf S., Mohorič A., Physica A 553 (2020) 124171.

ASSESSING THE MOLECULAR DYNAMICS IN PARAMAGNETIC LIQUID SYSTEMS

Maria J. Beira^{a,b} and Pedro J. Sebastião^{a,b}.

^a*Center of Physics and Engineering of Advanced Materials, Instituto Superior Técnico, Universidade de Lisboa, Av. Rovisco Pais, 1049-001 Lisbon, Portugal*

^b*Department of Physics, Instituto Superior Técnico, Universidade de Lisboa, Av. Rovisco Pais, 1049-001 Lisbon, Portugal*

NMR relaxometry is a widely used experimental technique that enables the study of dynamical processes ranging from fast internal molecular rotations to slower aggregate motions. This technique is particularly sensitive to the presence of paramagnetic species, such as iron, gadolinium, manganese and cobalt, just to name a few. In Figure 1 it is possible to observe the highlighted paramagnetic relaxation enhancement induced by the presence of around 1mM of gadolinium in a phosphonium-based ionic liquid system.

Paramagnetic relaxation can be induced by a temporary binding to the paramagnetic center (inner-sphere, IS) or by translational diffusion in its vicinity (outer-sphere, OS). The deconvolution of these two processes is non-trivial and generally requires one to perform multiple experiments, such as analyzing systems with different solvent proportions[1], varying the paramagnetic species concentration or varying the temperature at which the experiments are performed.

In the present work we achieve a consistent analysis of ionic liquid- and PEG-based paramagnetic systems, relying on the simultaneous analysis of data obtained for different temperatures and concentration of magnetic particles. Moreover, we show that the spin-spin relaxation time, T_2 , might be a more efficient alternative to discriminate between IS and OS paramagnetic relaxation. Finally, the subtly significant influence of metal impurities is also evidenced in the PEG-based systems.

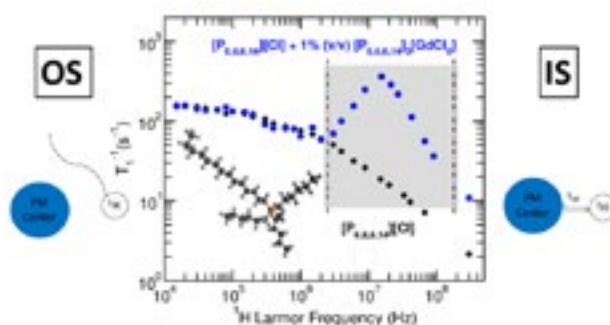


FIGURE 1. Gadolinium-induced paramagnetic relaxation enhancement in ionic liquid systems

Acknowledgements

M.J.B. acknowledges the PhD scholarships granted by the portuguese foundation for science and technology (PD/BD/142858/2018 and COVID/BD/152743/2022)

References

[1] Rui Cordeiro *et al.*, *Int. J. Mol. Sci.* 2021, **22**, 706

IONIC-LIQUID BASED HYBRID GEL POLYMER ELECTROLYTES AS SEEN BY NMR

Claudia Schmidt

Paderborn University, Department of Chemistry, 33098 Paderborn, Germany

Gel polymer electrolytes (GPEs) combine the advantages of liquid and solid electrolytes. They exhibit both high ion conductivity, similar to liquids, and the mechanical stability and high safety of solids, which makes them ideal candidates energy storage applications. Since GPCs are multicomponent systems, they exhibit quite complex behavior that can be studied at the molecular level by a variety of NMR methods using different nuclei. In this lecture, an introduction to NMR investigations of GPEs will be provided, focusing on our studies of GPEs based on the random copolymer poly(vinylidene fluoride co-hexafluoropropylene) (PVdF-HFP) swollen with electrolyte solutions (ES) of salt in an ionic liquid (IL) and containing inorganic fillers, making them hybrid organic/inorganic materials. The fillers are added to optimize conductivity [1] or electromagnetic shielding [2]. Figure 1 shows examples of diffusion coefficients and line shapes, reflecting molecular mobilities.

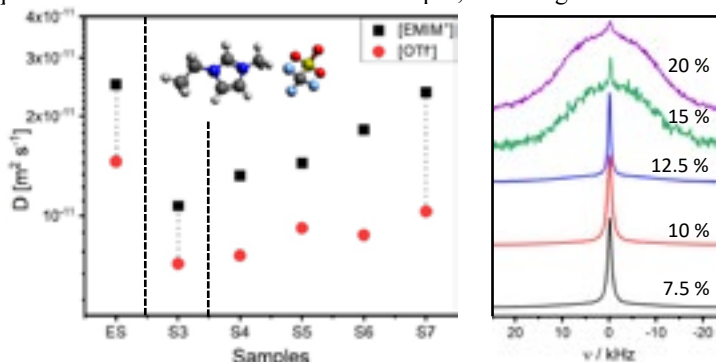


FIGURE 1. (a) Diffusion constants obtained from ^1H and ^{19}F measurements of the IL [EMIM][OTf] in the system PVdF-HFP/SiO₂/ES, where ES is the electrolyte solution of LiOTf in the IL, and S3 to S7 are GPE samples (S3: 65 % ES, no SiO₂; S4 to S7: 50, 55, 60, and 65 % ES, respectively, with SiO₂) [1]. (b) Static ^7Li spectra of the system PVdF-HFP/BaTiO₃/ES, where ES is LiBF₄ in [EMIM][BF₄], containing different mass fractions of BaTiO₃ [2].

Acknowledgements

The work by the (former) students and postdocs in my group, Dr. W. Keil, R. Duo, M. Beerbaum, S. Lansab, M. Siebrecht, Y. Zhao, and Dr. A. Ordikhani-Seyedlar, is gratefully acknowledged. Thanks go to Prof. A. Chandra (University of Delhi) and her former Ph.D. students, Dr. M. Kumar Vyas and Dr. S. Khurana, who provided most of the materials, to Dr. M. Dvoyashkin (University of Leipzig) for diffusion measurements, to Dr. R. Graf (Max-Planck-Institute for Polymer Research) for stimulating discussions, and to the Alexander von Humboldt Foundation for funding the Delhi-Paderborn research linkage.

References

- [1] Shilpa Khurana and Amita Chandra, *Solid State Ionics* 340, 115027 (2019).
- [2] Manoj Kumar Vyas and Amita Chandra, *J. Mater. Sci.* 54, 1304 (2019).

CHALLENGES OF NON-EXPONENTIAL NMR RELAXATION PROCESS

Adriane Consuelo Leal Auccaise, Elzbieta Masiewicz and Danuta Kruk

Department of Physics and Biophysics, University of Warmia and Mazury in Olsztyn, Oczapowskiego 4, 10-719 Olsztyn, Poland.

NMR relaxation processes give insight into molecular motion. In NMR experiments one monitors time evolution of magnetization (^1H , ^{19}F , *etc.*) The non-exponentiality can result from two sources: dynamical heterogeneity of the system or/and the quantum-mechanical framework of the relaxation process. It is well-known that even a very simple spin system, like two non-equivalent $\frac{1}{2}$ spins (such as ^1H , ^{19}F or ^1H , ^{13}C) exhibit, in principle, bi-exponential relaxation (and, hence, bi-exponential evolution of magnetization) as a result of joint spin transitions (cross-relaxation) caused by mutual dipole-dipole interactions [1-3]. However, to experimentally observe a bi-exponential magnetization evolution, two conditions must be met: the first one is a significant difference (let us say at least by an order of magnitude) between the relaxation rates, while the second one is comparable contributions of both relaxation components in terms of their amplitudes. The effect depends on several factors, such as: the magnetic field, the difference in the gyromagnetic factors of the participating spins, the amplitude of the dipole-dipole coupling, the time scale and the mechanism of the molecular motion— as shown in Fig.1. The non-exponentiality of relaxation processes will be discussed in detail and illustrated by experimental examples.

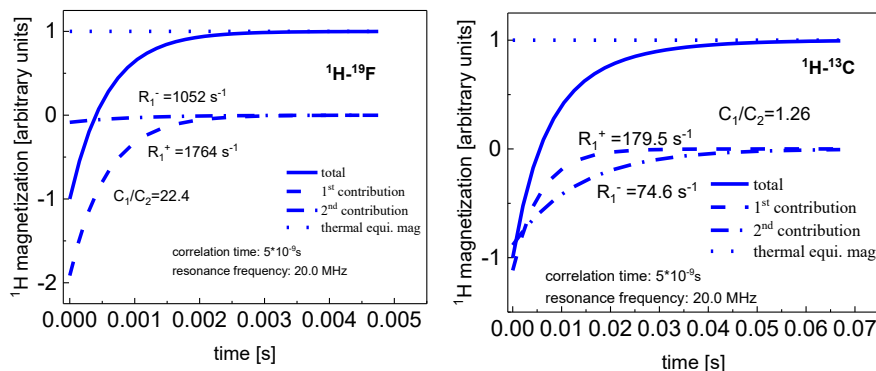


FIGURE 1. . Examples of bi-exponential magnetization evolution.

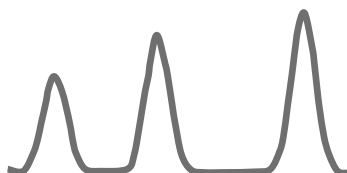
Acknowledgement

This research has received funding from the European Union's Horizon 2020 research and innovation program under grant agreement No 899683 (project "HIRES-MULTIDYN").

References

- [1] Kruk, D. *Understanding spin dynamics*; Pan Stanford Publishing: Singapore, 2015.
- [2] D. Kruk and M. Florek-Wojciechowska. Recent development in ^1H NMR relaxometry. *Annual Reports on NMR Spectroscopy*, 99, 119-184, 2020.
- [3] A. Consuelo-Leal, H.D.F. Sare, and R. Auccaise. Relaxation dynamics of an unlike spin pair system. arXiv.2212.08747.

ON-LINE LABORATORY TRAININGS



AMPERE NMR School

JASON workshop: practical aspects

Adolfo Botana^a and Peter Kiraly^b

^aJEOL UK Ltd, Silver Court, Watchmead, Welwyn Garden City AL7 1LT

^bJEOL UK Ltd, 4 Bankside, Long Hanborough, Witney OX29 8LJ

JASON is a new vendor agnostic analytical software with special emphasis on the automatic processing, analysis and reporting of NMR data [1]. In particular, JASON features a large work space, "Canvas," where 1D NMR, 2D NMR, and chemical structures are interlinked to support structural analysis. In this workshop we will present an overview of the software and how it can be used for structure verification and generation of reports. To fully benefit from this workshop it is recommended to bring a laptop with the software already installed.



FIGURE 1. Overview of JASON capabilities

References

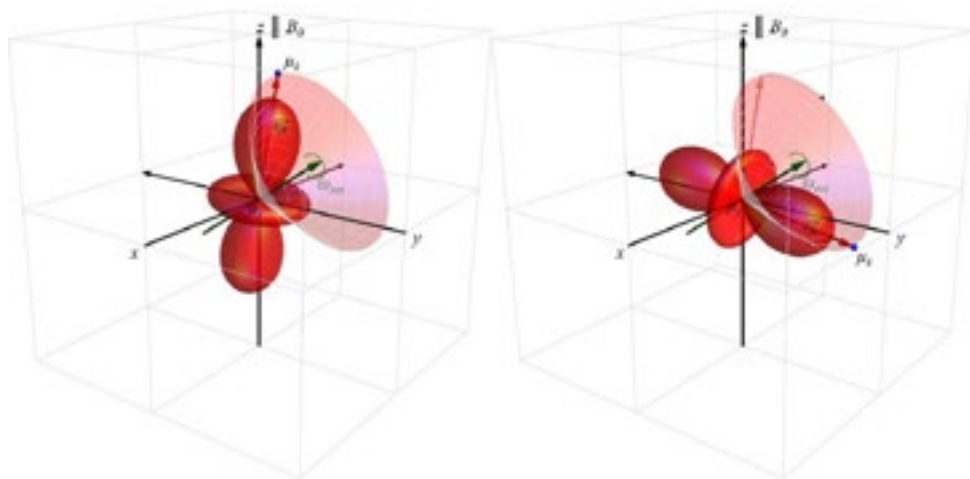
- [1] JASON <https://jeoljason.com/>

MAGIC ANGLE

Jacek Jenczyk

*NanoBioMedical Centre, Adam Mickiewicz University,
Wszchnicy Piasteowskiej 3, 61-614 Poznań, Poland*

There are number of exceptional examples indicating the unique position of tetrahedral symmetry in the vast landscape of different spatial organization pathways which can be sampled by matter. Very often the tetrahedral angle remains an intrinsic feature of the system or emerges spontaneously due to interactions. Quite remarkably, the same angle reappears in fundamental spin interactions i.e. the dipolar coupling between a pair of polarized spins (magnetic moments) vanishes when the inter-spin vector is tilted one half of the tetrahedral angle with respect to the polarization field direction. This specific condition is known as the magic angle in the NMR community and the effect is directly related to the inherent symmetry of a magnetic field generated by an isolated magnetic moment. Developed conceptually in the 1950s [1, 2] Magic Angle Spinning (MAS) has become a routine technique in solid state NMR spectroscopy. This unique concept, together with the exceptional progress made in the field of NMR probe engineering, has made possible the acquisition of high resolution spectra for a rigid phase samples. General idea regarding spin interactions under MAS conditions can be demanding to comprehend due to an experimentally introduced time evolution of the spin system and its anisotropic character of interactions. In order to thoroughly understand the concept of a MAS experiment it is vital to first describe the structure of coupling tensors and their subsequent orientational evolution during NMR experiments.



References

1. Andrew ER, Bradbury A, Eades RG. Nuclear Magnetic Resonance Spectra from a Crystal rotated at High Speed. *Nature* 1958;182:1659-1659.
2. Lowe IJ. Free Induction Decays of Rotating Solids. *Physical Review Letters* 1959;2:285-287.

FFC-NMR TUTORIAL

Elżbieta Masiewicz

*Department of Physics and Biophysics, University of Warmia and Mazury in Olsztyn,
Oczapowskiego 4, 10-719 Olsztyn, Poland, e-mail: elzbieta.masiewicz@uwm.edu.pl*

One of the fundamental topics of molecular science is to learn dynamical properties of biomolecules. Nuclear Magnetic Resonance (NMR) methods, especially FFC-NMR relaxation studies, give a deep insight into the dynamics of biomolecular systems i.e. tumbling-like motion, translation diffusion and internal dynamics. In FFC-NMR relaxation experiments at low frequencies (magnetic fields) one probes slow molecular motions in the scale of microseconds, while with increasing the frequency progressively faster dynamics up to nanoseconds are detected. The FFC-NMR relaxation studies stems as an extremely valuable source of information about the dynamics of biomolecules, nevertheless, they pose several challenges from the experimental as well as theoretical point of view.

In this context, the FFC-NMR tutorial will be divided into three parts: First, some general introduction to the Fast Field Cycling technique will be provided, along with the theory of basic pulse sequences and essential knowledge for setting of proper parameters to start an experiment. Next, step by step a simple FFC experiment will be performed remotely using one of the FFC-NMR Relaxometers (Stelar s.r.l.), located at the University of Warmia and Mazury in Olsztyn laboratory, including practical advice for beginner users. In other words, the tutorial Participants will simply learn “How to get started with the FFC-NMR measurements” - i.e. sample preparation, sample tuning, choosing the right sequence (depending on the type of sample), setting proper parameters, acquiring and evaluating FFC data. In the last part of the tutorial, some theoretical aspects of data analysis will be presented.

MRI: BASIC PRINCIPLES AND APPLICATION

Tomasz Zalewski and Marek Kempka

*NanoBioMedical Centre, Adam Mickiewicz University, Poznań, Poland
Wszechnicy Piastowskiej 3, 61-614 Poznań, Poland*

The tutorial aims to introduce the basics of the NMR phenomena and procedures in the MRI lab. Classes will be divided into two parts. In the first part, some basic information about NMR and MRI will be provided, and in the next step will be shown the preparation of an MRI research scanner, ie. tuning coil, and magnetic field shimming. Moreover, 1D NMR experiments will be carried out.

The second part will show the basic experiments using Fourier imaging methods with the introduction of the spin echo imaging technique. The building of k-space during MRI experiments will be shown, to highlight the significance of Fourier transform in Magnetic Resonance Imaging. Finally, the images for the object with a well-defined structure will be obtained with spin echo and gradient echo techniques.

The tutorial will be carried out with the use of ICT technology and remote access to an MRI scanner at NanoBioMedical Centre in Poznan.

NMR DIFFUSION

Michał Bielejewski

*Institute of Molecular Physics, Polish Academy of Sciences
Smoluchowskiego 17, 60-179 Poznań, Poland*

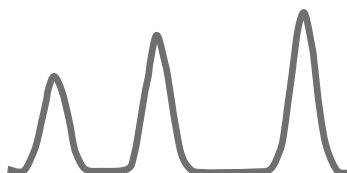
The word **diffusion** derives from the Latin word *diffundere*, which means "to spread out".

In the most general case, diffusion is a phenomenon that refers to the net movement of an object driven by a gradient of some magnitude factor. The process has a stochastic nature, and its concept plays an important role in many areas of physics, chemistry, biology, sociology, economics, and finance, constituting a broad field for research. In natural sciences, diffusion is not limited to a given state of matter but can occur in solids, liquids, and gases. It conditions the life processes by determining the transport through membranes, cells eventually, the whole body. In chemical processes, it is often the central rule driving many reactions. In physics, it defines many transport processes for atoms, ions, or molecules. A distinguishing feature of diffusion is that it depends on particle random walk and results in mixing or mass transport without requiring directed bulk motion. The first description of the diffusion phenomena was given by Adolf Fick in 1855. Fick's laws can be used to solve for the diffusion coefficient, ***D***. A diffusion process that obeys Fick's laws is called *normal* or *Fickian diffusion*. On the other hand, it is called anomalous diffusion or non-Fickian diffusion if the process does not follow these laws. This tutorial aims to give an overview of the wide range of applications of diffusion NMR and principles of NMR diffusometry methods that allow insight, for example, for accurate molecular size determination, in nanomedicine drug delivery, or separation of complex mixtures. The tutorial will be carried out with the assistance of dr hab Kosma Szutkowski from the NanoBioMedical Centre in Poznan and remote access to an NMR spectrometer at the NanoBioMedical Centre in Poznan.



PARTICIPANTS

POSTERS



AMPERE NMR School

Insights into Gelation Mechanisms and Gel Properties of LMWG/PC: A Comparative Study using DSC/TGA, NMR, and Confocal Fluorescence Microscopy

Farooq Ahmad^a, Natalia Bielejewska, Michał Bielejewski^a

^a*Institute of Molecular Physics Polish Academy of Sciences, Smoluchowskiego 17, 60-179
Poznań*

ABSTRACT

In this study, we present the LMWG, also referred to as a candidate for the gel-electrolytes functional material that exhibits promising potential for utilization in various electrochemical applications. Acquiring an understanding of the distinct properties exhibited by LMWG at the Sol-gel phase is crucial for analyzing and predicting the features they offer. The current investigation presents a comparative analysis including thermal analysis (DSC/TGA), intermolecular interactions (NMR spectroscopy), and microstructure elucidation (Confocal Fluorescence Microscopy) of a physical gel based on a low molecular weight gelator, specifically cyclo (L- β -2-ethylhexylasparaginyL-L-phenylalanine)2-ethylhexyl 2-((2S,5S)-5-benzyl-3, 6-dioxopiperazin-2-yl) acetate and solution of propylene carbonate. A physical gel's molecular structure, dynamics, and interactions were analyzed through NMR. The DSC/TGA technique provided us with the thermal characteristics of the gel. Optical polarization microscopy was employed to examine the internal microstructure of the gel. The studies were performed on an LMWG-based Gel using a propylene carbonate solvent.

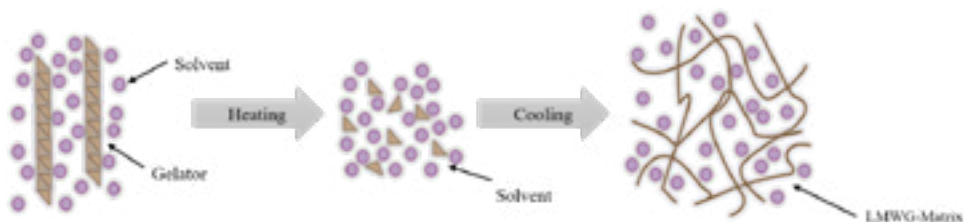


FIGURE 1. The preparation route of LMWG-based gel through the physical method

Acknowledgments

This work was supported by the National Science Centre, Poland [grant number 2021/43/O/ST5/01911].

Magnetic resonance imaging of hydrocarbon gas at various pressures

M. Anikeeva^a, A. N. Pravdivtsev^a, E. Peschke^a, and J-B. Hövener^a

^a *Section Biomedical Imaging, Molecular Imaging North Competence Center (MOIN CC), Kiel University, Am Botanischen Garten 14, 24118, Kiel, Germany*

Thermal reactions using heated gases are the driving force behind industrial production processes. However, a lack of understanding regarding the distribution of gas flow within reactors hampers the optimization of these chemical processes. We are proposing using magnetic resonance imaging (MRI) to visualize the gas flows inside the reaction chambers. In the current work, we study thermally polarized hydrocarbon gas, ethane, under slightly elevated pressures (1.5 – 6 bar) and evaluate their relaxation parameters and assess their utility for rapid imaging.

MRI experiments were done on a 7 T pre-clinical MRI (BioSpec, Bruker), using a ¹H transmit-receive quadrature volume resonator (86 mm diameter, Bruker). We used a 75 mL borosilicate flask (Synthware) filled with ethane (C₂H₆, 99.95% purity, Linde plc) as a phantom of the reactor. The longitudinal relaxation time constant, T₁, and the transverse relaxation time, T₂, of ethane were measured at various pressures in the range of 1.5 – 6 bar using an inversion recovery (IR) and a Carr-Purcell-Meiboom-Gill (CPMG) pulses sequences with a very short constant echo spacing of 2 τ = 600 μs (Figure 1 (a, insert)), respectively. Based on the measured relaxation times (Figure 1 (a)), we adjusted the MRI sequence parameters and acquired images of ethane using a fast low angle shot (FLASH), and a rapid acquisition with relaxation enhancement (RARE) (Figure 1 (c)) sequences. The SNR of sequences was maximised by taking into account dependence of relaxation on pressure. Each image was acquired within 100 s only with an signal to noise ratio (SNR) between 140 and 190 for FLASH and 170 – 280 for RARE pulse sequence. The experimental data were compared to the values of the gas-phase SNR expected for the corresponding pressures (Figure 1 (d)). Thus, we show the feasibility of fast imaging of gases within the reaction chamber.

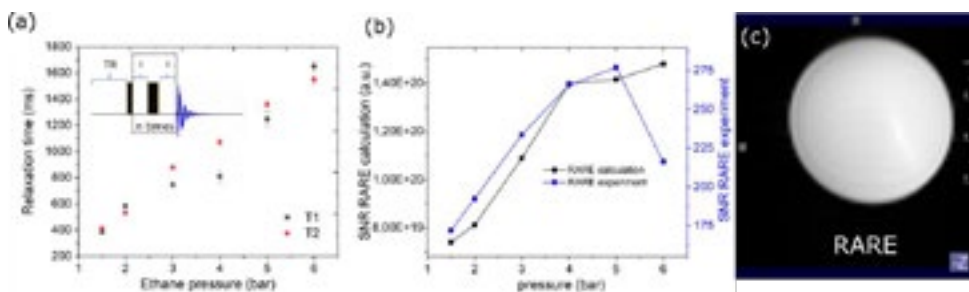


FIGURE 1. (a) Summary of of ethane longitudinal and transverse relaxation times measured in IR and CPMG with $\tau = 0.3$ ms (insert) experiments at different pressures. (b) Comparison of the calculated (black dots) and experimental (blue dots) SNR values for RARE imaging. (c) Axial RARE image of the flask filled with 4 bar ethane (slice thickness 80 mm, resolution 0.906 mm x 0.906 mm, TE = 15.36, RARE factor = 2, TR = 1.6 s, 2 averages, bandwidth = 5 kHz).

Acknowledgements

Sonderforschungsbereich/Transregio 287 BULK-REACTION (Projekt-ID 422037413) der Deutschen Forschungsgemeinschaft (DFG)

Synthesis of novel tracers for deuterium magnetic resonance imaging

Fatima Anum^a, Arne Brahms^b, Philip Saul^b, Maria Anikeeva^a, Rainer Herges^b,
Jan-Bernd Hövener^a, Andrey N. Pravdivtsev^a,

^aUniversity Medical Center Schleswig-Holstein, Kiel University, Department of Radiology and Neuroradiology, Section Biomedical Imaging, Molecular Imaging North Competence Center (MOIN CC), Am Botanischen Garten 14, 24118 Kiel Continue Here

^bOtto Diels Institute for Organic Chemistry, Kiel University, Otto-Hahn Platz 4, 24118 Kiel, Germany

Deuterium magnetic resonance imaging (DMI) is a non-invasive technique capable of generating high-resolution metabolic maps. This study explores the potential of deuterium-labeled DMI tracers for in vivo diagnostics and treatment monitoring. We present a novel deuterium based pH sensor for MRI, deuterium-labeled zymonic acid (ZA)-d₄.

Protonated ZA was synthesized from sodium pyruvate (Pyr) and its pH sensitivity was evaluated. Pyr (0.1-0.2 M) was dissolved in water and maintained at a pH of 12 for two days. Acidification with HCl (pH ~1) was followed by water removal using a freeze dryer. The resulting crude ZA was diluted in acetone, filtered to eliminate NaCl, and purified using flash column chromatography with a Biotage SNAP Ultra C18 60g column and a 2-10% acetonitrile linear gradient. The purified ZA was freeze-dried, yielding a dark yellow viscous mass with an experimental yield of 50.8%.

pH-dependent changes in the chemical shifts of CH and CH₃ resonances of ZA were investigated using ¹H NMR analysis at varying pH values (2-3, 6-8). Two pK_a values, 1.5±0.7 and 7.06±0.02, were confirmed. This chemical shift variation is planned to be utilized for pH mapping with DMI. Future steps involve synthesizing deuterated ZA and acquiring corresponding DMI pH maps.

In conclusion, deuterium-labeled zymonic acid (ZA)-d₄ shows promise as a pH sensor for MRI, with its pH-dependent chemical shifts opening a new avenues for non-invasive in vivo diagnostics and treatment monitoring.

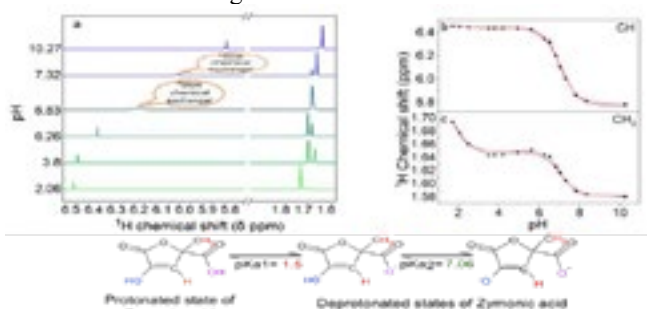


FIGURE 1: ¹H NMR spectra of ZA (a) and chemical shifts (b,c) as a function of pH. This experiment was conducted in 9.4 T at 290 K using 1:10 of H₂O:D₂O 49.64 mM ZA solution. Chemical shift variation of CH and CH₃ protons revealed to pH sensitive areas near pK_a values of ~1.5 and 7.06.

Acknowledgements: We acknowledge funding from BMBF (01ZX1915C), DFG (PR 1868/3-1, HO-4604/2-2, HO-4604/3, GRK2154-2019, FOR5042, SFB1479, TRR287, HO 4604/3-1), Cluster of Excellence (EXC 2167), European Regional Development Fund (ERDF) and the Zukunftsprogramm Wirtschaft of Schleswig-Holstein (Project no. 122-09-053) and intramural CAU funding.

INSIGHTS TO NMR RELAXATION AND SUSCEPTIBILITY REPRESENTATION

Ruben Auccaise^a, Adriane Consuelo Leal Auccaise^a and Danuta Kruk^b

^a*Department of Physics, State University of Ponta Grossa, Av. General Carlos Cavalcanti 4748, CEP 84030-900 Ponta Grossa, Paraná, Brazil.*

^b*Department of Physics and Biophysics, University of Warmia and Mazury in Olsztyn, Oczapowskiego 4, 10-719 Olsztyn, Poland.*

Nuclear Magnetic Resonance Relaxation is a powerful experimental tool to study a spin particle's system interacting with its surroundings. Behind the experimental technique's success, there is a theoretical background well established, such as the Redfield master equation, which is one of the main formal backgrounds used to decode information from an environment monitoring the spin particle system. Consequently, applying the Redfield master equation, the magnetization dynamics is non-exponential for some heteronuclear cases. The highlighted dynamics are less frequent in experimental implementations, often mixed or overlapped with the mono-exponential relaxation evolution of the magnetization. Therefore, it is interesting to establish some procedures to identify the non-exponential signature from the magnetization evolutions. In this study, we considered that the magnetization time evolutions are well known, such that the relaxation rates can be computed and established, showing the characteristic dependence of the spectral density functions, which allows us to figure out the most suitable kinds of molecular motion. Together with the relaxation rates, there are the susceptibility functions. It is a physical definition that will help us find some insights about the non-exponential relaxation and the regimes in which the non-exponential signature could, or not, be more evident.

In this discussion, we explored the relaxation rates of a heteronuclear spin system generated from a theoretical development found in Ref. [1,2]. Next, we applied the definition of susceptibility function $\chi = \omega R_1$, where ω is the angular frequency and R_1 is the relaxation rate. The susceptibility function was analyzed at different angular frequency regimes and using the spectral density function of the force-free hard-sphere model [1]. Those results were compared with susceptibility functions considering the mono-exponential relaxation, and the differences were highlighted.

References

- [1] D. Kruk and M. Florek-Wojciechowska. Recent development in ¹H NMR relaxometry. Annual Reports on NMR Spectroscopy, 99, 119-184, 2020.
- [2] A. Consuelo-Leal, H.D.F. Sare, and R. Auccaise. Relaxation dynamics of an unlike spin pair system. arXiv.2212.08747.

SYNTHESIS AND CHARACTERIZATION OF Gd-BASED DENDRITIC POLYMERS AS A POTENTIAL CONTRAST AGENT

Nataliya Babayevska, Katarzyna Fiedorowicz, Jacek Jenczyk

*NanoBioMedical Centre, Adam Mickiewicz University,
ul. Wszechnicy Piastowskiej 3, 61-614 Poznań, Poland*

As new multifunctional materials, dendritic hyperbranched polymers have drawn much attention because of their unique fluorescence properties, perfect mechanical toughness, and good chemical stability. These features allow to use it in the fields of photoluminescence, electroluminescence, optics, lasers, and solar–energy conversion systems [1,2]. Due to high water solubility and low toxicity, dendrimers have emerged as one of the most promising nanocarrier systems for biomedical applications, especially for drug delivery or medical imaging. Among rare earth elements gadolinium Gd due to the 7 unpaired electrons in its 4f subshell is a well-known MRI/NIR dual-modality imaging agent due to their high r_1 relaxation and paramagnetism [3]. At the same time, Gd is a well-known green-emission phosphor ($\lambda_{lum.}$ at 545 nm) and can be used as a biomarker for the detection of cancer cells.

The present study focused on the synthesis of Gd-based dendritic hyperbranched polymers, *in vitro* biocompatibility evaluation for potential use in magnetic resonance imaging contrast agents.

The binding of Gd^{3+} ions to the dendrimer complex was confirmed by photoluminescence, FT-IR, and NMR spectroscopies. The complexes show characteristic photoluminescence peaks in the visible green region - emission characteristic of gadolinium. FT-IR spectroscopies confirmed that the carboxyl group of the dendrimer is coordinated with the Gd ions. Results from NMR measurements showed, that Gd ions may reside within terminal, dendritic regions and thus lead to vanishing of NMR signals characterized by higher chemical shift values. Cytotoxicity studies showed that Gd-based dendrimers do not have a significant negative effect on human cardiomyocyte cell line up to the highest concentration tested - 100 $\mu g/ml$.

Acknowledgment

The authors gratefully acknowledge the financial support by the WPC2/nanoHEART/2021 project.

- [1]. B. Gao, L. Fang, R. Zhang, J. Men. *Synthetic Metals*, 2012, 162(5), 503-510.
- [2] D. Liu, Z. Wang, H. Yu, J. You. *Eur. Polym. J.*, 2009, 45(8), 2260-2268.
- [3] P. Chandrasekharan, C.-X. Yong, Z. Poh et al., *Biomaterials*, 2012, 33, 9225-9231.

Fast pKa determination for lead optimisation Application of Chemical Shift Imaging and Chemical Gradients into Analysis of APIs

K. Baj;^a A. Hindle;^b S.H. Marsden;^b J. Brammer;^a S. Demanze;^c M. Wallace;^d
J.A. Iggo^a

^a Department of Chemistry, University of Liverpool, L69 7ZDD, United Kingdom

^b School of Chemistry, University of Leeds, LS2 9JT, United Kingdom

^c Oncology R&D, AstraZeneca, Cambridge, CB4 0WG, United Kingdom

^d School of Pharmacy, University of East Anglia, NR4 7TJ, United Kingdom

¹H Chemical Shift Imaging [1] with a chemical gradient (CSI-CG) provides an efficient, one-shot method for the determination of pKa, using little analyte [2]. The technique can be readily used in DMSO-d₆ [3] and has been used to analyse basicity patterns in a homologous series of bridged anilines. Density-Functional Theory (DFT) geometry optimisation and charge distribution calculations have been used to rationalise the results [4,5].

We have developed mixed solvent water-DMSO pH indicator ladders. That allows the determination of pKa in any water-DMSO ratio in a single-shot experiment and the reduction in the number of experiments required to extrapolate mixed-solvent pKa determinations to an aqueous value. As a result, we can successfully extrapolate to an aqueous pKa regardless of solvation effects on the analyte with a precision greater than that offered by computational methods.

Several pulse sequences for water suppression have been evaluated, and automation routines developed to allow the use of sample changers for high throughput of data acquisition in an industrial setting [3]. Water signals are suppressed using excitation sculpting, while pre-saturation can be used to suppress a second solvent peak if required, Figure 1.

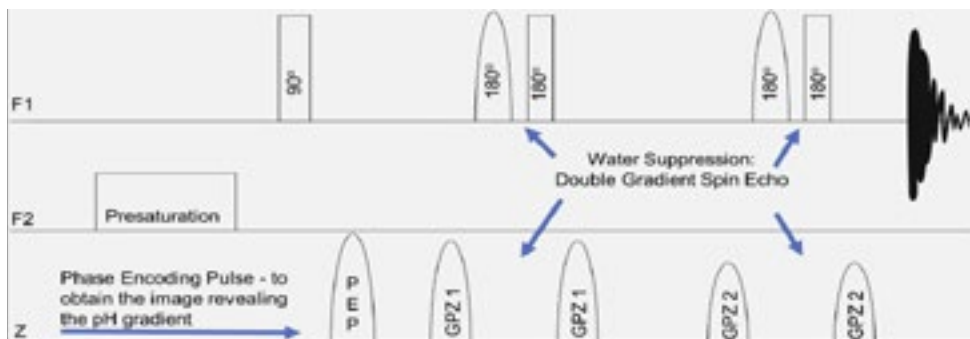


Figure 1. Pulse sequence for double solvent suppression ¹H Chemical Shift Imaging.

References

- [1] P. Trigo-Mourino et al., Chem. – Eur. J. 2013, 19, 7013-7019.
- [2] M. Wallace et al., Anal. Chem., 2018, 90, 4160-4166.
- [3] G. Schenck et al., Anal. Chem., 2022, 94, 23, 8115–8119
- [4] D. Bochevarov et al., Int. J. Quantum Chem., 2013, 113(18), 2110-2142.
- [5] A. Hindle et al., Chem Commun., 2023, 59, 6239-6242.

UNDERSTANDING WATER AND OIL HOLDING PROPERTIES OF COCOA FIBER-GUM MIXTURES WITH NMR RELAXOMETRY

Murad Bal^a, Mecit H. Oztop^a

^a*Department of Food Engineering, Middle East Technical University, Üniversiteler Mah. Dumlupınar Blv. No:1 06800 Çankaya Ankara*

Cocoa bean husk is a byproduct of chocolate industry and discarded as waste or animal feed. The husk has a high fiber content with considerable water and oil holding properties, but the cocoa aroma and flavor limits its use in ranging food applicants. Once the aroma and flavor of the husk is removed through a solvent extraction process, the aroma free mass is called cocoa fiber which is a potential stabilizer. In addition, its physical properties can be improved by incorporation of commercially available gums such as xanthan and gum arabic. In this study, water holding properties of cocoa fiber mixed with varying arabic gum (5, 10, 20%) and xanthan gum (5, 10, 20%) were measured. In order to understand the interactions of the hydrocolloid mixtures at a molecular level, T_2 (*spin-spin relaxation time*) times of the water and hydrocolloid mixes were also measured. Relaxation spectra were also obtained for the wet mixes. Addition of arabic gum did not improve the water holding properties of cocoa fiber significantly but increased T_2 of the samples. A strong correlation between water holding capacity and T_2 was obtained ($R^2 > 0.81$). Differences were also detected in the effect of gum type and oil binding capacities.

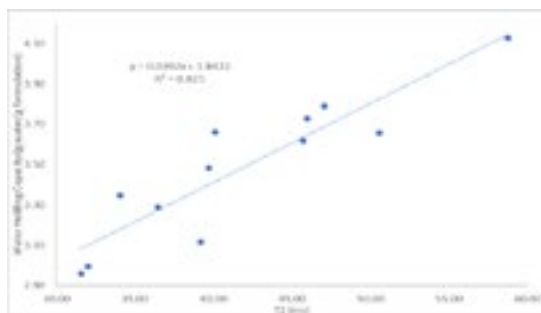


FIGURE 1. Water Holding Capacity and T_2

THREE MUSKETEERS OF MRI CONTRASTING: INFLUENCE OF METAL ADDITION ON PHOTOTHERMAL AND RELAXIVITY PROPERTIES OF POROUS POLYDOPAMINE NANOPARTICLES

Magdalena J. Bigaj-Józefowska^a, Emerson L. Coy^a, Karol Załęski^a, Radosław Mrówczyński^b, Bartosz F. Grześkowiak^a

^a*NanoBioMedical Centre, Adam Mickiewicz University, Poznań, Poland*

^b*Faculty of Chemistry, Adam Mickiewicz University, Poznań, Poland*

Polydopamine (PDA) nanoparticles have been extensively studied for their photothermal and therapeutic properties, making them promising candidates for cancer treatment [1]. During the synthesis of PDA nanoparticles, metal ions can be incorporated into the polymer matrix through coordination bonds with the functional groups of dopamine. The addition of metal ions can influence the physicochemical properties of PDA nanoparticles, including photothermal and relaxivity properties [2]. However, the influence of different metal dopants on the photothermal and relaxivity properties of porous PDA nanoparticles has yet to be fully explored. In this study, we aim to assess the influence of different metal dopants on the photothermal and relaxivity properties of PDA nanoparticles.

We synthesized porous PDA nanoparticles using a simple one-pot method. The nanoparticles were then doped with different metal ions: iron, manganese, and gadolinium. The physicochemical properties of the nanoparticles were characterized using various techniques, including HR-TEM with EDX, DLS, ICP-OES, and SQUID. We also assessed the photothermal properties of the nanoparticles using a laser irradiation system and evaluated the relaxivity properties of the nanoparticles using NMR spectroscopy. The photothermal and relaxivity properties of the nanoparticles were found to be dependent on the type of metal dopants. Our findings provide insights into the potential of metal-doped PDA nanoparticles for cancer theranostics and combined therapy. The porosity of nanoparticles enables loading additional cargo such as small molecule drugs, whereas the metal doping-induced paramagnetism of the nanoformulations makes them suitable for use as MRI contrasting agents.

Acknowledgments

The research was financed by The National Science Centre (NCN), Poland, under project number UMO-2018/31/D/ST8/02434.

References

- [1] J. Liebscher, *et al.*, Structure of Polydopamine: A Never-Ending Story?, *Langmuir*. 29 (2013) 10539–10548.
- [2] Xu, N., *et al.*, (2022). Fe (III)-Chelated Polydopamine Nanoparticles for Synergistic Tumor Therapies of Enhanced Photothermal Ablation and Antitumor Immune Activation. *ACS Applied Materials & Interfaces* (2022)

SPEEDING UP RESTRICTED DIFFUSION NMR MEASUREMENTS FOR POROUS STRUCTURE DETERMINATION OF BIOCOMPATIBLE GELS

Marek Czarnota^a, Sylwester Domański^b and Mateusz Urbańczyk^a.

^a*Institute of Physical Chemistry, Polish Academy of Sciences, Kasprzaka 44/52, 01-224 Warsaw, Poland*

^b*Polbionica Sp. z o.o. Aleja Prymasa Tysiąclecia 79A, 01-242 Warszawa, Poland*

Restricted diffusion measurements with Nuclear Magnetic Resonance spectroscopy provide us detailed information about porous structures. Restricted diffusion measurements utilize the behavior of molecules with movement limited by porous structures since the diffusion coefficient is lower than expected for free movement. The disadvantage of this measurement is its duration, which can be shortened significantly by applying fast Time-Resolved methodology[1]. In our research, we study samples of Gelatin Methacryloyl hydrogels dissolved in water. The sample is used as a backbone structure for a 3D-printed bionic pancreas. In our work, we show the relationship between the concentration of Gelatin Methacryloyl, its degree of substitution, and its structure.

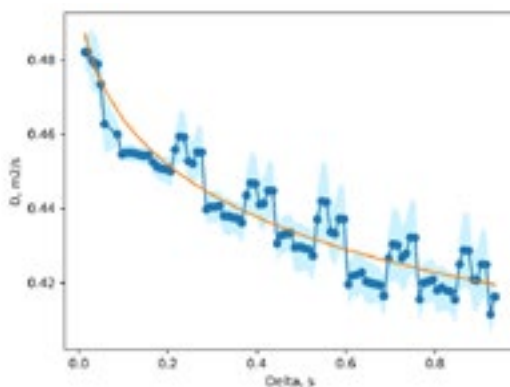


FIGURE 1. The exemplary plot of restricted diffusion of Gelatin Methacryloyl sample. Diffusion coefficient values are multiplied by the factor of 10^{-9} . Light blue color is error of diffusion calculation.

Acknowledgements

The authors would like to thank the National Science Centre, Poland, for its support in the form of an OPUS Grant (2021/41/B/ST4/01286).

References

- [1] Accelerating Restricted Diffusion NMR Studies with Time-Resolved and Ultrafast Methods, Mateusz Urbańczyk, Yashu Kharbanda, Otto Mankinen, and Ville-Veikko Telkki Analytical Chemistry 2020 92 (14), 9948-9955

GMO@DTPA-BSA-GD NANOPARTICLES AS NOVEL POTENTIAL MRI CONTRAST AGENTS

K.Gębicka^{1,2}, D.Flak¹, T.Zalewski¹, M.Kempka^{1,2}, G.Nowaczyk¹, M.Banaszak^{1,2}

¹*NanoBioMedical Centre, Adam Mickiewicz University, Wszechnicy Piastowskiej 3, 61-614 Poznań, Poland*

²*Faculty of Physics, Adam Mickiewicz University, Uniwersytetu Poznańskiego 2, 61-614 Poznań, Poland*

Current challenges in the design of new contrast agents is a search for new Gd-based paramagnetic CAs or their substitutes, whose low concentration (micromolar or even submicromolar) would make it possible to achieve the desired contrast with a low risk of systemic toxicity [1]. Nanoparticle-based CAs represent promising new platforms that next to the biocompatibility can provide high resolution and sensitivity MR imaging. Another alternative nanocarrier-approach is lipid-based nanoparticles modified with Gd-chelating lipids, where the Gd-chelating lipids are a part of the formed lipid bilayer next to the GMO lipid matrix. Among lipid nanoparticles used in bioimaging, lipid-based lyotropic liquid crystal nanoparticles (LLCNPs) stand out, particularly cubosomes and hexosomes, next to solid lipid nanoparticles (SLNPs) or other types [2]. These structures exhibiting long-range internal ordering are promising nanocarriers of CAs. In particular, these self-organized structures appear to offer a large loading of coordinated Gd(III) ions, and their extensive water channels may enable efficient water exchange between the inner and outer spheres surrounding the Gd(III) ions, resulting in better relaxivity.

Undertaken studies confirmed that proposed new lipid-based NPs show great potential as new CAs for MR imaging, particularly obtaining T₁-weighted images. At a magnetic field induction of 0.47 T, GMO@DTPA-BSA-Gd dispersed phases showed increased relaxivity r_1 compared to commercial contrast agents: Magnevist, Gadovist and Dotarem [3]. These features of LLCNPs, therefore, allow to conclude that proposed Gd-chelating lipid-enriched GMO-lipid nanoparticles may be the promising new contrast agents in MR imaging, thereby the type of nanocarriers for further development of multifunctional systems combining diagnostics and therapy in a single system.

Acknowledgments

The work was supported by the research grant DWM/WPC2/285/2020 funded by the National Centre for Research and Development.

References

- [1] M.A. Hahn, et al., *Analytical and Bioanalytical Chemistry*. 399 (2011) 3–27.
- [2] N. Tran, et al., *Materials Science and Engineering: C*. 71 (2017) 584–593.
- [3] M. Rohrer, et al., *Investigative Radiology*. 40 (2005) 715–724

CHARACTERIZATION OF POLYMER-CERAMIC COMPOSITE ELECTROLYTES USING MULTIDIMENSIONAL SOLID-STATE NMR

Pedram Ghorbanzade^{a,b,c} and Juan Miguel López del Amo^a

^a *Centre for Cooperative Research on Alternative Energies (CIC energiGUNE), Basque Research and Technology Alliance (BRTA), Alava Technology Park, Albert Einstein 48, Vitoria-Gasteiz 01510, Spain*

^b *University of Basque Country (UPV/EHU), Barrio Sarriena, s/n, 48940 Leioa, Spain*

^c *ALISTORE-European Research Institute, 80039, Amiens, France.*

Electrification of vehicles, which is an effective approach to mitigate climate change requires the development of safer batteries with solid-state electrolytes. A composite polymer electrolyte (CPE) consisting of Li⁺ conductor inorganic particles dispersed in a polymer matrix is a promising concept that combines the high ionic conductivity and electrochemical stability of ceramics with the flexibility and processability of the polymers.¹ Although CPEs have improved the performance and stability of the electrolytes, their ionic conductivity is insufficient for high-rate applications. One possible approach to improve the ionic conductivity is the heat treatment of the ceramic particles to modify the ceramic surface and form a better interphase with the polymer.²

In this work, solid-state NMR spectroscopy was used to closely follow the chemical and phase evolutions of LLZO garnets during the heat treatment process and its impact on the local Li⁺ dynamics. The presence and degradation of LiOH and Li₂CO₃ as secondary phases on the LLZO surface were monitored by relaxometry and ⁷Li-1H heteronuclear correlations. Thereafter, 2D ⁷Li-⁷Li and ⁶Li-⁶Li EXSY NMR experiments were employed to analyze the polymer-ceramic interface and detect the Li-ion exchange, as well as to quantify the exchange rates.^{3,4} Using pseudo-3D experiments, LiOH was identified as an intermediate phase for the interfacial Li exchange. Finally, using ⁷Li → ⁶Li trace exchange experiments, the Li-ion pathway through the electrolyte was determined.

Acknowledgements

P.G as a part of the DESTINY PhD programme acknowledges funding from the European Union's Horizon2020 research and innovation programme under the Marie Skłodowska-Curie Actions COFUND - Grant Agreement No: 945357.

This work was supported by the “Ministerio de Ciencia e Innovación / Agencia Estatal de Investigación”, under the project grant TED2021-129663B-C52.

References

- [1] S. Li, S.-Q. Zhang, L. Shen, Q. Liu, J.-B. Ma, W. Lv, Y.-B. He and Q.-H. Yang, *Advanced Science*, 2020, 7, 1903088.
- [2] P. Ghorbanzade, A. Pesce, K. Gómez, G. Accardo, S. Devaraj, P. López-Aranguren and J. M. López del Amo, *J. Mater. Chem. A*, 2023.
- [3] P. Ranque, J. Zagórski, S. Devaraj, F. Aguesse and J. M. L. del Amo, *J. Mater. Chem. A*, 2021, 9, 17812–17820.
- [4] J. Zagórski, J. M. López del Amo, M. J. Cordill, F. Aguesse, L. Buannic and A. Llordés, *ACS Appl. Energy Mater.*, 2019, 2, 1734–1746.

INVESTIGATING SYNERGISTIC EFFECTS BETWEEN CELLULOSE AND LIGNIN FOR ADVANCED FOREST CARBON FIBERS: MASS TRANSPORT CHARACTERIZATION WITH MAGNETIC RESONANCE METHODS

F. Guerroudj^a, J. Bengtsson^b, K. Jedvert^b and D. Bernin^a.

^a Chalmers University of Technology, Gothenburg, Sweden

^b Research Institutes of Sweden, Mölndal, Sweden

Carbon fibers (CFs) have a high specific strength and stiffness, which makes them very efficient reinforcements in composite materials for light-weight applications. The production of CFs requires a polymeric precursor that later can be carbonized. Forest-based products: lignin and cellulose are an attractive alternative to the fossil-based polymer commonly used. To obtain fibers, these materials need first to be dissolved in e.g. ionic liquids before being coagulated in a non-solvent e.g. water. It has been shown that wet spinning of lignin-cellulose ionic liquid solutions is a promising method for producing forest-based CFs precursors [1]. Several synergistic effects of using lignin and cellulose have been identified and affect the performance during spinning and consequently the produced CFs. These effects are very poorly understood and not deeply explored.

In this study, a special focus is on the mass transport of the solvent and non-solvent occurring during the coagulation process, where cellulose and lignin precipitate to form a rigid fiber. Complementary to some theoretical and experimental studies [2,3], in-situ NMR- and MRI-based methodologies are used to characterize the mass transport and solvent exchange under different coagulation conditions, as well as morphological analysis of the coagulated cellulose-lignin films.

A single shot RARE sequence combined with slice saturation was applied and 2D signal intensity maps were recorded throughout the coagulation process. In addition, spectroscopic information in a voxel was measured to characterize and follow the coagulation bath composition over time. ¹³C solid-state NMR spectroscopy was used to study the morphological structure of cellulose and its crystallinity of the obtained cellulose-lignin films.

The results showed that the coagulation conditions, such as the use of different solvent, non-solvent, or types of lignin, affect the dynamics of the mass transport during the coagulation process, as well as the morphological properties of the obtained cellulose-lignin films.

The use of NMR/MRI methods reveals how variations in the raw materials affect the quality of the fibers, and how the process, and consequently the CFs, can be further optimized

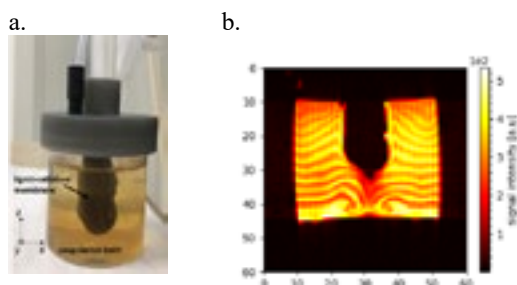


FIGURE. Mass transport measurements: (a) study set-up and (b) 2D signal intensity map in xz plan (geometric axis in $174^\circ/171^\circ$) showing the dynamics of solvent exchange.

References

- [1] Bengtsson A, *ACS Omega* (2022);
- [2] Bengtsson J, *Holzforschung* (2019);
- [3] Hedlund A, *Macromolecules* (2017).

1D 1H NMR SPECTRA OF NOVEL GLYCERYL MONOOLEATE / GLYCERYL MONOLAURATE LIPID LIQUID CRYSTALLINE NANOPARTICLES

Jakub Jagielski, Łukasz Popenda, Karolina Gębicka, Grzegorz Nowaczyk

NanoBioMedical Centre, Wszechnicy Piastowskiej 3, 61-614 Poznań, Poland

In recent years, lipid liquid crystalline nanoparticles (LLCNPs) have garnered significant attention as potential drug delivery systems due to their biocompatibility and versatile properties. In this study, we present a preliminary investigation of newly developed lipid liquid crystalline nanoparticles composed of glyceryl monooleate (GMO) and glyceryl monolaurate (GML) using nuclear magnetic resonance (NMR) spectroscopy.

The synthesis of the LLCNPs was accomplished using a top-down approach with sonication as the homogenization method. The nanoparticles were characterized using dynamic light scattering (DLS), cryogenic transmission electron microscopy (cryo-TEM), and small-angle X-ray scattering (SAXS). The DLS analysis revealed a narrow size distribution with an average diameter of 140.23 nm. Cryo-TEM images demonstrated the presence of spherical nanoparticles with a well-defined structure. SAXS results suggest that the nanoparticles exhibit a crystalline structure with cubic Pn3m symmetry.

In addition to the aforementioned methods, nuclear magnetic resonance is another approach to gain insights into the internal structure and molecular dynamics of the LLCNPs [1]. In the presented study, a one-dimensional proton nuclear magnetic resonance (1D 1H NMR) spectrum was evaluated to investigate the degree of internalization of GMO and GML into the structure of the nanoparticles.

In conclusion, this study presents the successful synthesis and characterization of novel lipid liquid crystalline nanoparticles composed of GMO and GML. Further investigations are warranted to explore their performance as drug carriers and optimize their formulation for specific therapeutic applications.

Acknowledgements

The studies were financially supported by The National Centre for Research and Development through grant DWM/WPC2/285/2020.

References

[1] Li, Dianfan, and Martin Caffrey. "Structure and functional characterization of membrane integral proteins in the lipid cubic phase." *Journal of molecular biology* 432.18 (2020): 5104-5123.

¹H-NMR low temperature spectroscopy and relaxometry studies of hydration from gaseous phase of foliose lichenized fungi: *Psoroma Hypnorum* from Antarctica.

D. Jakubiec^{a,b}, K. Kubat^a, M. A. Olech^{d,e}, A. Casanova-Katny^c, K. Strzałka^{f,g} and H. Harańczyk^a

^a*Institute of Physics, Jagiellonian University, ul. Prof. Stanisława Łojasiewicza 11, 30-348 Kraków, Poland*

^b*Doctoral School of Exact and Natural Sciences, Jagiellonian University in Cracow, Poland*

^c*Faculty of Natural Resources, Catholic University of Temuco, Chile*

^d*Institute of Botany, Jagiellonian University, ul. Kopernika 27, 31-501 Kraków, Poland*

^e*Institute of Biochemistry and Biophysics, Polish Academy of Sciences, ul. Pawińskiego 5a, 02-106 Warsaw, Poland*

^f*Malopolska Centre of Biotechnology, Jagiellonian University, ul. Gronostajowa 7A, 30-387 Kraków, Poland*

^g*Faculty of Biochemistry, Biophysics and Biotechnology, Jagiellonian University, ul. Gronostajowa 7A, 30-387 Kraków, Poland*

The rehydration process of the extremely dehydrated lichenized fungi (*Psoroma Hypnorum*) from the Antarctica were studied. Low temperature (210-295K) relaxometry and ¹H-NMR spectroscopy were used - methods allowing one to monitor molecular dynamics of bound water in order to distinguish several fractions of water present in a living cryptobiotic organism (in thallus of dehydrated lichenized fungus). For the dehydrated thallus of *P. hypnorum*, an Antarctic lichenized fungus, the course of gas phase hydration shows a sequential bonding of very tightly bound water fraction, tightly bound water, and finally loosely bound water. The rehydration process for *P. hypnorum* is slower, compared to desert species from less humid region, reflecting the availability of water in the environment[1]. For *P. hypnorum*, the ¹H-NMR spectra make it possible to distinguish several water signals, namely the signal from loosely bound water, and the signal from tightly bound water fraction. In the ¹H-NMR spectra a chemical shift of the lines can be seen.

Acknowledgements

The research was carried out as a part of Chile grant from INACH (Instituto Antártico Chileno, Ministerio de Relaciones Exteriores, Chile): Sistema de Proyectos INACH, RT_27_16; Concurso: Título: XXII Concurso Nacional de Proyectos de Investigación Científica y Tecnológica, Antártica, 2016, Project: "Ecophysiology of Antarctic and Atacama desert lichens: freezing and deep dehydration mechanism under natural conditions and under passive warming experiments", supervisor: Investigador Principal prof. Angélica Casanova-Katny, Universidad Católica de Temuco, Temuco, Chile.

References

- [1] H. Harańczyk, K. Strzałka, K. Kubat; A. Andrzejowska; M. Olech, D. Jakubiec; P. Kijak; Angelica Casanova-Katny, " A comparative analysis of gaseous phase hydration properties of two lichenized fungi: *Niebla tigrina* (Follman) Rundel & Bowler from Atacama Desert and *Umbilicaria antarctica* Frey & I. M. Lamb from Robert Island, Southern Shetlands Archipelago, maritime Antarctica", 2021, *Extremophiles*, **25**(3), 267-283.

Insights into structure and dynamics of minimal HDV like ribozyme Drz-Mtgn-1

Soumyadip Jana, Silke Johannsen, Roland K.O. Sigel

Department of Chemistry, University of Zurich, Winterthurerstrasse 190, 8057 Zürich

Email: soumyadip.jana@chem.uzh.ch

Hepatitis delta virus (HDV)-like ribozymes are self-cleaving RNAs belonging to the class of small ribozymes, and their widespread occurrence [1] in all aspects of life implies crucial functions in various biological processes. The catalytic reaction follows a general acid-base mechanism assisted by divalent metal ions and directly involves a conserved cytosine to initiate the nucleophilic attack of the 2'-hydroxyl group on the adjacent phosphodiester bond. This ribozyme family differs greatly in length and sequence but adopts a conserved nested double pseudoknot structure with the catalytically important cytosine in the core [2]. So far, only the HDV ribozyme, the eponym and first representative of this family, has been studied in detail regarding structure and catalytic mechanism. However, to understand which structural motives are responsible for the wide range of cleavage rates observed in this family, further structural studies are required.

Here we investigate the Drz-Mtgn-1 ribozyme, which originates from the human gut microbiome and shows a unique bell-shaped self-cleavage activity in the presence of divalent metal ions. This ribozyme belongs to the minimal HDV-like ribozymes, as it lacks a non-essential domain for catalytic activity [3]. Using NMR spectroscopy, we want to determine the three-dimensional structure and disentangle the intricate interplay of this RNA with metal ions. Initial NMR studies reveal that the Drz-Mtgn-1 ribozyme folds into the nested double pseudoknot structure even in the absence of divalent metal ions, thereby forming two critical G·U wobble pairs that are potentially important for the generation of specific metal ion binding sites in the catalytic core.

This study will enlighten the structural basis and the role of metal ions that determine the dynamics of the cleavage reaction and help to bridge the gap between ribozyme's structure and function.

Acknowledgements:

I thank to Dr. Silke Johannsen and Prof. Roland K.O. Sigel for their guidance and all Sigel lab members for their input in this project.

References:

- [1]: Chiu-Ho T Webb, Andrej Lupták, RNA Biology, 8 (5), 719-727.
- [2]: A R Ferré-D'Amaré, K Zhou, J A Doudna, Nature 1998, 395 (6702), 567–574.
- [3]: Nathan J Riccitelli, Eric Delwart, Andrej Lupták, Biochemistry 2014, 53 (10), 1616–1626.

MECHANISMS OF MOLECULAR MOTION BY MEANS OF NMR RELAXOMETRY

Adam Kasperek, Maciej Osuch, Danuta Kruk

*Department of Physics and Biophysics, University of Warmia and Mazury in Olsztyn,
Oczapowskiego 4, 10-719 Olsztyn, Poland*

The development of Fast Field Cycling technology has enabled NMR relaxation experiments in a broad frequency range from about 10 KHz to 40 MHz (referring to ^1H resonance frequency). There are two main advantages of NMR relaxometry – the first one is the opportunity to probe dynamical processes occurring on much different time scales from ms to ps in a single experiment, while the second one is the unique opportunity of revealing the mechanism of the motion.

This is due to the fact that relaxation rates can be described by linear combination of spectral density functions. As spectral density functions are Fourier transforms of the corresponding time correlation functions, their mathematical forms depend on the mechanism of the motion. The poster presents a guideline for analysing NMR relaxometry data for hydrated macromolecules, illustrated by examples. In the first step, it is shown that the data can always be parametrized in terms of relaxation contributions associated with Lorentzian spectral densities. Such approach, although useful, does not give a deeper insight into the mechanism of motion. Thus, in the next step, it is demonstrated how to attempt to reveal the mechanism of translation diffusion on the basis of the mathematical form of the frequency dependencies of the relaxation rates, exploiting characteristic properties of the spectral density functions.

Acknowledgements

This project has received funding from the European Union's Horizon 2020 research and innovation programme under grant agreement No 101008228 (project SuChAQuality).

A TD-NMR investigation for the food-grade pickering emulsions

Esranur Kaya^a, Esmanur Ilhan^a and Mecit Halil Oztop^a

^aDepartment of Food Engineering, Middle East Technical University, Ankara, Turkey

TD-NMR relaxometry is a powerful, non-invasive method to investigate the molecular interactions in food systems. Food systems usually show a multi-component relaxation behaviour thus generating a relaxation spectrum from a T_2 decay curve can and be a great tool to examine the components that are present [1]. T_2 relaxation spectra can provide information about the *water/oil contents and status, physical properties of the water, and interaction of the water with the surrounding macromolecules* [2]. In this study, we examined pickering emulsions which are emulsions stabilized by hydrocolloidal particles. Pickering emulsions were prepared by pea protein isolate and quince seed mucilage as the hydrocolloids. Sunflower oil was used at a ratio of %20. In order to better visualize this interaction, emulsions with different polysaccharide-protein ratios of 0.01, 0.02, 0.05, 0.10 were prepared and T_2 relaxation times were measured for 14 days. T_2 times were expressed as a biexponential model and the two components were associated with the protons coming from (T_{2a}) water that is restricted by the pickering particles and (T_{2b}) oil droplets that were stabilized. Higher hydrocolloid concentrations (0.5 & 1) were expected to decrease the T_2 times due to higher viscosities. However, this was not the observed case until the end of 1st week. It is likely that pickering particles adsorbed to the oil droplets and decreased the relaxation times. The increase in both T_{2a} and T_{2b} values was less in high concentration emulsions after the 7th day. This trend was also confirmed by the particle size measurements, and low concentration emulsions (0.01 & 0.02) were observed to undergo phase separation in the following days. Differences in the relaxation times were interpreted as different stability mechanisms for the studied emulsions.

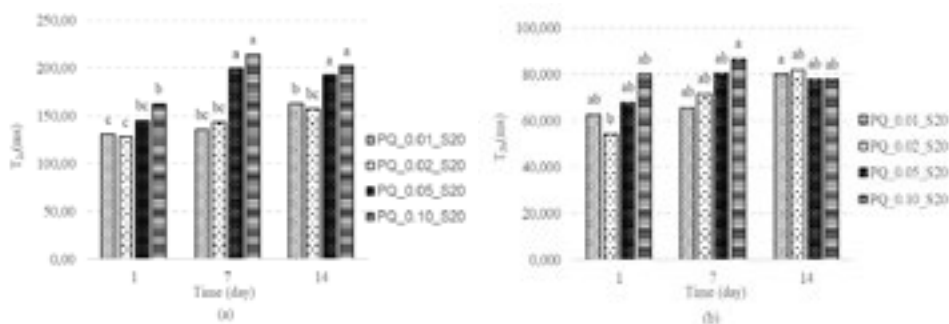


FIGURE 1. T_{2a} (a) and T_{2b} (b) spin-spin relaxation times of pea protein isolate(P) quince seed mucilage(Q) and emulsions containing 20% oil (S20) according to the biexponential model. Different lowercase letters indicate significant difference for each sample ($p < 0.05$).

Acknowledgements

This study was funded by the Scientific and Technological Research Council of Turkey (TUBITAK) COST 2519 Grant No 121O091.

References

- [1] Acri, G., Sansotta, C., Ruello, E. V., Denaro, L., Salmeri, F. M., & Testagrossa, B. (2020). The Use of Time Domain NMR in Food Analysis: A Review. *Current Nutrition & Food Science*, 17(6), 558–565. <https://doi.org/10.2174/1573401316999201126212143>
- [2] Kirtil, E., & Oztop, M. H. (2016). 1H Nuclear Magnetic Resonance Relaxometry and Magnetic Resonance Imaging and Applications in Food Science and Processing. *Food Engineering Reviews*, 8(1), 1–22. <https://doi.org/10.1007/s12393-015-9118->

METHODS OF FUNCTIONALIZATION OF SMART HYDROGEL SURFACES BASED ON HYALURONIC ACID.

Marietta Koźlarek^{a,b}, Roksana Markiewicz^a and Grzegorz Nowaczyk^a.

^a Adam Mickiewicz University, NanoBioMedical Centre, Poznań, Poland

^b Adam Mickiewicz University, Faculty of Physics, Poznań, Poland

Intelligent hydrogels have the potential for application in therapeutic systems due to their mechanical strength, physicochemical properties, and biocompatibility. Intelligent hydrogels can regulate their hydrophilicity, swelling capacity, and permeability to molecules under the influence of external physical and chemical stimuli such as pH, temperature, electric and magnetic fields, light, ionic strength, and the presence of specific biomolecules. As a result, hydrogels can reduce the frequency of dosing, maintain the desired therapeutic concentration in a single dose, and minimize the side effects of drugs by preventing their accumulation in target tissues. Additionally, they are also used in wound dressings, biosensors, and medical implants [1,2].

The main aim of our study was to design and develop surface-functionalized hydrogels based on hyaluronic acid for post-myocardial infarction therapy. Hyaluronic acid is a natural anionic polysaccharide with a wide range of physicochemical and functional properties, making it highly useful in biomedical applications such as tissue engineering and drug delivery systems [3]. It is characterized by biodegradability, non-toxicity, and the ability to modify its properties through chemical conjugation of functional groups [4].

To prepare potential therapeutic systems characterized by drug loading capability, long lifespan, increased active surface area, selectivity, and good membrane permeability and ease of transport in the body, we synthesized three types of hyaluronan-based nanoparticles. Using an ion gelation method, we obtained a polycationic nanocomplex - pure sodium hyaluronate (SH-NP). As a second hydrogel type, an amphiphilic hyaluronans modified with lithocholic acid (HA-LCA) were obtained. Subsequently, using amine coupling, hyaluronic acid complexes functionalized with β -cyclodextrin with hydrophobic cavities (HA-CD). The structure and composition of the obtained nanomaterials were confirmed using nuclear magnetic resonance spectroscopy, moreover, fourier-transform infrared spectroscopy was employed to examine the diverse surface of the hydrogels and evaluate the network properties of the polymer layers. The obtained systems can be characterized with physical properties similar to living tissues, making them suitable for further investigations as conjugates of Bis-MPA PEG pseudodendrimers functionalized with Apelin-13 polypeptide.

Acknowledgements

Project number DWM/WPC2/285/2020, entitled “Construction of Multifunctional Nanosystems for Theranostics of Ischemic Heart Diseases”, funded from the National Centre of Research and Development is kindly acknowledged. Moreover, M.K. would like to acknowledge project ID-UB 076/34/UAM/0070 funded by Adam Mickiewicz University.

References

- [1] S. Mantha, et al. Materials. 12 (2019) 3323.
- [2] A. Bordbar-Khiabani, et al. International Journal of Molecular Sciences. 23 (2022) 3665.
- [3] S. Peralta, et al. European Polymer Journal. 112 (2019) 433–441.
- [4] W.H. Lee, et.al ACS Nano. 16 (2022) 20057–20074.

EVALUATION OF MIXING EFFICIENCY IN BUBBLE REACTORS FOR CARBON DIOXIDE CAPTURE USING MRI

Feryal Guerroudj, Emmanouela Leventaki, Saeed Khoshhal Salestan, Francisco M. Baena-Moreno, Diana Bernin.

Department of Chemistry and Chemical Engineering, Chalmers University of Technology, Gothenburg, Sweden

CO₂ absorption is a potential solution to hamper further climate changes. A promising alternative to amine absorbents are alcohol solvents with sodium hydroxide [1]. The efficiency of the CO₂ capture depends heavily on the mixing of the liquid and the gas. Here we evaluated the mixing efficiency of our 3D-printed bubble reactor without forced mixing over time using fast MRI techniques. The absorbent solutions were prepared with 96% ethanol, 4% water and NaOH at concentrations of 2-10 g/L. The gas was a mixture of 30% CO₂ and 70% N₂. Experiments were conducted in a 3D-printed bubble column reactor at ambient pressure and temperature. The reactor was placed inside an MRI (Bruker Avance III 300MHz with a H¹ transmit/receive probe of 66 mm diameter) and the gas was sparged continuously into the reactor. Figure 1(a) depicts the experimental setup. One-shot RARE images and flow maps were recorded throughout the reaction. During CO₂ absorption, a gel is formed containing most likely a mixture of inorganic and organic carbonates. This gelation hinders further absorption as it inhibits good mixing and further dissolution of CO₂. One-shot RARE images (Figure 1(b) and (c)) enabled monitoring of the liquid which became gradually more viscous. High signal intensity (bright yellow) corresponds to the liquid, while low intensity corresponds to regions where the gas is creating turbulence. Good mixing regions could be identified based on the intensity of the signal. For the 2 g/L NaOH solution, better mixing was observed due to less gel formation. We also found that the positioning of the sparger is crucial to minimize regions with bad mixing. MRI provided an understanding of the fluid dynamics inside a bubble column. In cases where the liquid phase is opaque, or physicochemical changes affect the process, conventional methods like high-speed cameras tend to fail. Fast MRI can enable the optimization of bubble reactor designs [2].

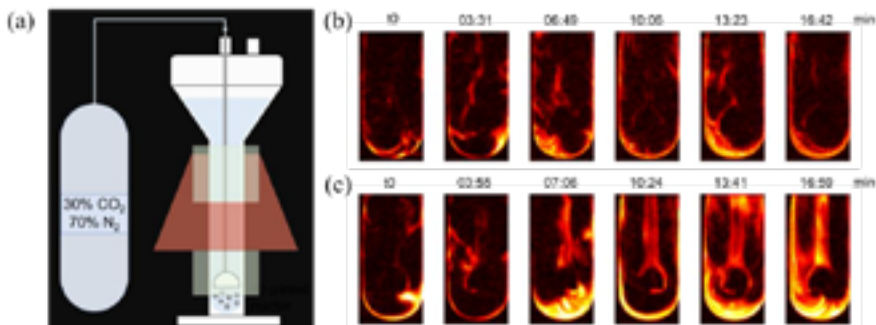


FIGURE 1. (a) Experimental setup and sagittal RARE images over time during sparging gas into a solution of (b) 2 g/L of NaOH in ethanol and (c) 10 g/L of NaOH in ethanol.

References

- [1] Baena-Moreno, Heliyon (2023).
- [2] Tayler, Doctoral thesis (2011).

In-House Fabrication of Microwave Waveguides and Resonators for Efficient Dynamic Nuclear Polarization

Jake Lumsden^a, Zhenfeng Pang^a, Utsab Banerjee^a, Kong Ooi Tan^a

^a *Laboratoire des Biomolécules, LBM, Département de Chimie, École Normale Supérieure, PSL University, Sorbonne Université, CNRS, 75005 Paris, France*

Dynamic nuclear polarization (DNP) is an NMR hyperpolarization technique that facilitates the transfer of polarization from unpaired electron spins to nuclear spins. To achieve efficient DNP performances, low-loss corrugated microwave waveguides and tunable high- Q dual resonance (RF and microwave) TE₀₁₁ resonator is required [1, 2]. We will present the methods to fabricate the 9.4 T/ 263 GHz microwave components using additive (3D printing) or subtractive (CNC machining) manufacturing processes. For the additive approach, we will first 3D print the components with plastic (ABS or similar) materials, followed by either electro or electroless plating with copper. For the subtractive method, we will machine a manual tap using a combined 5-axis CNC machine and a manual lathe fabrication process. The tap will then be heat treated (via tempering and/or annealing) for more favorable mechanical properties. These microwave accessories are expected to yield better DNP and EPR performances.

References

- [1] Woskov, P. P., Nanni, E. A., Shapiro, M. A., Jawla, S. K., Hummelt, J. S., Temkin, R. J., & Barnes, A. B. (2011). 330 GHz helically corrugated waveguide. *IRMMW-THz 2011 - 36th International Conference on Infrared, Millimeter, and Terahertz Waves*. <https://doi.org/10.1109/irmmw-THz.2011.6105103>
- [2] Smith, A. A., Corzilius, B., Bryant, J. A., Derocher, R., Woskov, P. P., Temkin, R. J., & Griffin, R. G. (2012). A 140 GHz pulsed EPR/212 MHz NMR spectrometer for DNP studies. *Journal of Magnetic Resonance*, 223. <https://doi.org/10.1016/j.jmr.2012.07.008>

Novel 1D ZnO Nanomaterials with Promising Photoelectrochemical Properties for Biosensing and Water Splitting Applications

Andrii Lys^{a*}, Irfan Hanif^{a*}, and Igor Iatsunskyi^a

^a*NanoBioMedical Centre, Adam Mickiewicz University, Wszechnicy Piastowskiej 3, 61-614, Poznań, Poland*

Antigen rapid detection tests are more frequently used to identify the SARS-CoV-2 viral proteins. Despite being less sensitive than molecular tests, antigen rapid detection tests have the advantages of being inexpensive and providing results quickly at the point of care. Additionally, they can detect target analytes with low concentrations which makes them advantageous for early diagnosis of the disease ¹. To reduce the spread of the virus, it is necessary to develop diagnostic tests that can rapidly identify the infected individual. ZnO possesses good physical and chemical stability, sustainability, high energy conversion efficiency, sensitivity, and abundance, which make it promising for photoelectrochemical applications, such as SARS-CoV-2 antibodies detection ² and water splitting ³.

In this work, we present ZnFe₂O₄/ZnO core-shell electrospun fibers as working electrode in standard three-electrode configuration, the studied nanostructures revealed catalytic activity without applied solar-light radiation and up to 45% incremental photocurrent growth with solar-light radiation. And 1D ZnO nanorods used as photoelectrochemical immunosensor. In comparison with traditional methods of antibody detection, the present study offers several advantages such as low cost, portability, and high accuracy. With continuous research and development, the 1D ZnO based electrochemical sensor will play an important role in rapid and sensitive diagnostic tools for the monitoring of infectious diseases.

Acknowledgments

The authors also acknowledge the financial support from the National Science Centre of Poland (NCN) through the SONATA-Bis grant 2020/38/E/ST5/00176. The financial support of Marie Skłodowska-Curie Research and Innovation Staff Exchange (CanBioSe 778157) is gratefully acknowledged.

References

1. Biby, A. *et al.* Rapid testing for coronavirus disease 2019 (COVID-19). *MRS Communications* (2022) doi:10.1557/s43579-021-00146-5.
2. Nunez, F. A. *et al.* Electrochemical Immunosensors Based on Zinc Oxide Nanorods for Detection of Antibodies Against SARS-CoV-2 Spike Protein in Convalescent and Vaccinated Individuals. *ACS Biomater. Sci. Eng.* (2023) doi:10.1021/acsbiomaterials.2c00509.
3. Kolaei, M., Tayebi, M., Masoumi, Z. & Lee, B. K. A novel approach for improving photoelectrochemical water splitting performance of ZnO-CdS photoanodes: Unveiling the effect of surface roughness of ZnO nanorods on distribution of CdS nanoparticles. *J. Alloys Compd.* (2022) doi:10.1016/j.jallcom.2022.164314.

*Both authors contributed equally to this research.

STRUCTURE AND MOLECULAR INTERACTIONS IN AMMONIUM IONIC LIQUIDS

Roksana Markiewicz^a, Adam Klimaszyk^{a,b}, Marcin Jarek^a, Michał Taube^b.

^a *Adam Mickiewicz University, NanoBioMedical Centre, Wszechnicy Piastowskiej 3, 61-614 Poznań, Poland*

^b *Adam Mickiewicz University, Faculty of Physics, Uniwersytetu Poznańskiego 2, 61-614 Poznań, Poland*

Ionic liquids, organic/inorganic salts with melting points below 100 °C, are typically characterized by a variety of characteristics, from which common to great group of ILs are low vapor pressure, a wide range of liquids, high thermal, electrochemical and chemical stability, and the ability to dissolve many organic and inorganic compounds, including some polymers. The construction of the anion and cation determines their unique properties, which can be changed to create an ionic liquid with the required physical and chemical properties. The key advantage that sets ILs apart from conventional solvents is that they may be projected, and for this reason, ILs might be referred to as green solvents utilized in industrial and laboratory applications.

This study chose cations of different structure (aromatic, cyclic, and aliphatic), different alkyl chain length attached to the quaternary nitrogen, and bis(trifluoromethanesulfonyl)imide anion, which results in three homologous series of ionic liquids with the cation of different geometry, with different alkyl chain lengths attached to the quaternary nitrogen. The main aim was to evaluate the macro- and microscopic structure of the synthesized ILs.

After structure confirmation by means of NMR and FTIR (collected with a FT/IR-4700, JASCO), phase transition temperatures were determined by means of differential scanning calorimetry technique (with a DSC 8000, Perkin Elmer unit). Moreover, Small-angle X-ray scattering studies were performed using the Xeuss 2.0 SAXS/WAXS system. Finally, self-diffusion coefficients were determined for series of the prepared ILs measurements at 14,4 T Agilent NMR spectrometer techniques (DOTY DSI-1372, $g_z=28$ T/m, VnmrJ 4.2; Pulse sequence: PGSE (Pulsed Gradient Spin-Echo).

Acknowledgements

A.K. would like to acknowledge the project: "Interdisciplinary PhD studies in nanotechnology" No. POWR.03.02.00-00-I032/16 under the European Social Fund.

WATER DYNAMICS IN ARTIFICIAL TISSUES BY MEANS OF NMR RELAXOMETRY

Elzbieta Masiewicz, Farman Ullah, Adrianna Mieloch and Danuta Kruk

*Department of Physics and Biophysics, University of Warmia and Mazury in Olsztyn,
Oczapowskiego 4, 10-719 Olsztyn, Poland.*

^1H NMR relaxometry experiments have been performed for examples of materials used in regenerative medicine (“artificial tissues”). The experiments have been performed in the frequency range from 10kHz to 20MHz at 25°C and 38°C. The purpose of the studies is to reveal dynamical and structural properties of selected materials used in regenerative medicine in connection to their macroscopic properties (such as viscoelasticity) and get insight into the mechanism of water motion and interactions of water molecules with the macromolecular matrix. In Fig.1 (left) examples of the ^1H spin-lattice relaxation data are shown in comparison with solid collagen, considered as a model system. In Fig.1 (right) one sees examples of ^1H magnetization for the hydrated material – the relaxation process has turned out to be single-exponential.

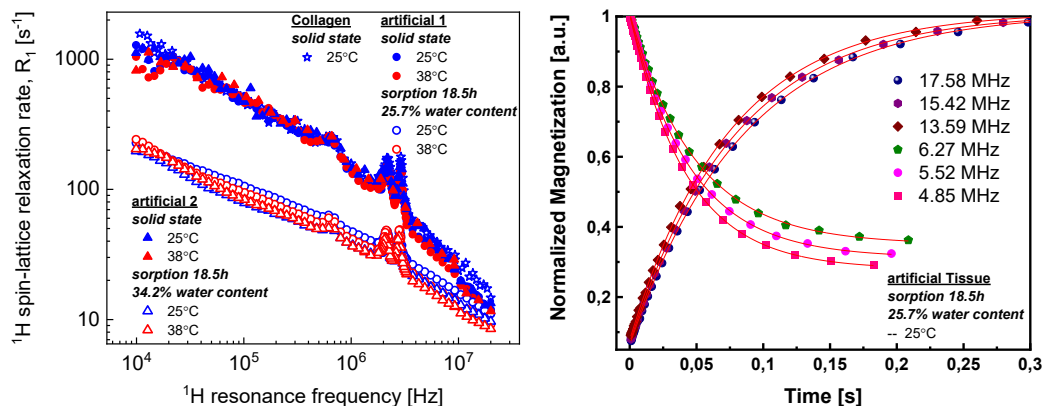


FIGURE 1. (left) ^1H spin-lattice relaxation data for artificial tissues compared with analogous data for solid collagen; (right) examples of ^1H magnetization versus time for hydrated artificial tissues.

The data have been thoroughly analyzed in terms of advanced models of relaxation processes, including Quadrupole Relaxation Enhancement effects [1]. The analysis has led to a series of parameters characterizing the dynamics of different molecular fractions present in the materials and revealed the mechanism of water diffusion in the vicinity of the macromolecular surfaces.

Acknowledgements

The work was supported by National Science Centre, Poland, project number: 2021/43/B/NZ5/01602.

References

[1] Kruk, D., Masiewicz, E., Borkowska, A. M., Rochowski, P., Fries, P. H., Broche, L. M., & Lurie, D. J. (2019). Dynamics of solid proteins by means of nuclear magnetic resonance relaxometry. *Biomolecules*, 9(11), 652.

Analysis molecular dynamic processes in the complex of human S100B protein with A β peptide on base ^{15}N relaxation data

Thomas Okoth^{a,b}, Wojciech Kwiatek^c, Maciej Kozak^{d,e}, and Igor Zhukov^a

^aInstitute of Biochemistry and Biophysics, Polish Academy of Sciences, 02-106 Warsaw, Poland

^bDepartment of Chemistry, Warsaw University of Technology, 00-661 Warsaw, Poland

^cInstitute of Nuclear Physics Polish, Academy of Sciences, 31-342 Kraków, Poland

^dDepartment of Biomedical Physics, Faculty of Physics, Adam Mickiewicz University, 61-614 Poznań, Poland.

^eNational Synchrotron Radiation Centre SOLARIS, Jagiellonian University, 30-392 Kraków, Poland

S100B proteins are a type of calcium-binding protein that play a crucial role in the regulation of various processes associated with Alzheimer's disease (AD). In AD patients, neuroinflammation leads to an increase in the levels of S100B proteins in the brain. This heightened presence of S100B proteins plays a significant role in the processing of the amyloid precursor protein (APP), the regulation of amyloid beta peptides (A β), and the phosphorylation of Tau. The interactions between S100B and A β amyloid suggest that S100B has a regulatory role, which can vary depending on the stage of AD and the level of A β presented in cell [1].

In our studies we explore structural alterations observed under interaction of the uniformly ^{15}N -labeled human S100B in Ca-loaded form with A β_{1-40} peptide utilizing heteronuclear NMR spectroscopy. Analysis of chemical shift perturbations reveals the α -helices I – I' together with the α -helices IV – IV' as a structural motif involved in binding of the A β_{1-40} peptide (Figure 1), as previously reported by other group for A β_{1-42} [2].

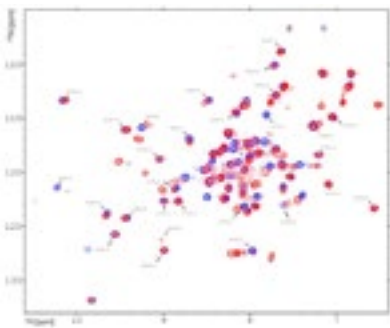


Figure 1. Overlay of ^1H - ^{15}N HSQC spectra collected for ^{15}N -labeled S100B (blue) and after addition A β_{1-40} peptide (red).

backbone upon interaction with the A β_{1-40} peptide. Specifically, a decrease in the $J(\omega_N)$ function was observed for the majority of the ^{15}N , indicating a reduction in molecular dynamic processes in the S100B backbone within the μs – ns time-frame. Simultaneously, increased mobility was observed for the residues Ser41 and His42, which are located in the loop between α -helices II and III.

Acknowledgments

The research was supported by a research grant (2021/41/B/ST4/03807) from National Science Centre (Poland).

References

1. Wang, X., et al. (2014) *Biochim. Biophys. Acta*, **1842**, 1240–1247
2. Cristóvão, J.S., et. al. (2018) *Science Advance*, **4**, eaaq1702

FREQUENCY OPTIMIZATION IN MULTIDIMENSIONAL DIFFUSION-RELAXATION CORRELATION MRI ON A FIXED MOUSE BRAIN

Pak Shing Kenneth Or^a, Maxime Yon^{a,b}, Omar Narvaez^b, Alejandra Sierra Lopez^b, Dan Benjamini^c and Daniel Topgaard^a.

^aPhysical Chemistry, Lund University, Sweden

^bA.I. Virtanen Institute for Molecular Sciences, University of Eastern Finland, Finland

^cMultiscale Imaging and Integrative Biophysics Unit, National Institute on Aging, NIH, USA

Multidimensional diffusion-relaxation correlation magnetic resonance imaging (mdMRI) is a recently-developed technique that simultaneously measures and correlates diffusion and relaxation times to overcome the limitations of traditional measurements. At the core of our mdMRI technique is the tensor-valued encoding of the diffusion measurements[1], which provides control over the range of frequencies probed in the diffusion spectra. Having a wide range is useful for probing restricted diffusion[2]. However, due to hardware constraints, achieving higher frequencies at constant b-values requires increasing echo time (TE), sacrificing signal-to-noise ratio (SNR). How large of a range is achievable without losing too much SNR is a particularly important problem for samples with short T_2 , like our mouse brain sample fixed in 2% formaldehyde, T_2 approximately 25 ms.

To find the optimal experimental settings for our sample, we designed several acquisition protocols covering different frequency ranges at each b-value and correspondingly different minimum TEs. At the max b-value of $6.7 \cdot 10^9 \text{ s/m}^2$, the protocol with the smallest range of 45-111 Hz has minimum TE 46 ms. The protocol with the largest range of 30 – 228 Hz has minimum TE 63 ms. Fitting was done with a custom Monte-Carlo inversion algorithm[3], producing distributions for each voxel in the solution space from which we extract statistical descriptors for the solution distribution.

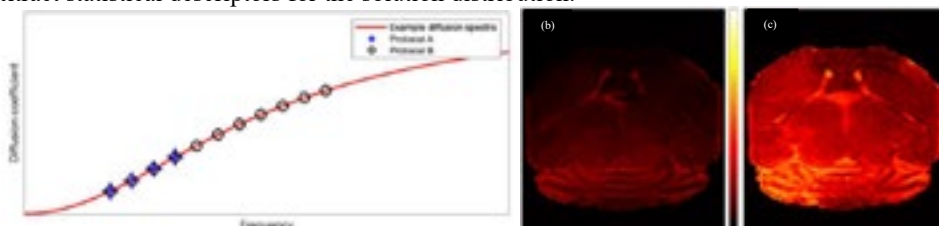


FIGURE 1. (a) Illustrative plot of experimental design and result. Plotted on a generic diffusion spectra, protocol A represents one with a small frequency range, while protocol B represents one with a large frequency range. Plots (b) and (c) show the change in $D_{||}$ per unit frequency, obtained from a protocol with the smallest and largest frequency range respectively. Color bar range: 0-6e-12 m^2 .

We observed the strongest sensitivity to frequency for both mean isotropic diffusivity ($D_{||}$) and squared normalized anisotropy (D_{Δ}^2) values for the protocol having an intermediate frequency range of 33-215 Hz, minimum TE 54 ms at max b-value. While in general larger ranges should result in higher sensitivities, the associated decrease in SNR counteracts that effect.

References

- [1] Jiang, H.; Svenningsson, L; and Topgaard, D., *Magn. Reson.* **2023**, 4: 73-85,
- [2] Stepišnik, J.; Callaghan, P.T., *Physica B* **2000**, 270, 110-117,
- [3] de Almeida Martins, J.P.; Topgaard, D., *Sci. Rep.* **2018**, 8, 2488,

LUNG CANCER RADIOMICS INVESTIGATION: CT-MRI FEATURES COMPARISON AND SOFTWARE CONSISTENCY

Agnese RobustelliTest^{a,b}, Alessandra Pinto^d, Chandra Bortolotto^{d,e}, Raffaella Cabini^{b,f}, Francesca Brero^b, Manuel Mariani^{a,c}, Ian Postuma^b, Lorenzo Preda^{d,e}, Alessandro Lascialfari^{a,b}

^aDepartment of Physics, University of Pavia, Via Bassi 6, 27100 Pavia, Italy

^bINFN, Pavia Unit, Via Bassi 6, 27100, Pavia, Italy

^cINFN, Milano Unit, Via Celoria 16, 20133, Milano, Italy

^dRadiology Institute, Fondazione IRCCS Policlinico San Matteo, 27100, Pavia, Italy

^eDiagnostic Imaging and Radiotherapy Unit, Department of Clinical, Surgical, Diagnostic, and Pediatric Sciences, University of Pavia, 27100, Pavia, Italy.

^fDepartment of Mathematics, University of Pavia, Via Ferrata5, 27100 Pavia, Italy.

Radiomics is a quantitative method that allows to extract mineable data from medical images. The aim of Radiomics is to improve clinical decision-making effectiveness defining novel imaging biomarkers, labelled *radiomic features*, able to reflect tissue properties. Currently, Radiomics has not yet been introduced in clinical routine mainly because of its poor generalizability and reproducibility [1]. Within this framework, our purpose is to preliminary investigate the statistical reliability of radiomics features extracted from Computed Tomography (CT) and Magnetic Resonance Imaging (MRI) lung cancer images, and the consistency between two open-source radiomics platforms, LIFEx [2] and Pyradiomics [3]. 26 lung cancer patients were retrospectively included in the considered cohort. For each patient, both CT and MRI images have been manually segmented using the ITK SNAP tool. Three different images pre-processing methods were considered, acting on voxels resampling and grey-level discretization. From the pre-processed images, 66 features *IBSI-compliant* [4] common to the two radiomics software were extracted and organized in datasets. At this point, the correlation between Pyradiomics and LIFEx features, for each imaging technique, and the correlation between CT and MRI features, for each radiomics platform, were investigated. The correlation was analysed both graphically, through graphs, and quantitatively, by the *Spearman test* and the *Intraclass correlation coefficient* (ICC). Among LIFEx and PyRadiomics software, statistically significant correlations were found for 88% of CT-derived features and 91% of MR-derived features. Comparing CT and MRI images, significant correspondences were found for 15% of LIFEx features and 12% of PyRadiomics features. The obtained results suggest that the IBSI standardization is quite effective even when two radiomic software are considered, and that CT and MRI images contain different, non-redundant information, paving the way for a future multi-modal radiomics analysis.

References

- [1] DOI: <https://doi.org/10.2967/jnumed.118.222893>
- [2] <https://www.lifexsoft.org/>
- [3] <https://pyradiomics.readthedocs.io/en/latest/>
- [4] <https://doi.org/10.1148/radiol.2020191145>

Insight into Mass Transfer within a Superabsorbent Polymer Using MRI

Saeed Khoshhal Salestan^a, Emmanouela Leventaki^a, Feryal Guerroudj^a, Diana Bernin^a

^a *Department of Chemistry and Chemical Engineering, Chalmers University of Technology*

Absorption-based technologies are widely used for many applications, particularly in hygiene products for the absorption of body fluids. Designing efficient absorbents with high capacity requires better insight into the mechanism of the absorption. It means an attempt to unravel the role of intermolecular interactions and swelling on the behavior of absorbing fluids. Although it is a commonly accepted fact that the absorption performance of hygiene pads can be affected by operational conditions, such as the ratio of used materials, determining the extent to which parameters modify the behavior of absorbed fluid has proven to be challenging and contentious [1,2]. To further elucidate the water and salt behavior at a molecular scale in these environments, the magnetic resonance imaging (MRI) technique was implemented to evaluate water absorbed in the super absorbent polymers (SAPs). Some principal parameters, including the T_2 relaxation time, were noticed to be significantly dependent on the ratio of the fluid/polymer, as well as the particle size of the absorbents. The outcome elucidated that the absorption inside the SAP samples is not homogeneous and the salt ions enhance the observed heterogeneity. In this regard, the intermolecular forces between ions and the polymer chains seem to make the polymer act like a filter. It means that sites on the polymer chains are occupied by sodium ions and, consequently, the number of possible interactions between water molecules and polymer chains seems to drop [1]. Moreover, T_2 relaxation time showed a descending trend as the fluid/polymer ratio and particle size were reduced expressing more interaction or lower mobility due to higher chain density per volume.

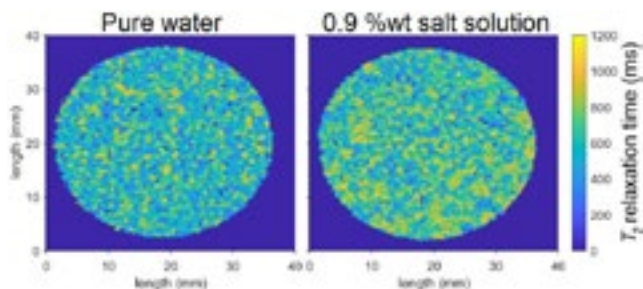


FIGURE 1. Axial maps of long T_2 relaxation times of fluids within the SAP sample with a particle size 300-600 μm .

Acknowledgments

This project has financially been supported by Bo Rydin Foundation.

References

- [1] G.S. Pell, et al., NMR investigation of the nature of water in disposable incontinence pads containing superabsorbent polymers and fluffed wood pulp, *Colloid Polym. Sci.* 281 (2003)
- [2] B. MacMillan, et al., An n.m.r. investigation of the dynamical characteristics of water absorbed in Nafion, *Polymer (Guildf)*. 40 (1999)

Investigation of the interaction of sodium ions with ZIF-8 in sodium-ion battery electrolytes using ^{23}Na and ^1H NMR.

Dominika Tubacka^a, Kosma Szutkowski, Patryk Florczak^a

^a*NanoBioMedical Centre Adam Mickiewicz University in Poznań (Wszechnicy Piastowskiej 3, 61-614 Poznań)*

Sodium-ion batteries (SIBs) are attracting a lot of investigation and commercial interest at present. They are considered the most promising alternative to lithium-ion batteries (LIBs) due to their similar chemical properties, far greater availability of natural resources and resultant low cost, reduced carbon footprint, and, above all, increased safety [1].

Because sodium and lithium batteries have comparable structures and operating mechanisms, many advances in lithium-ion technology can be leveraged to increase the performance of SIBs through optimization of electrode materials and electrolytes. In this context, ^{23}Na NMR and ^1H NMR techniques are used to explore the incorporation of sodium electrolytes with a porous MOF (Metal Organic Framework) material, such as the highly porous ZIF-8 (Zeolitic Imidazolate Frameworks) [2]. These methods were chosen because of their capacity to precisely follow sodium ion and proton dynamics, which is critical for understanding the interaction between the electrolyte and the porous ZIF-8 material. The findings of these investigations can help evaluate whether sodium ions interact with MOFs and flow inside the structure or are maintained on the surface, and how this impacts ionic conductivity. This understanding can help researchers grasp how MOFs can be utilized to improve the performance of sodium-ion batteries, particularly those used to store energy. The combined use of electrolytes with MOFs is an intriguing area of research for future advancements in battery technology.

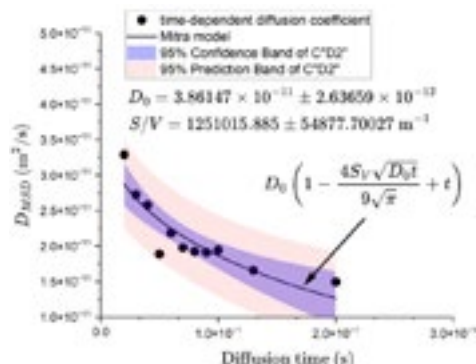


FIGURE 1. Time-dependent diffusion coefficients of PC as obtained in ZIF-8-PC. [3]

Acknowledgements

OPUS UMO-2019/35/B/ST8/02550

IDUB 054/13/SNŚ/0044

References

- [1] Tapia-Ruiz N., et al. *JPhys Energy*, **2021**;3(3).
- [2] Karatrantos A.V., et al. *Jenny Stanford Publishing*, **2023**;52.
- [3] Moutal N., et al. *IEEE Transactions on Medical Imaging*, **2019**;38(11):2507-2522.

¹³C SOLID-STATE NMR PROVIDING CRUCIAL INSIGHTS INTO PULPING OF NON-WOODEN CELLULOSE RESOURCES

Joanna Wojtasz-Mucha^a, Diana Bernin^a

^a *Department of Chemistry and Chemical Engineering, Chalmers University of Technology, Gothenburg, Sweden*

The demand for textile fibres continues to increase due to the steady growth of the world's population. Cotton being one of the main resources for textile fibre production cannot meet the market needs due to a limited production capacity. During the last century wood was the primary resource for cellulose for both paper and textile industry. Its pulp is preferred due to its long fibres and all-year availability.

Albeit containing cellulose and enabling a circular cellulose economy, very little is known about pulping of non-wooden resources such as straw, bamboo, bagasse and reeds, corn straw, reed, grass, jute, flax, sisal etc. In comparison to wood, the hierarchical organization differs severely due to different purposes e.g. oat husks' purpose is to protect the grain.

Apart from this, cellulose consists not only of amorphous and crystalline fractions—the crystalline fraction has many allomorphs. The most common ones being native cellulose—cellulose I and regenerated cellulose II. The production of textile fibres includes dissolving the cellulose pulp and coagulation in an anti-solvent during the spinning process. One sustainable dissolution system is cold alkali. It was however observed that the dissolution of the cellulose II allomorph in cold alkali is impaired. Pulping is a multiple step process—prehydrolysis, cooking and post-treatments such as bleaching. Each of these steps might if not optimized cause partial transformation of cellulose from native cellulose to cellulose II—preventing the pulp from dissolution.

¹³C solid-state NMR is a crucial and common technique to analyse cellulose and their existing allomorphs (see Fig. 1). Here we applied ¹³C solid-state NMR to follow the cellulose pulp from oat husks and wheat straw during the different pulping steps. We aim to optimize the pulping process to enable dissolution in cold alkali for the production of sustainable textile fibres.

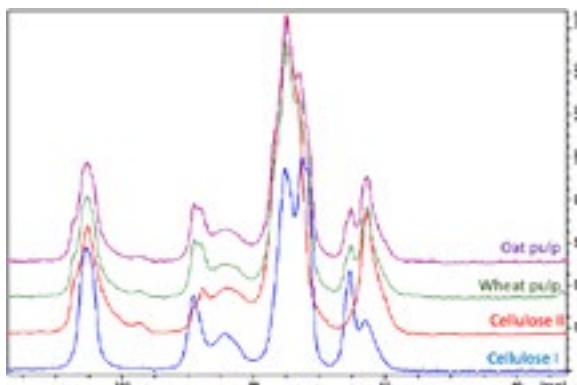


FIGURE 1. Solid state NMR spectra of various cellulose samples

Acknowledgments

This project acknowledges funding from Vinnova and TreeToTextile.

THE POSITIVE INTERPLAY BETWEEN IMAGING AND THERAPEUTIC AGENTS ENCAPSULATED IN THERANOSTIC LIPOSOMES TARGETING ORAL CANCER

Tomasz Zalewski^a, Grzegorz Nowaczyk^a and Paulina Skupin-Mrugalska^b.

^a NanoBioMedical Centre, Adam Mickiewicz University, Wszechnicy Piastowskiej 3, 61-614 Poznan, Poland

^b Department of Inorganic and Analytical Chemistry, Poznan University of Medical Sciences, Rokietnicka 3, 60-806 Poznan, Poland

The theranostic liposomes are a multifunctional approach that combines diagnosis and treatment [1]. We reported an improved relaxation (resulting from the presence of zinc phthalocyanine, ZnPc), possibly improving MRI contrast and potentially allowing a reduction of the dose of co-administered lipid analog of Magnevist® (PE-DTPAGd), keeping the performance unmodified [2, 3]. The aim of the study was to replace ZnPc with a marketed photosensitizer, verteporfin (VRP), and verify our previous observations. Additionally, the theranostic liposomes were conjugated with an anti-EGFR antibody and its efficacy was evaluated in a cellular model of head and neck squamous cell carcinoma (HNSCC).

Liposomes were prepared by the microfluidic method (MF). Loading efficacy was determined using HPLC (VRP, ZnPc) or NMR (PE-DTPAGd). Vesicle size and zeta potential were characterized by dynamic light scattering. Relaxometric measurements were performed at different magnetic fields at 23°C and 37 °C. *In vitro* cytotoxicity and photosensitizing activity were evaluated in two HNSCC cell lines in 2D and 3D cell culture models.

The size of theranostic liposomes prepared by MF was 30-50 nm, while a slight increase in diameter was noted for antibody-conjugated liposomes (*ca.* 60 nm). The presence of VRP in the liposomal bilayer led to increased relaxivity of Gd(III) ions in theranostic liposomes compared to paramagnetic vesicles (without VRP but with PE-DTPAGd), which is in agreement with results obtained for ZnPc-loaded liposomes. The VRP encapsulated in targeting theranostic liposomes effectively inhibited cancer cell growth in a 2D model of SCC-25 and FaDU with IC₅₀ of 16 nM and 45.3 nM, respectively, as well as in a 3D model with corresponding IC₅₀ values of 61.5 nM (SCC-25) and 108.3 nM (FaDu).

Changes inside the liposomal bilayer upon dye incorporation among phospholipids' molecules result in increased water permeability across the liposomal membrane and relaxivity of incorporated MRI CA. Theranostic liposomes allow the delivery of higher doses of VRP than can be achieved for the free drug allowing the effective photodynamic treatment of HNSCC spheroids.

Acknowledgements

The authors acknowledge the financial support for the project from the Polish National Science Centre, No 2016/21/D/NZ7/01607

References

- [1] T. Lammers, S. Aime, W.E. Hennink, G. Storm, F. Kiessling, *Acc. Chem. Res.* 44 (2011) 1029–1038.
- [2] P. Skupin-Mrugalska, L. Sobotta, A. Warowicka, B. Wereszczynska, T. Zalewski, P. Gierlich, M. Jarek, G. Nowaczyk, M. Kempka, J. Gapinski, S. Jurga, J. Mielcarek, *J. Inorg. Biochem.* 180 (2018) 1–14.
- [3] P. Skupin-Mrugalska, T. Zalewski, P.A. Elvang, G. Nowaczyk, M. Czajkowski, H. Piotrowska-Kempisty, *Colloids Surf. B Biointerfaces.* 205 (2021) 111871.

NMR DEPTH PROFILING OF PAINTED WALLS: OSTIA ANTICA

Matea Urbanek,¹ Jan Bader,² Daniel Krüger,² A. Yong,³
 Jürgen Frick,¹ Jens Anders,² E. Del Federico,³ P. Tomassini,⁴ Bernhard
 Blümich⁵

¹ *Materialprüfungsanstalt Stuttgart,*

² *University of Stuttgart,*

³ *Pratt Institute Brooklyn,*

⁴ *UC Louvain,*

⁵ *RWTH Aachen University*

The mortar-layer stratigraphy of Roman wall paintings at Ostia Antica, the historic port of ancient Rome, was studied at two occasions with nuclear magnetic resonance (NMR) depth profiling [1] to explore manufacturing details in the context of the use and history of the buildings. In the first campaign in 2019 the NMR signature of covered wall paintings was studied [2,3], while in the second campaign in 2022, depth profiles were compared to answer the question if different painted walls were prepared for painting at the same time or by the same workshop [4]. The experience gained in handling the portable NMR hardware for onsite measurements has stimulated the development of an improved NMR depth-profiling instrument [5,6]. The information provided by NMR depth profiling is illustrated with experimental data, and progress in hardware development is reported.

Acknowledgements

Supported by DFG grant DFG AN 984/24-1 and FR 2912/2-1

References

- [1] B. Blümich, Concepts and Applications of the NMR-MOUSE, in: D.M. Bastidas, E. Cano, eds., *Advanced Characterization Techniques, Diagnostic Tools and Evaluation Methods in Heritage Science*, Springer Nature, Cham, 2018, 61-75
- [2] B. Blümich, E. Del Federico, D. Jaschtschuk, M. Küppers, K. Fallon, A. Steinfeld, P. Tomassini, *Nondestructive Analysis of Wall Paintings at Ostia Antica*, *Heritage 4* (2021) 4421–44
- [3] B. Blümich, D. Jaschtschuk, C. Rehorn, *Advances and Adventures with Mobile NMR*, in: S. Haber-Pohlmeier, B. Blümich, L. Ciobanu, *Magnetic Resonance Microscopy*, Wiley-VCH, Weinheim, 2022, chapter 7, pp. 155-172
- [4] M. Urbanek, S. Haber-Pohlmeier, D. Krüger, J. Bader, E. Del Federico, K. Fallon, A. Steinfeld, J. Zöldföldi, J. Frick, J. Anders, H. Becker, B. Blümich, P. Tomassini, *Lessons on the history of buildings from NMR depth profiles of painted walls at Ostia Antica*, manuscript in preparation
- [5] B. Blümich, J. Anders, *When the MOUSE leaves the house*, *Magn. Reson. 2* (2021) 149–160

Contrast Enhancement in MRI Using Combined Double Action Contrast Agents and Image Post-Processing in the Breast Cancer Model

D. MacDonald^a, A. Dash^b, F.C.J.M. van Veggel^b, B. Tomanek^{a,c}, and B. Błasiak^a

^a *Institute of Nuclear Physics Polish Academy of Science, Kraków, Poland*

^b *Department of Chemistry, University of Victoria, British Columbia, Canada*

^c *Department of Oncology, University of Alberta, Edmonton, Canada*

MRI provides the best soft tissue contrast when comparing with other diagnostic modalities. Relaxation times T_1 and T_2 of normal tissue and tumor create the contrast in MRI. Contrast agents shortening T_1 and T_2 relaxation times further improve detection of small pathologies such as early stages breast or brain cancers [1]. Furthermore, images can be post-processed to improve contrast. We studied changes in tumor contrast before and after non-targeted NaDyF₄/NaGdF₄ contrast injection. Then to further increase the contrast we applied an image subtraction and addition. Therefore, we performed theoretical calculations of MR signal in a tumor model using T_1 -weighted, T_2 -weighted, and combined images for T_1 -, T_2 -, and T_1/T_2 -targeted contrast agents. We imaged a mouse with triple negative breast cancer (TNB) before and after an injection of a nontargeted NaDyF₄/NaGdF₄ nanoparticles (NP). We applied the RARE (T_1 -weighted), and MSME (T_2 -weighted) pulse sequences, using a 9.4 T MRI system. The results show that subtraction of T_2 -weighted from T_1 -weighted MR images provides additional increase in the tumor contrast: over two-fold in the tumor model and 12% in the in vivo experiment. We concluded that an image subtraction improved tumor contrast hence it may improve the accuracy of cancer detection [2].

Acknowledgements

Acknowledgements: This work was funded by the National Science Center, Poland. Grant number: OPUS 2018/31/B/ST5/03605.

References

- [1] L. Smith et al., J. Nanomat., (2012) 1-7
- [2] D. MacDonald, A. Dash , F. C. J. M. van Veggel , B. Tomanek, B. Błasiak., Materials 2023, 16(8), 3096; <https://doi.org/10.3390/ma16083096>

EXPLORING TEMPERATURE RELATED PROTON DYNAMICS IN HYDRATED STARCH BY TIME DOMAIN NMR

Jana van Rooyen^a, Leonid Grunin^b, Mecit Oztot^c and Marena Manley^a

^a*Department of Food Science, Stellenbosch University, Stellenbosch, 7602, South Africa; 20783353@sun.ac.za; mman@sun.ac.za*

^b*Resonance Systems GmbH, 28 Seestrasse, Kirchheim unter Teck, Baden-Wuerttemberg, 73230, Germany; mobilenmr@hotmail.com*

^c*Department of Food Engineering, Middle East Technical University, Ankara, Turkey; mecit@metu.edu.tr*

The use of various dry thermal treatment techniques to modify starch properties have gained increasing attention in recent years [1]. However, its effect on the hydrothermal transformation upon heating is not fully understood. Wheat starch isolated from roasted (115°C for 165 s) and unroasted wheat as well as maize starch were used to investigate the temperature-dependent changes in starch-water mixtures by Time Domain-Nuclear Magnetic Resonance (TD-NMR). T_2 relaxation spectra are appropriate for analysis of heterogeneous food samples to investigate its multi-component behaviour [2]

Molecular properties of starch-water systems at 50% moisture content were characterised from 20 to 90°C by Rhim Kessmeier-Radiofrequency Optimised Solid Echo (RK-ROSE) and Carr-Purcell-Meiboom-Gill (CPMG) pulse sequence for detection of the solid and liquid phases, respectively. Six proton populations were identified. For the component of shortest relaxation time (T_{2r}^*), the contribution of the amorphous and crystalline part within the semicrystalline structure were detected by comparing the second moment values to the relaxation times. Water absorption by the different starches and the associated granule swelling were observed up to 50°C by the lowered relaxation times (T_{2i}^* , $T_{2(2)}$ and $T_{2(3)}$). The displacement of the proton relaxation time distribution ($T_{2(3)}$) towards shorter times suggests a reduction in proton mobility. This is due to water migration from the outer to the inner region of the granule. On the other hand, the reduction in the fraction of the shortest component (T_{2r}^*) suggests the loss of structured semicrystalline regions due to the increase in proton mobility upon heating.

The second, and most abundant component detected by CPMG provides information on the onset of gelatinisation. A stabilisation in the reduction of $T_{2(2)}$ occurred at similar temperatures as the onset of gelatinisation detected by differential scanning calorimetry and initial structural deformation detected by the complex modulus (G^*). This study proved that TD-NMR can be used to accurately demonstrate the fast changes in water mobility during heating of starch-water systems; as observed for dry heat treated wheat and maize starches.

Acknowledgements

The work has been part of the H2020 MSCA RISE Consortium 'SuChAQuality' (Grant agreement: 101008228) funded by the EU. J.v.R. acknowledges Stellenbosch University for the Postgraduate Scholarship granted.

References

- [1] van Rooyen, J., Simsek, S., Oyeyinka, S.A. & Manley, M. (2022). Foods, 11(2), pp. 1–19.
- [2] Bosmans, G.M. & Delcour, J.A. (2017). Modern Magnetic Resonance. Pp 1-18.

LIST OF SCHOOL SPEAKERS

Esteban Anoardo

Laboratorio de Relaxometría y Técnicas Especiales (Larte),
FaMAF – Universidad Nacional de Córdoba and IFEG-CONICET.
Córdoba, Argentina

Adriana Auccaise

Department of Physics and Biophysics, University of Warmia
and Mazury in Olsztyn,
Oczapowskiego 4, 10-719 Olsztyn, Poland

Maria Beira

Center of Physics and Engineering of Advanced Materials,
Instituto Superior Técnico, Universidade de Lisboa,
Av. Rovisco Pais, 1049-001 Lisboa, Portugal
Department of Physics, Instituto Superior Técnico,
Universidade de Lisboa,
Av. Rovisco, Pais, 1049-001 Lisboa, Portugal

Bernhard Blümich

Institut für Technische und Makromolekulare Chemie,
RWTH Aachen University,
Germany

Anja Böckmann

Molecular Microbiology and Structural Biochemistry,
UMR5086 CNRS/University of Lyon,
France

Adolfo Botana

JEOL UK Ltd, Silver Court, Watchmead,
Welwyn Garden City AL7 1LT, UK

Lucia Calucci

Istituto di Chimica dei Composti Organometallici,
Consiglio Nazionale delle Ricerche,
Via G. Moruzzi 1, 56124 Pisa, Italy

Leonid Grunin

Resonance Systems GmbH,
28 Seestrasse, Kirchheim unter Teck, Baden-Wuerttemberg,
73230, Germany

Wiktor Koźmiński

Faculty of Chemistry, Biological and Chemical Research
Centre, University of Warsaw,
Żwirki i Wigury 101, 02-089 Warsaw, Poland

Daunta Kruk

Department of Physics and Biophysics, University of Warmia
and Mazury in Olsztyn,
Oczapowskiego 4, 10-719 Olsztyn, Poland
NanoBioMedical Centre, Adam Mickiewicz University
in Poznań, Wszechnicy Piastowskiej 3, 61-614 Poznań, Poland

Olivier Lafon

Univ. Lille, CNRS, UCCS,
Lille, France

Arkadiusz Leniak

Celon Pharma SA.
Ogrodowa 2A, 05-092 Kielpin, Poland

David Lurie

School of Medicine, Medical Sciences & Nutrition,
University of Aberdeen,
Foresterhill, Aberdeen AB25 2ZD, Scotland, UK

Beat Meier

Physical Chemistry,
ETH Zürich, 8093 Zürich, Switzerland

Mecit Oztop

Department of Food Engineering,
Middle East Technical University,
Ankara, Turkey

Giacomo Parigi

Magnetic Resonance Center (CERM), University of Florence,
and CIRMMP,
via Luigi Sacconi 6, 50019 Sesto Fiorentino, Italy

Claudia Schmidt

Paderborn University, Department of Chemistry,
33098 Paderborn, Germany

Pedro Jose Sebastiao

Center of Physics and Engineering of Advanced Materials,
Instituto Superior Técnico,
Universidade de Lisboa, Av. Rovisco Pais, 1049-001 Lisboa,
Portugal
Department of Physics, Instituto Superior Técnico,
Universidade de Lisboa, Av. Rovisco, Pais, 1049-001 Lisboa,
Portugal

Siegfried Stapf

Department of Technical Physics II, TU Ilmenau,
PO Box 100 565, 98684 Ilmenau, Germany

Janez Stepisnik

Faculty of Mathematics and Physics, University of Ljubljana,
Slovenia

Ville-Veiko Telkki

NMR Research Unit, University of Oulu,
P.O. Box 3000, FI-90014, Finland

Daniel Topgaard

Department of Chemistry, Lund University,
Lund, Sweden

Magdalena Wencka

Jožef Stefan Institute,
Jamova 39, SI-1000, Slovenia
Institute of Molecular Physics, Polish Academy of Sciences,
Smoluchowskiego 17, 60-179 Poznań, Poland

LIST OF TRAINERS

Michał Bielejewski

Institute of Molecular Physics, Polish Academy of Sciences,
Smoluchowskiego 17, 60-179 Poznań,
Poland

Adolfo Botana

JEOL UK Ltd, Silver Court, Watchmead,
Welwyn Garden City AL7 1LT, UK

Jacek Jencyk

NanoBioMedical Centre, Adam Mickiewicz University in
Poznań, Wszechnicy Piastowskiej 3, 61-614 Poznań, Poland

Marek Kempka

NanoBioMedical Centre, Adam Mickiewicz University in
Poznań, Wszechnicy Piastowskiej 3, 61-614 Poznań, Poland

Elżbieta Masiewicz

Department of Physics and Biophysics, University of Warmia
and Mazury in Olsztyn, Oczapowskiego 4, 10-719 Olsztyn,
Poland

Kosma Szutkowski

NanoBioMedical Centre, Adam Mickiewicz University in
Poznań, Wszechnicy Piastowskiej 3, 61-614 Poznań, Poland

Tomasz Zalewski

NanoBioMedical Centre, Adam Mickiewicz University in
Poznań, Wszechnicy Piastowskiej 3, 61-614 Poznań, Poland

LIST OF PARTICIPANTS

Ahmad Farooq

Institute of Molecular Physics, Polish Academy of Sciences,
Smoluchowskiego 17, 60-179 Poznań, Poland

Anikeeva Maria

Section Biomedical Imaging (SBMI) Molecular Imaging
North Competence Center (MOIN CC) Dept. Radiology and
Neuroradiology University Hospital Schleswig-Holstein (UKSH)
Christian-Albrechts-Universität zu Kiel (CAU)
Am Botanischen Garten 14 24118 Kiel Deutschland

Anum Fatima

Section Biomedical Imaging (SBMI) Molecular Imaging
North Competence Center (MOIN CC) Dept. Radiology and
Neuroradiology University Hospital Schleswig-Holstein (UKSH)
Christian-Albrechts-Universität zu Kiel (CAU)
Am Botanischen Garten 14 24118 Kiel Deutschland

Auccaise Ruben

Universidade Estadual de Ponta Grossa,
Av. General Carlos Cavalcanti, 4748 – Uvaranas,
Ponta Grossa-Brasil

Babayevska Nataliya

NanoBioMedical Centre, Adam Mickiewicz University in Poznan,
Wszechnicy Piastowskiej 3, 61-614 Poznań, Poland

Baj Krzysztof

Department of Chemistry, University of Liverpool, UK

Bal Murad

Middle East Technical University, Orta Doğu Teknik Üniversitesi,
Üniversiteler Mahallesi
Dumlupınar Bulvarı No:1 06800 Çankaya Ankara, Turkey

Bigaj-Józefowska Magdalena

NanoBioMedical Centre, Adam Mickiewicz University in Poznan,
Wszechnicy Piastowskiej 3, 61-614 Poznań, Poland

Blasiak Barbara

Instytut Fizyki Jądrowej im. Henryka Niewodniczańskiego
Polskiej Akademii Nauk,
Radzikowskiego 152 31-342 Kraków, Poland

Czarnota Marek

Institute of Physical Chemistry, Polish Academy of Sciences
Marcina Kasprzaka 44/52, 01-224 Warszawa, Poland

Farinone Marco

Ryvu Therapeutics,
Sternbacha 2; 30-394 Kraków, Poland

Florczak Patryk

NanoBioMedical Centre, Adam Mickiewicz University in Poznan,
Wszechnicy Piastowskiej 3, 61-614 Poznań, Poland

Gębicka Karolina

NanoBioMedical Centre, Adam Mickiewicz University in Poznan,
Wszechnicy Piastowskiej 3, 61-614 Poznań, Poland

Ghorbanzade Pedram

CIC energiGUNE,
C/Albert Einstein 48. 01510 Vitoria-Gasteiz. Spain

Guerroudj Feyral

Chalmers University of Technology 412 96 Gothenburg, Sweden

Hanif Irfan

NanoBioMedical Centre, Adam Mickiewicz University in Poznan,
Wszechnicy Piastowskiej 3, 61-614 Poznań, Poland

Jagielski Jakub

NanoBioMedical Centre, Adam Mickiewicz University in Poznan,
Wszechnicy Piastowskiej 3, 61-614 Poznań, Poland

Jakubiec Daniel

Uniwersytet Jagielloński, Szkoła doktorska Nauk Ścisłych
i Przyrodniczych, Wydział Fizyki Astronomii i Informatyki
Stosowanej,
ul. prof. S. Łojasiewicza 11 30-348 Kraków

Jana Soumyadip

University of Zurich,
Winterthurerstrasse 190, 8057, Zurich

Jencyk Jacek

NanoBioMedical Centre, Adam Mickiewicz University in Poznan,
Wszechnicy Piastowskiej 3, 61-614 Poznań, Poland

Jorasz Alija

NanoBioMedical Centre, Adam Mickiewicz University in Poznan,
Wszechnicy Piastowskiej 3, 61-614 Poznań, Poland

Kasperek Adam

University of Warmia and Mazury in Olsztyn,
Michała Oczapowskiego 2, 10-719 Olsztyn, Poland

Kaya Esranur

Middle East Technical University, Orta Doğu Teknik Üniversitesi,
Üniversiteler Mahallesi
Dumlupınar Bulvarı No:1 06800 Çankaya Ankara, Turkey

Khoshhal Salestan Saeed

Chalmers University of Technology
412 96 Gothenburg, Sweden

Koźłarek Marietta

Faculty of Physics, Adam Mickiewicz University in Poznań,
Uniwersytetu Poznańskiego 2, 61-614 Poznań, Poland

Leventaki Emmanouela

Chalmers University of Technology
412 96 Gothenburg, Sweden

Lumsden Jake

ENS Paris,
24 Rue Lhomond, 75005 Paris

Lys Andrii

NanoBioMedical Centre, Adam Mickiewicz University
in Poznań,
Wszechnicy Piastowskiej 3, 61-614 Poznań, Poland

MacDonald David

Instytut Fizyki Jądrowej im. Henryka Niewodniczańskiego
Polskiej Akademii Nauk,
Radzikowskiego 152 31-342 Kraków, Poland

Markiewicz Roksana

NanoBioMedical Centre, Adam Mickiewicz University
in Poznań,
Wszechnicy Piastowskiej 3, 61-614 Poznań, Poland

Masiewicz Elżbieta

Institute of Molecular Physics, Polish Academy of Sciences,
Smoluchowskiego 17, 60-179 Poznań, Poland

Nowaczyk Grzegorz

NanoBioMedical Centre, Adam Mickiewicz University
in Poznań,
Wszechnicy Piastowskiej 3, 61-614 Poznań, Poland

Okoth Thomas

Institute of Biochemistry and Biophysics, Polish Academy
of Sciences, Pawińskiego 5a, 02-106 Warszawa Poland

Or Pak

Physical Chemistry, Department of Chemistry, Faculty
of Science, Lund University,
Naturvetarvägen 14 / Solvegatan 39 A, 223 62 Lund

Robustelli Test Agnese

University of Pavia,
via Agostino Bassi 6, Pavia (PV), Italy

Römer Armin

Forschungszentrum Jülich GmbH, IEK-9

Tubacka Dominika

Adam Mickiewicz University in Poznań,
Uniwersytetu Poznańskiego 8, 61-614 Poznań, Poland

Ullah Farman

University of Warmia and Mazury in Olsztyn,
Michała Oczapowskiego 2, 10-719 Olsztyn, Poland

Wojtasz-Mucha Joanna

Chalmers University of Technology
412 96 Gothenburg, Sweden

Yio Marcus

Imperial College London, Department of Civil
and Environmental Engineering,
239, Skempton Building, London, UK

Zalewski Tomasz

NanoBioMedical Centre, Adam Mickiewicz University
in Poznań, Wszechnicy Piastowskiej 3, 61-614 Poznań, Poland

NOTES

NOTES

NOTES

NOTES

NOTES

NOTES

NOTES

NOTES

NOTES

NOTES

NOTES

NOTES

NOTES

NOTES

NOTES

NOTES

NOTES

NOTES

NOTES

NOTES

NOTES

NOTES

June 18th - June 24th 2023, Zakopane, Poland

Introduction

SUNDAY June 18 th	Afternoon Arrivals & Accommodation				SATURDAY June 24 th	
MONDAY, June 19 th	TUESDAY, June 20 th	WEDNESDAY, June 21 st	THURSDAY, June 22 nd	FRIDAY, June 23 rd	Breakfast	
8:00-9:00	Breakfast	Breakfast	Breakfast	Breakfast		
Anja Beckmann	Adolfo Botana	Pedro José Sebastião	Olivier Laton	Leonid Grinin		
Solid-state NMR of the Mitochondr ABC Transporter Bm1A	Practical aspects of 13C QMNR	Observing short-range orientational order from liquid crystals to small molecule liquids	NMR of quadrupolar nuclei at high magnetic fields	Analysis of Strongly Dipolar Coupled Solids by Time-Domain NMR		
9:45-10:30	Siegrfried Stapf	Meeti Oztop	Esteban Anaroto	Magdalena Wondka		
Bicomponent fluids in porous media: what NMR can do for you	TD-NMR & MRI applications in Food Systems	Low field MRI solutions: fixed field, pre-polarized or field-cycled	69Ga and 71Ga as probes of local symmetry in diamagnetic complex metallic phases	Chemical exchange rate studied by NMR CPMG method		
10:30-11:00	Coffee Break	Coffee Break	Coffee Break	Coffee Break		
Beat Meier	David Lurie	Bernhard Blumich	Lucia Calucci	Marta Bera		
Protein fast MAS experiments at high field	Basics of MRI & Field-cycling Imaging	Asymmetry in Three-Site Relaxation-Exchange NMR	Looking into porous materials with solid-state NMR and relaxometry	Assessing the Molecular Dynamics in paramagnetic liquid systems		
11:45-12:30	Adolfo Botana	Ville-Veiko Telkki	Daniel Topgaard	Giacomo Parrigi		Claudia Schmitz
The magical world of pure shift NMR	Effect of surfactant aggregation on lipid formation	Translational motion and magnetic field gradients	Field-cycling NMR relaxometry of paramagnetic-labeled proteins	Ionic-liquid based hybrid gel polymer electrolytes as seen by NMR		
12:30-13:15	Wiktor Kozminski	Felice D'Alia/ Ahmed Dhifonzi	Arkadiusz Leniak	Danuta Kruk	Adriane Anceschi	
High dimensionality and high resolution NMR experiments for biomolecules	JEOL - The Luminaire NMR on cloud formation	Expanding NMR Laboratory Operations in Medical Oncology: Insights & Challenges at Odon Pharma SA	NMR relaxation processes in solutions of superparamagnetic nanoparticles	Challenges of non-exponential NMR relaxation processes		
13:15-14:00	Lunch	Lunch	Lunch	Lunch	Lunch	
14:00-16:15	Free Time	Free Time	Free Time	Free Time	Free Time	
16:15-16:30	Coffee Break	Coffee Break	Coffee Break	Coffee Break	Coffee Break	
On-line laboratory training	On-line laboratory training	Excursion	On-line laboratory training	On-line laboratory training	On-line laboratory training	
16:30-17:15	Adolfo Botana	Jacek Jenczyk	Magik Angle	Adolfo Botana	Jacek Jenczyk	
JASCO workshop: practical aspects	Magik Angle	JASCO workshop: practical aspects	Magik Angle	JASCO workshop: practical aspects	Magik Angle	
Group 1	Group 2	Group 1	Group 2	Group 1	Group 2	
17:15-18:00	Jacek Jenczyk	Adolfo Botana	Magik Angle	JASCO workshop: practical aspects	Magik Angle	
Group 1	Group 2	Group 1	Group 2	Group 1	Group 2	
18:45 - walk to...	18:45 - walk to...	18:45 - walk to...	18:45 - walk to...	18:45 - walk to...	18:45 - walk to...	
Dinner	Dinner	Dinner	Dinner	Dinner	Dinner	
19:00	Dinner	Dinner	Dinner	Dinner	Dinner	
19:45	Dinner	Dinner	Dinner	Dinner	Dinner	
20:45	Dinner	Dinner	Dinner	Dinner	Dinner	
21:45	Dinner	Dinner	Dinner	Dinner	Dinner	
22:45	Dinner	Dinner	Dinner	Dinner	Dinner	
23:45	Dinner	Dinner	Dinner	Dinner	Dinner	
24:45	Dinner	Dinner	Dinner	Dinner	Dinner	
25:45	Dinner	Dinner	Dinner	Dinner	Dinner	
26:45	Dinner	Dinner	Dinner	Dinner	Dinner	
27:45	Dinner	Dinner	Dinner	Dinner	Dinner	
28:45	Dinner	Dinner	Dinner	Dinner	Dinner	
29:45	Dinner	Dinner	Dinner	Dinner	Dinner	
30:45	Dinner	Dinner	Dinner	Dinner	Dinner	
31:45	Dinner	Dinner	Dinner	Dinner	Dinner	
32:45	Dinner	Dinner	Dinner	Dinner	Dinner	
33:45	Dinner	Dinner	Dinner	Dinner	Dinner	
34:45	Dinner	Dinner	Dinner	Dinner	Dinner	
35:45	Dinner	Dinner	Dinner	Dinner	Dinner	
36:45	Dinner	Dinner	Dinner	Dinner	Dinner	
37:45	Dinner	Dinner	Dinner	Dinner	Dinner	
38:45	Dinner	Dinner	Dinner	Dinner	Dinner	
39:45	Dinner	Dinner	Dinner	Dinner	Dinner	
40:45	Dinner	Dinner	Dinner	Dinner	Dinner	
41:45	Dinner	Dinner	Dinner	Dinner	Dinner	
42:45	Dinner	Dinner	Dinner	Dinner	Dinner	
43:45	Dinner	Dinner	Dinner	Dinner	Dinner	
44:45	Dinner	Dinner	Dinner	Dinner	Dinner	
45:45	Dinner	Dinner	Dinner	Dinner	Dinner	
46:45	Dinner	Dinner	Dinner	Dinner	Dinner	
47:45	Dinner	Dinner	Dinner	Dinner	Dinner	
48:45	Dinner	Dinner	Dinner	Dinner	Dinner	
49:45	Dinner	Dinner	Dinner	Dinner	Dinner	
50:45	Dinner	Dinner	Dinner	Dinner	Dinner	
51:45	Dinner	Dinner	Dinner	Dinner	Dinner	
52:45	Dinner	Dinner	Dinner	Dinner	Dinner	
53:45	Dinner	Dinner	Dinner	Dinner	Dinner	
54:45	Dinner	Dinner	Dinner	Dinner	Dinner	
55:45	Dinner	Dinner	Dinner	Dinner	Dinner	
56:45	Dinner	Dinner	Dinner	Dinner	Dinner	
57:45	Dinner	Dinner	Dinner	Dinner	Dinner	
58:45	Dinner	Dinner	Dinner	Dinner	Dinner	
59:45	Dinner	Dinner	Dinner	Dinner	Dinner	
60:45	Dinner	Dinner	Dinner	Dinner	Dinner	
61:45	Dinner	Dinner	Dinner	Dinner	Dinner	
62:45	Dinner	Dinner	Dinner	Dinner	Dinner	
63:45	Dinner	Dinner	Dinner	Dinner	Dinner	
64:45	Dinner	Dinner	Dinner	Dinner	Dinner	
65:45	Dinner	Dinner	Dinner	Dinner	Dinner	
66:45	Dinner	Dinner	Dinner	Dinner	Dinner	
67:45	Dinner	Dinner	Dinner	Dinner	Dinner	
68:45	Dinner	Dinner	Dinner	Dinner	Dinner	
69:45	Dinner	Dinner	Dinner	Dinner	Dinner	
70:45	Dinner	Dinner	Dinner	Dinner	Dinner	
71:45	Dinner	Dinner	Dinner	Dinner	Dinner	
72:45	Dinner	Dinner	Dinner	Dinner	Dinner	
73:45	Dinner	Dinner	Dinner	Dinner	Dinner	
74:45	Dinner	Dinner	Dinner	Dinner	Dinner	
75:45	Dinner	Dinner	Dinner	Dinner	Dinner	
76:45	Dinner	Dinner	Dinner	Dinner	Dinner	
77:45	Dinner	Dinner	Dinner	Dinner	Dinner	
78:45	Dinner	Dinner	Dinner	Dinner	Dinner	
79:45	Dinner	Dinner	Dinner	Dinner	Dinner	
80:45	Dinner	Dinner	Dinner	Dinner	Dinner	
81:45	Dinner	Dinner	Dinner	Dinner	Dinner	
82:45	Dinner	Dinner	Dinner	Dinner	Dinner	
83:45	Dinner	Dinner	Dinner	Dinner	Dinner	
84:45	Dinner	Dinner	Dinner	Dinner	Dinner	
85:45	Dinner	Dinner	Dinner	Dinner	Dinner	
86:45	Dinner	Dinner	Dinner	Dinner	Dinner	
87:45	Dinner	Dinner	Dinner	Dinner	Dinner	
88:45	Dinner	Dinner	Dinner	Dinner	Dinner	
89:45	Dinner	Dinner	Dinner	Dinner	Dinner	
90:45	Dinner	Dinner	Dinner	Dinner	Dinner	
91:45	Dinner	Dinner	Dinner	Dinner	Dinner	
92:45	Dinner	Dinner	Dinner	Dinner	Dinner	
93:45	Dinner	Dinner	Dinner	Dinner	Dinner	
94:45	Dinner	Dinner	Dinner	Dinner	Dinner	
95:45	Dinner	Dinner	Dinner	Dinner	Dinner	
96:45	Dinner	Dinner	Dinner	Dinner	Dinner	
97:45	Dinner	Dinner	Dinner	Dinner	Dinner	
98:45	Dinner	Dinner	Dinner	Dinner	Dinner	
99:45	Dinner	Dinner	Dinner	Dinner	Dinner	
100:45	Dinner	Dinner	Dinner	Dinner	Dinner	
101:45	Dinner	Dinner	Dinner	Dinner	Dinner	
102:45	Dinner	Dinner	Dinner	Dinner	Dinner	
103:45	Dinner	Dinner	Dinner	Dinner	Dinner	
104:45	Dinner	Dinner	Dinner	Dinner	Dinner	
105:45	Dinner	Dinner	Dinner	Dinner	Dinner	
106:45	Dinner	Dinner	Dinner	Dinner	Dinner	
107:45	Dinner	Dinner	Dinner	Dinner	Dinner	
108:45	Dinner	Dinner	Dinner	Dinner	Dinner	
109:45	Dinner	Dinner	Dinner	Dinner	Dinner	
110:45	Dinner	Dinner	Dinner	Dinner	Dinner	
111:45	Dinner	Dinner	Dinner	Dinner	Dinner	
112:45	Dinner	Dinner	Dinner	Dinner	Dinner	
113:45	Dinner	Dinner	Dinner	Dinner	Dinner	
114:45	Dinner	Dinner	Dinner	Dinner	Dinner	
115:45	Dinner	Dinner	Dinner	Dinner	Dinner	
116:45	Dinner	Dinner	Dinner	Dinner	Dinner	
117:45	Dinner	Dinner	Dinner	Dinner	Dinner	
118:45	Dinner	Dinner	Dinner	Dinner	Dinner	
119:45	Dinner	Dinner	Dinner	Dinner	Dinner	
120:45	Dinner	Dinner	Dinner	Dinner	Dinner	
121:45	Dinner	Dinner	Dinner	Dinner	Dinner	
122:45	Dinner	Dinner	Dinner	Dinner	Dinner	
123:45	Dinner	Dinner	Dinner	Dinner	Dinner	
124:45	Dinner	Dinner	Dinner	Dinner	Dinner	
125:45	Dinner	Dinner	Dinner	Dinner	Dinner	
126:45	Dinner	Dinner	Dinner	Dinner	Dinner	
127:45	Dinner	Dinner	Dinner	Dinner	Dinner	
128:45	Dinner	Dinner	Dinner	Dinner	Dinner	
129:45	Dinner	Dinner	Dinner	Dinner	Dinner	
130:45	Dinner	Dinner	Dinner	Dinner	Dinner	
131:45	Dinner	Dinner	Dinner	Dinner	Dinner	
132:45	Dinner	Dinner	Dinner	Dinner	Dinner	
133:45	Dinner	Dinner	Dinner	Dinner	Dinner	
134:45	Dinner	Dinner	Dinner	Dinner	Dinner	
135:45	Dinner	Dinner	Dinner	Dinner	Dinner	
136:45	Dinner	Dinner	Dinner	Dinner	Dinner	
137:45	Dinner	Dinner	Dinner	Dinner	Dinner	
138:45	Dinner	Dinner	Dinner	Dinner	Dinner	
139:45	Dinner	Dinner	Dinner	Dinner	Dinner	
140:45	Dinner	Dinner	Dinner	Dinner	Dinner	
141:45	Dinner	Dinner	Dinner	Dinner	Dinner	
142:45	Dinner	Dinner	Dinner	Dinner	Dinner	
143:45	Dinner	Dinner	Dinner	Dinner	Dinner	
144:45	Dinner	Dinner	Dinner	Dinner	Dinner	
145:45	Dinner	Dinner	Dinner	Dinner	Dinner	
146:45	Dinner	Dinner	Dinner	Dinner	Dinner	
147:45	Dinner	Dinner	Dinner	Dinner	Dinner	
148:45	Dinner	Dinner	Dinner	Dinner	Dinner	
149:45	Dinner	Dinner	Dinner	Dinner	Dinner	
150:45	Dinner	Dinner	Dinner	Dinner	Dinner	
151:45	Dinner	Dinner	Dinner	Dinner	Dinner	
152:45	Dinner	Dinner	Dinner	Dinner	Dinner	
153:45	Dinner	Dinner	Dinner	Dinner	Dinner	
154:45	Dinner	Dinner	Dinner	Dinner	Dinner	
155:45	Dinner	Dinner	Dinner	Dinner	Dinner	
156:45	Dinner	Dinner	Dinner	Dinner	Dinner	
157:45	Dinner	Dinner	Dinner	Dinner	Dinner	
158:45	Dinner	Dinner	Dinner	Dinner	Dinner	
159:45	Dinner	Dinner	Dinner	Dinner	Dinner	
160:45	Dinner	Dinner	Dinner	Dinner	Dinner	
161:45	Dinner	Dinner	Dinner	Dinner	Dinner	
162:45	Dinner	Dinner	Dinner	Dinner	Dinner	
163:45	Dinner	Dinner	Dinner	Dinner	Dinner	
164:45	Dinner	Dinner	Dinner	Dinner	Dinner	
165:45	Dinner	Dinner	Dinner	Dinner	Dinner	
166:45	Dinner	Dinner	Dinner	Dinner	Dinner	
167:45	Dinner	Dinner	Dinner	Dinner	Dinner	
168:45	Dinner	Dinner	Dinner	Dinner	Dinner	
169:45	Dinner	Dinner	Dinner	Dinner	Dinner	
170:45	Dinner	Dinner	Dinner	Dinner	Dinner	
171:45	Dinner	Dinner	Dinner	Dinner	Dinner	
172:45	Dinner	Dinner	Dinner	Dinner	Dinner	
173:45	Dinner	Dinner	Dinner	Dinner	Dinner	
174:45	Dinner	Dinner	Dinner	Dinner	Dinner	
175:45	Dinner	Dinner	Dinner	Dinner	Dinner	
176:45	Dinner	Dinner	Dinner	Dinner	Dinner	
177:45	Dinner	Dinner	Dinner	Dinner	Dinner	
178:45	Dinner	Dinner	Dinner	Dinner	Dinner	
179:45	Dinner	Dinner	Dinner	Dinner	Dinner	
180:45	Dinner	Dinner	Dinner	Dinner	Dinner	
181:45	Dinner	Dinner	Dinner	Dinner	Dinner	
182:45	Dinner	Dinner	Dinner	Dinner	Dinner	
183:45	Dinner	Dinner	Dinner	Dinner	Dinner	
184:45	Dinner	Dinner	Dinner	Dinner	Dinner	
185:45	Dinner	Dinner	Dinner	Dinner	Dinner	
186:45	Dinner	Dinner	Dinner	Dinner	Dinner	
187:45	Dinner	Dinner	Dinner	Dinner	Dinner	
188:45	Dinner	Dinner	Dinner	Dinner	Dinner	
189:45	Dinner	Dinner	Dinner	Dinner	Dinner	
190:45	Dinner	Dinner	Dinner	Dinner	Dinner	
191:45	Dinner	Dinner	Dinner	Dinner	Dinner	
192:45	Dinner	Dinner	Dinner	Dinner	Dinner	
193:45	Dinner	Dinner	Dinner	Dinner	Dinner	
194:45	Dinner	Dinner	Dinner	Dinner	Dinner	
195:45	Dinner	Dinner	Dinner	Dinner	Dinner	
196:45	Dinner	Dinner	Dinner	Dinner	Dinner	
197:45	Dinner	Dinner	Dinner	Dinner	Dinner	
198:45	Dinner	Dinner	Dinner	Dinner	Dinner	
199:45	Dinner	Dinner	Dinner	Dinner	Dinner	
200:45	Dinner	Dinner	Dinner	Dinner	Dinner	
201:45	Dinner	Dinner	Dinner	Dinner	Dinner	
202:45	Dinner	Dinner	Dinner	Dinner	Dinner	
203:45	Dinner	Dinner	Dinner	Dinner	Dinner	
204:45	Dinner	Dinner	Dinner	Dinner	Dinner	
205:45	Dinner	Dinner	Dinner	Dinner	Dinner	
206:45	Dinner	Dinner	Dinner	Dinner	Dinner	
207:45	Dinner	Dinner	Dinner	Dinner	Dinner	
208:45	Dinner	Dinner	Dinner	Dinner	Dinner	
209:45	Dinner	Dinner	Dinner	Dinner	Dinner	
210:45	Dinner	Dinner	Dinner	Dinner	Dinner	
211:45	Dinner	Dinner	Dinner	Dinner	Dinner	
212:45	Dinner	Dinner	Dinner	Dinner	Dinner	
213:45	Dinner	Dinner	Dinner	Dinner	Dinner	
214:45	Dinner	Dinner	Dinner	Dinner	Dinner	
215:45	Dinner	Dinner	Dinner	Dinner	Dinner	
216:45	Dinner	Dinner	Dinner	Dinner	Dinner	
217:45	Dinner	Dinner	Dinner	Dinner	Dinner	
218:45	Dinner	Dinner	Dinner	Dinner	Dinner	
219:45	Dinner	Dinner	Dinner	Dinner	Dinner	
220:45	Dinner	Dinner	Dinner	Dinner	Dinner	
221:45	Dinner	Dinner	Dinner	Dinner	Dinner	
222:45	Dinner	Dinner	Dinner	Dinner	Dinner	
223:45	Dinner	Dinner	Dinner	Dinner	Dinner	
224:45	Dinner	Dinner	Dinner	Dinner	Dinner	
225:45	Dinner	Dinner	Dinner	Dinner	Dinner	
226:45	Dinner	Dinner	Dinner	Dinner	Dinner	
227:45	Dinner	Dinner	Dinner	Dinner	Dinner	
228:45	Dinner	Dinner	Dinner	Dinner	Dinner	
229:45	Dinner	Dinner	Dinner	Dinner	Dinner	
230:45	Dinner	Dinner	Dinner	Dinner	Dinner	
231:45	Dinner	Dinner	Dinner	Dinner	Dinner	
232:45	Dinner	Dinner	Dinner	Dinner	Dinner	
233:45	Dinner	Dinner	Dinner	Dinner	Dinner	
234:45	Dinner	Dinner	Dinner	Dinner	Dinner	
235:45	Dinner	Dinner	Dinner	Dinner	Dinner	
236:45	Dinner	Dinner	Dinner	Dinner	Dinner	
237:45	Dinner	Dinner	Dinner	Dinner	Dinner	
238:45	Dinner	Dinner	Dinner	Dinner	Dinner	
239:45	Dinner	Dinner	Dinner	Dinner	Dinner	
240:45	Dinner	Dinner	Dinner	Dinner	Dinner	
241:45	Dinner	Dinner	Dinner	Dinner	Dinner	
242:45	Dinner	Dinner	Dinner	Dinner	Dinner	
243:45	Dinner	Dinner	Dinner	Dinner	Dinner	
244:45	Dinner	Dinner	Dinner	Dinner	Dinner	
245:45	Dinner	Dinner	Dinner	Dinner	Dinner	
246:45	Dinner	Dinner	Dinner	Dinner	Dinner	
247:45	Dinner	Dinner	Dinner	Dinner	Dinner	
248:45	Dinner	Dinner	Dinner	Dinner	Dinner	
249:45	Dinner	Dinner	Dinner	Dinner	Dinner	
250:45	Dinner	Dinner	Dinner	Dinner	Dinner	
251:45	Dinner	Dinner	Dinner	Dinner	Dinner	
252:45	Dinner	Dinner	Dinner	Dinner	Dinner	
253:45	Dinner	Dinner	Dinner	Dinner	Dinner	
254:45	Dinner	Dinner	Dinner	Dinner	Dinner	
255:45	Dinner	Dinner	Dinner	Dinner	Dinner	
256:45	Dinner	Dinner	Dinner	Dinner	Dinner	
257:45	Dinner	Dinner	Dinner	Dinner	Dinner	
25						